STUDY ON MULTIPLE *KIR* GENE POLYMORPHISMS AND THEIR CORRELATION WITH PLASMA VIRAL LOAD IN SIV-INFECTED RHESUS MACAQUES

PORNTIP CHAICHOMPOO

A THESIS SUBMITTED IN PARTIAL FULFILLMENT
OF THE REQUIREMENTS FOR
THE DEGREE OF DOCTOR OF PHILOSOPHY
(IMMUNOLOGY)
FACULTY OF GRADUATE STUDIES
MAHIDOL UNIVERSITY
2010

Thesis
entitled

STUDY ON MULTIPLE *KIR* GENE POLYMOPHISMS AND THEIR CORRELATION WITH PLASMA VIRAL LOAD IN SIV-INFECTED RHESUS MACAQUES

Porntip Ch.

Miss.Porntip Chaichompoo
Candidate

K. Pattanapanyasat

Prof.Kovit Pattanapanyasat,
Ph.D.
Major-advisor

Wannee Kantakamalakul

Assoc.Prof.Wannee Kantakamalakul,
Ph.D.
Co-advisor

Jaruda Kobkitjaroen

Lect.Jaruda Kobkitjaroen,
M.D.
Co-advisor

B. Mahaisavariya

Prof. Banchong Mahaisavariya,
M.D.
Dean
Faculty of Graduate Studies
Mahidol University

K. Pattanapanyasat

Prof. Kovit Pattanapanyasat,
Ph.D.
Program Director
Doctor of Philosophy
Program in Immunology
Faculty of Medicine Siriraj Hospital
Mahidol University

Thesis
entitled

STUDY ON MULTIPLE *KIR* GENE POLYMOPHISMS AND THEIR CORRELATION WITH PLASMA VIRAL LOAD IN SIV-INFECTED RHESUS MACAQUES

was submitted to the Faculty of Graduate Studies, Mahidol University
for the degree of Doctor of Philosophy (Immunology)
on
March 31, 2010

Porntip Ch.

Miss.Porntip Chaichompoo
Candidate

Prof.Aftab A. Ansari,
Ph.D.
Chair

K. Pattanapayasat

Prof.Kovit Pattanapanyasat,
Ph.D.
Member

Wannee Kantakamalakul

Assoc.Prof.Wannee Kantakamalakul,
Ph.D.
Member

Jaruda Kobkitjaroen

Lect.Jaruda Kobkitjaroen,
M.D.
Member

B. Mahaisavariya

Prof. Banchong Mahaisavariya,
M.D.
Dean
Faculty of Graduate Studies
Mahidol University

T. Kulthanan

Clin.Prof. Teerawat Kulthanan,
M.D., F.I.M.S., F.R.C.S.T., F.I.C.S.,
Certificate in Orthopedics (Essen)
Dean
Faculty of Medicine Siriraj Hospital
Mahidol University

ACKNOWLEDGEMENTS

This thesis arose in part out of years of research, by that time, I have worked with a great number of people whose contribution in assorted ways to the research and the making of the thesis deserved special mention. It is a pleasure to convey my gratitude to them all in my humble acknowledgment. First of all, I am heartily thankful to my major advisor, Prof. Dr.Kovit Pattanapanyasat, for giving me the valuable opportunity to study at the Department of Immunology. His kindness, valuable guidance, attention and encouragement are greatly appreciated. I would like to express the deepest appreciation to my co-advisor, Prof. Dr.Aftab A. Ansari, who has the attitude and the substance of a genius: he continually and convincingly conveyed a spirit of adventure in regard to research. I would like to record my gratitude to my supervisor, Assoc. Prof. Dr.Pavel Bostik, for his supporting from the initial to the final level enabled me to develop an understanding of the subject. Without his guidance and persistent help this dissertation would not have been possible. It is an honor for me to my thesis committee, Assoc. Prof. Dr.Wannee Kantakamalakul and Lect.Jaruda Kobkitjaroen, whose work demonstrated to me that concern for global affairs supported by an engagement in technique research and provide a quest for our times. I owe my deepest gratitude to the Thailand Research Fund for the financial support through the Royal Golden Jubilee Ph.D. Program. I am deeply indebted to Prof. Dr.Francois Villinger, Dr.Susan T. Stephenson, Ms.Dawn M. Little and my colleagues from Department of Pathology and Laboratory Medicine, Emory University, Atlanta, Georgia, USA, for their kind, gorgeous supports, understanding, and advices while I was learning in United State. Special appreciations also go to Dr.Lara E. Pereira for NK cell isolation. To the Yerkes National primate Research Center for collection of samples for this study. I would also acknowledge all staff of the Department of Immunology and Division of Instruments for Research, Faculty of Medicine, Siriraj Hospital, Mahidol University, Bangkok, Thailand, for their friendship, helpfulness and encouragement. Finally, my special thanks go to my parents and my friends for their understanding, warmly, and friendships. Last but not least, I offer my regards and blessings to all of those who supported me in any respect during the completion of the project.

Porntip Chaichompoo

STUDY ON MULTIPLE *KIR* GENE POLYMORPHISMS AND THEIR CORRELATION WITH PLASMA VIRAL LOAD IN SIV-INFECTED RHESUS MACAQUES

PORNTIP CHAICHOMPOO 5037259 SIIM/D

Ph.D. (IMMUNOLOGY)

THESIS ADVISORY COMMITTEE: KOVIT PATTANAPANYASAT, Ph.D., AFTAB A. ANSARI, Ph.D., WANNEE KANTAKAMALAKUL, Ph.D., JARUDA KOBKITJAROEN, M.D.

ABSTRACT

Natural killer (NK) cells are one of the major cell lineages in the innate immune system. HIV/SIV infection has been shown to decrease in both the frequency and function within this cell lineage. Among the many receptors expressed by NK cells that regulate their functions are the family of killer-cell immunoglobulin-like receptors (KIR's) which are encoded by a series of genes which are highly polymorphic. The natural ligands for KIR's are gene products of the major histocompatibility complex (MHC). KIR's are expressed on the cell surface with 1 to 3 extracellular domains (D0 to D2) and include a transmembrane and a cytoplasmic domain. The cytoplasmic domain is either a long (L), which contains an "inhibitory" immunoreceptor tyrosine based motif (ITIM), or a short cytoplasmic tail (S) containing an "activatory" immunoreceptor tyrosine based motif (ITAM). Only the ITAM molecules can bind adaptive molecules to activate signalling. Recent findings of a strong association between select KIR genes with MHC alleles and the rate of disease progression in HIV-1 infected individuals prompted our laboratory to examine whether such a relationship also exists for KIR genes, disease progression and plasma viral loads in SIV infected rhesus macaques. In this study, we characterized *KIR* loci including *Mamu-KIR1D, KIR2DL4,* and *KIR2DL5* in SIV-infected rhesus macaques with high or low plasma viral loads. The cDNA samples prepared from RNA obtained from purified NK cells were amplified for the 3 *KIR* genes using a series of primer sets and the products were ligated into a pGEM-T vector. The reactivated plasmids were transformed into JM109 cells. A sample of 5 single positive colonies was isolated, purified, and analyzed for DNA sequences. Among the *KIR* loci expressed in our cohort, we found 11 alleles from *KIR1D* characterized with the absence or presence of ITIMs in their cytoplasmic tail, and 7 alleles from *KIR2DL4* characterized with >98% homology. Data from this study appear to show a trend of SIV replication and KIR genotypes: there is a high expression of *KIR1D* alleles with ITIMs and *KIR2DL4 allele-1* in SIV-infected rhesus macaques that exhibited high plasma viral loads. These data support the view that the genetic inheritance of select KIR alleles and their corresponding natural ligands of the MHC class I molecules may play a deterministic role in the outcome of viral infection during the acute infection period.

KEY WORDS: KILLER IMMUNOGLOBULIN-LIKE RECEPTORS/ NK CELLS/ GENETIC POLYMORPHISMS/ SIMIAN IMMUNODEFICIENCY VIRUS/ RHESUS MACAQUES

110 pages

ความหลากหลายทางพันธุกรรมของเคอร์รีเซพเตอร์ในลิงวอกที่ติดเชื้อไวรัสเอสไอวี

STUDY ON MULTIPLE *KIR* GENE POLYMORPHISMS AND THEIR CORRELATION WITH PLASMA VIRAL LOAD IN SIV-INFECTED RHESUS MACAQUES

พรทิพย์ ชัยชมภู 5037259 SIIM/D

ปร. ด. (วิทยาภูมิคุ้มกัน)

คณะกรรมการที่ปรึกษาวิทยานิพนธ์ : โกวิท พัฒนาปัญญาสัตย์, Ph.D., แอฟแทป เอ แอนซารี, Ph.D., วรรณี กัณฐกมาลากุล, Ph.D., จารุดา กอบกิจเจริญ, M.D.

บทคัดย่อ

เอ็นเคเซลล์ (NK cells) เป็นเซลล์ที่มีความสำคัญในระบบภูมิคุ้มกันของร่างกายในการกำลังทำลายเชื่อไวรัสโดยเฉพาะอย่างยิ่งเชื้อไวรัสเอชไอวี/เอสไอวี ซึ่งมีผลกระทบต่อทั้งปริมาณและหน้าที่การทำงานของเซลล์ชนิดนี้ เคอร์รีเซพเตอร์ (KIR) เป็นโมเลกุลชนิดหนึ่งที่อยู่บนผิวของ NK cells ซึ่งโมเลกุลนี้มีความหลากหลายทางพันธุกรรมสูงและมีความสำคัญต่อการจับจำเพาะต่อ MHC class I องค์ประกอบของ KIR ประกอบด้วย โดเมนที่อยู่บนผิวเซลล์ และโดเมนที่อยู่ภายในเซลล์ ซึ่งแบ่งได้เป็น 2 แบบ คือ แบบหางสายยาวที่มีโมทีฟในการทำหน้าที่ยับยั้งการทำงานของเซลล์ (ITIMs) และแบบหางสายสั้นซึ่งไม่มีโมทีฟดังกล่าว ซึ่ง KIR ชนิดแบบหางสั้นนี้จะทำหน้าที่กระตุ้นโมเลกุลอื่นแล้วส่งผลต่อการกระตุ้นการทำงานของเซลล์เพื่อไปทำลายเซลล์เป้าหมาย จากหลักฐานงานวิจัยที่ผ่านมา พบว่าความหลากหลายทางพันธุกรรมของ KIR และ MHC class I มีความเกี่ยวข้องกับการชะลอความรุนแรงของโรคเอดส์ ซึ่งทางคณะวิจัยมีความสนใจศึกษาลักษณะการแสดงออกทางพันธุกรรมของ KIR โดยศึกษาเปรียบเทียบในลิงวอกที่ติดเชื้อเอสไอวี ในงานวิจัยนี้จะเน้นถึงการแสดงออกของ KIR ชนิด 1D, 2DL4, และ 2DL5 ในลิงวอกที่ติดเชื้อเอสไอวี ทั้งกลุ่มที่มีระดับไวรัสในพลาสม่าสูงและกลุ่มที่มีระดับไวรัสในพลาสม่าต่ำ โดยการศึกษา KIR ยีนทำโดย ศึกษาจาก cDNA ซึ่งสังเคราะห์มาจาก RNA ที่ได้มาจาก NK cells ของลิงแต่ละตัว จากนั้นจึงใช้เทคนิคการโคลนิ่ง เพื่อศึกษาสายพันธุกรรม จากการทดลองพบว่ามีการแสดงออกของ KIR1D ทั้งหมด 11 อัลลีน โดยแบ่งออกเป็น 2 กลุ่มใหญ่ ตามการแสดงออกของ ITIMs ส่วน KIR2DL4 พบทั้งหมด 7 อัลลีน แยกตามความคล้ายคลึงกันของสายพันธุกรรมที่ >98% จากการศึกษาวิจัยครั้งนี้พบว่าลิงที่มีการแสดงออกของ KIR1D แบบที่มี ITIMs และ KIR2DL4 allele-1 มีความสัมพันธ์กับลิงวอกที่ติดเชื้อไวรัสในกลุ่มที่มีระดับไวรัสในกระแสเลือดสูง งานวิจัยนี้ได้สนับสนุนข้อสมมุติฐานต่อการศึกษาหาความสัมพันธ์ทางพันธุกรรมของ KIR ร่วมทั้งโมเลกุลที่จับจำเพาะต่อ KIR ในการช่วยพยากรณ์และการตรวจติดตาม ตลอดจนการรักษาผู้ติดเชื้อไวรัสเอชไอวี/เอสไอวี

110 หน้า

CONTENTS

CONTENTS (cont.)

CONTENTS (cont.)

LIST OF TABLES

LIST OF TABLES (cont.)

LIST OF FIGURES

LIST OF FIGURES (cont.)

LIST OF ABBREVIATIONS

Abbreviations	Term
χ^2	The chi-square
aa	Amino acid
ac no	Accession number
ADCC	Antibody-dependent cell-mediated cytotoxicity
AIDS	Acquire immunodeficiency syndrome
BAC	Bacterial Artificial Chromosome
BCM	The Baylor College of Medicine
bp	Base pair
BSA	Bovine serum albumin
cat #	Catalog number
cDNA	Complementary deoxyribonucleic acid
CTL	Cytotoxic T cell
DC	Dendritic cell
DNA	Deoxyribonucleic acid
EC	Extracellular-like domain
FCS	Fetal calf serum
FL	Flt3 ligand
GAPDH	Glyceraldehyde 3-phosphate dehydrogenase
Gg	*Gorilla gorilla*
GM-CSF	Granulocyte/macrophage colony-stimulating factor
HCR	Human-chimpanzee-rhesus macaque
HGNC	The HUGO Genome Nomenclature Committee
HGSC	Human Genome Sequencing Center
HIV-1	Human immunodeficiency virus-1
HLA	Human leukocyte antigen
Hu	*Homo sapien*s

LIST OF ABBREVIATIONS (cont.)

Abbreviations	Term
IFN-γ	Interferon-γ
Ig	Immunoglobulin
iNKR	Inhibitory NK cell receptor
ITAM	Immunoreceptor tyrosine-based activation motif
ITIM	Immunoreceptor tyrosine-based inhibitory motif
KIR	Killer immunoglobulin-like receptor
KL	c-kit ligand
KLR	Killer cell lectin-like receptor
LAK	Lymphokine-activated killer
LRC	Leukocyte receptor complex
LTNP	Long term non-progressive
Mf	*Macaca fascicularis*
MHC	Major histocompatibility complex
MICA	MHC-class-I-polypeptide-related sequence A
Mm	*Macaca mulatta*
mRNA	Messenger ribonucleic acid
Mya	Million year ago
NCBI	National Center for Biotechnology Information
NCR	Natural cytotoxicity receptor
NHGRI	The National Human Genome Research Institute
NIH	National Institutes of Health
NK cell	Natural killer cell
NKG2D	NK group 2-member D
NKp30	NK cell protein 30
NKR-P1A	NK-cell receptor protein 1A
nRTIs	Reverse transcriptase inhibitors
OR	The odds ratio

LIST OF ABBREVIATIONS (cont.)

Abbreviations	Term
p-allele-5	Predicted Mamu-KIR2DL4 allele-5
PBMC	Peripheral blood mononuclear cell
PBS	Phosphate buffered saline
PCR	Polymerase chain reaction
PGI	Pooled Genomic Indexing
PMPA	9-[2-(phosphonomethoxy)propyl]adenine
Popy	*Pongo pygmaeus*
Pp	*Pan paniscus*
Pt	*Pan troglodytes*
qcPCR	Real time PCR
RM	Rhesus macaque
RNA	Ribonucleic acid
RT	Room temperature
SHP1	SRC-homology-2-domain-containing protein tyrosine phosphatase 1
SIV	Simian immunodeficiency virus
SM	Sooty mangabey
SNP	Single nucleotide polymorphism
sv	Splice variants
TM	Transmembrane domain
TNF	Tumor necrosis factor
ULBP	UL16-binding protein
VL	Viral load

CHAPTER I
INTRODUCTION

Natural killer (NK) cells are responsible for natural cytotoxicity and chemokine-cytokine production that play an important role in the innate immunity to viral infection and their ability to the adaptive immunity development (1). The balance of the natural cytotoxicity receptors (NCRs) and the inhibitory NK cell receptors (iNKRs) regulates the signal transduction to kill the lacking major histocompatibility complex (MHC) class I cells as known in the 'missing-self hypothesis', which refers to iNKR recognition of self-proteins that expresse on normal cells. The MHC class I molecules are altered or absent from the surface during viral infection and in tumour cells (Figure 1.1) (1). The killer immunoglobulin-like receptors (KIRs) express on NK cells and lymphocytes and display either activate or inhibit NK cell functions. KIR molecules contains the extracellular immunoglobulin (Ig)-like domain (EC), stem, transmembrane domain (TM), and either short (S) or long (L) cytoplasmic tails (Figure 1.2) (2). The activating KIR molecules (the short cytoplasmic tail) have a positive charge lysine (K) or arginine (R) in their TM. These amino acids can bind to a negative charge aspartic acid (D) in an adaptor molecule, usually DAP12 molecule which contains a short cytoplasmic domains containing immunoreceptor tyrosine-based activation motifs (ITAMs; protein consensus: Y-XX-I/L-$X_{(6–12)}$Y-XX-I/L), in cell-cell interaction (1, 3). All iNKRs have employ negative regulators bearing immunoreceptor tyrosine-based inhibitory motifs (ITIMs; protein consensus: S/I/V/L-X-Y-XX-I/V/L), which mediate to inhibit NK cell activity (1). Interestingly, KIR2DL4 molecules have intrinsic ITIMs in their cytoplasm and positively charged 'R' in their TM (4). Thus, KIR2DL4 can physically interact with the TM adaptor protein FcεRI-γ, which is believed to be mediated through the 'D' residue to transduce activity signals via ITAMs (5).

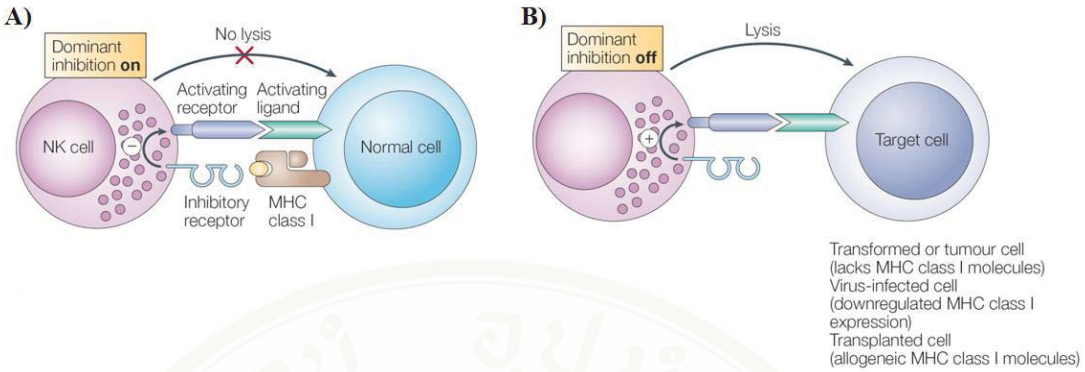

Fauci AS, et al. Nat Rev Immunol. (2005)

Figure 1.1. Natural-killer-cell recognition of target cells. In the presence of the major histocompatibility complex (MHC) class I molecules on normal cells, the inhibitory NK cell receptors (iNKRs) are triggered, leading to the delivery of inhibitory signals and, consequently, results in no lysis of target cells (A). In the case of tumor cells or virus-infected cells, the cell-surface expression of MHC class I molecules is downregulated, thus, iNKRs are not triggered. Instead, the positive signals through activating receptors are dominated, which induce lysis of target cells (B) (1).

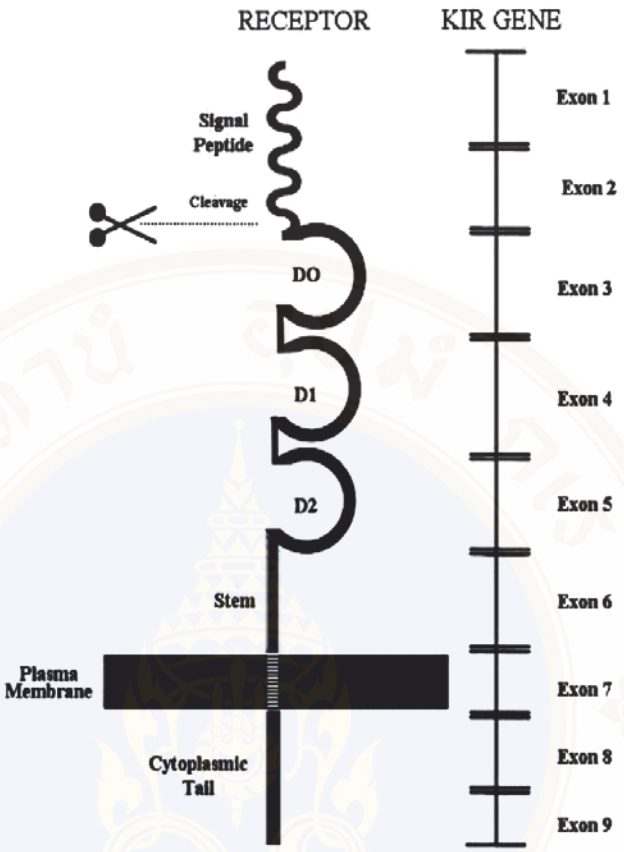

Iannello A, et al. J Leukoc Biol. (2008)

Figure 1.2. Killer immunoglobulin-like receptor (KIR) structure. The KIRs contain signal peptide, either one or two or three extracellular domain (D0, D1, and D2), stem, transmembrane domain, and short or long cytoplasmic tail (6).

There are several studies on the effects of human immunodeficiency virus-1 (HIV-1) and simian immunodeficiency virus (SIV) infection are decreased NCR expression and increased iNKR expression on NK cell surface. The hallmark of the relationship between *KIR* genetic individuals and disease's stages has been shown by Martin *et al* (7) and Alter *et al* (8). They proposed that the elevated expressions of the activating and/or the inhibitory KIR molecules on NK cells were related to HIV-1 infection at acute and chronic phases (8). The results showed that *Hu-KIR3DS1* expression in acute HIV-1 infected patients with human leukocyte antigen (HLA)-*B Bw4* allotypes presenting an isoleucine (I) at position 80 (*HLA-B Bw4*80I*) was 32-fold higher than HIV-1 serotype negative individuals with *HLA-B Bw4*80I* positive (p = 0.01). Meanwhile *Hu-KIR3DS1* combined with *HLA-B Bw4*80I* was associated with delayed progression to acquire immunodeficiency syndrome (AIDS) in patients with HIV-1 infection. They also investigated the various distinct allelic combinations of the *Hu-KIR3DL1* and *HLA-B Bw4*80I* that showed a significant and strong influence on both AIDS progression and plasma viral load (VL) in a consistent manner (9). A trend towards increased levels of *Hu-KIR3DL1* transcript levels in acutely infected individuals that encoded for at least one copy of *HLA-B Bw4*80I* were 6-fold higher than in *HLA-B Bw6* positive individuals (p = 0.07). *Hu-KIR3DL1* transcript levels were 5-fold higher in *HLA-B Bw4*80I* positive with acute infection compared to *HLA-B Bw4*80I* positive HIV-1 negative controls. Both *Hu-KIR3DS1* and *Hu-KIR3DL1* expression were differented in chronic HIV-1 infected patients with *HLA-B Bw4*80I* positive individuals when compared to acutely infected individuals (8, 9). The expression of *Hu-KIR3DS1* in chronic infected individuals with *HLA-B Bw4*80I* was higher than patients with *HLA-B Bw6* but was lower than HIV-1 negative individuals. In contrast, *Hu-KIR3DL1* expression was substantially increased in chronically infected subjects with *HLA-B Bw4*80I* when compared with acutely infected individuals and HIV-1 negative individuals (8).

Studies on the mechanisms of the pathogenesis of SIV-infected rhesus macaques (RMs, *Macaca mulatta*) showed similar finding to that of HIV-1-infected human in the phenotypic changes and NK cell functions that occur during either acute or chronic phases of SIV-infected RMs. Bostik *et al* investigated the *Mamu-KIR3DL* allelic expression to genetic relationship in the fast progressive and the long term

non-progressive (LTNP) SIV-infected RMs (2). They found 14 *Mamu-KIR3DL* alleles that showed two *Mamu-KIR3DL* alleles (allele-13 and allele-14, GenBank accession number (ac. no.) FJ562120 and FJ562121) which were characterized by a single nucleotide polymorphism (SNP) 159 H/Q was associated with RMs who exhibited high plasma VL. This data for the first time defined multiple alleles of *Mamu-KIR3DL* and showed association between viral control, NK cell function and genetic polymorphisms of KIR3DL receptors in RMs (2). Our laboratory is interested in a different KIR family - *Mamu-KIR1D*, *2DL4*, *2DL5*, *3DH*, and *3DL* - with the aim to perform analysis on relatively large population of RMs and define sequence variations that are common in RM population (2). We are also interested in polymorphism of other *Mamu-KIRs* in our RM cohort which has been divided into fast progressive infection or high VL (RM-HVL cohort) and LTNP infection or low VL (RM-LVL cohort) (2). Although some of *Mamu-KIRs* are available for database sequences as proposed by Hershberger *et al* (10), these data represent single sequence from individual animals and therefore do not compile a database large enough to identify sequence patterns or alleles. Because changes in the expression of KIR molecules have been previously shown to be associated with differences of disease course in HIV-1 infected human (8, 9) and in SIV-infected RMs (2), our initial attempt to characterize the genetic variations of *Mamu-KIR1D*, *2DL4*, and *2DL5* in RM cohort as described in Bostik *et al* (2) and to extend our perform analysis on these genes in a relatively large population of RMs (n = 38) as well as to define sequence variations that are common in this RM population. Moreover, we are also interested in the association between VL and genetic polymorphisms of KIRs. Some animals in our cohort were treated with 9-[2-(phosphonomethoxy)propyl]adenine (PMPA) (new name, tenofovia) which is antiretroviral drug, belong to a class of antiretroviral drugs known as nucleotide analogue reverse transcriptase inhibitors (nRTIs), which block reverse transcriptase, an enzyme crucial to viral production in HIV-infected people (http://en.wikipedia.org/wiki/Tenofovir). The antiviral drug treatement was not interfere to the genetic variations of *KIR* gene (11, 12).

CHAPTER II
OBJECTIVES

The objectives of this study are:

1. To determine the polymorphisms of *Mamu-KIR1D, Mamu -KIR2DL4,* and *Mamu-KIR2DL5* genes in purified NK cells obtained from SIV-infected rhesus macaques.
2. To determine the association of genetic variations of *KIR* genes to viral replication.

CHAPTER III
LITERATURE REVIEW

3.1. The Natural Killer cells

Cells of the innate immune system are basically non-antigen specific effector cells with primary function is to eliminate non-self cellular elements (cancer cells within our body) or serve to non-specifically mount an immune response against infectious agents such as viruses, bacteria, and other microbes (1). NK cells constitute a potent, rapid part of the innate immune response to infection or transformation, and also generate a link to priming of adaptive immunity. Their function can encompass direct cytotoxicity as well as the release of cytokines and chemokines (13). It is now becoming increasingly clear that cell lineages, in particular, the NK cell lineages have in fact a far more sophisticated biological role (1).

3.1.1. NK cell subsets

NK cells are large granular lymphocytes that are not of T cell or B cell lineage, they express CD16 and CD56, but do not express CD3 (Figure 3.1) (14). Generally, human NK cells comprise approximately 15% of all lymphocytes and are divided into two subsets based on their cell-surface density of $CD3^{-}CD16^{bright}CD56^{dim}$ and $CD3^{-}CD16^{dim}CD56^{bright}$ cells. The majority (~90%) of human NK cells have high expression of CD16 ($CD16^{bright}$, FcγRIII) but low-density expression of CD56 ($CD56^{dim}$), whereas only ~10% of NK cells are $CD16^{neg/dim}CD56^{bright}$ cells (15, 16). The development of human NK cells can be divided into two phases (Figure 3.2). The early phase, NK progenitor cell ($CD34^{+}Lin^{-}$) responds to growth factors such as flt3 ligand or c-kit ligand that influences cell development of an NK-cell precursor intermediate with the basic phenotype $CD34^{+}IL\text{-}15R^{+}$ cells. The secondly phase, IL-15 induces the development of mature $CD56^{bright}$ NK cells (15). It is important to note that human culture systems have shown the differentiation of $CD56^{bright}$ NK cells from various other starting progenitor populations including cord blood $CD34^{+}$, fetal

liver $CD34^{+}CD38^{+/-}$ and thymocyte T and/or NK progenitors in the presence of IL-15 (15). Potential hypothesis for the development of $CD56^{dim}$ NK cells include three probably ways (i) the existence of a unique $CD56^{dim}$ NK-cell precursor; (ii) an alternate signal (e.g. a novel cytokine) that could induce the differentiation of $CD56^{dim}$ cells from a common NK-cell precursor; or (iii) maturation of $CD56^{bright}$ cells into $CD56^{dim}$ NK cells (15). Like human NK cells, rhesus NK cells have divided into two subsets based on CD16 and CD56 expression as defined the $CD3^{-}CD16^{+}CD56^{-}$ or the $CD3^{-}CD16^{-}CD56^{+}$ cells (17).

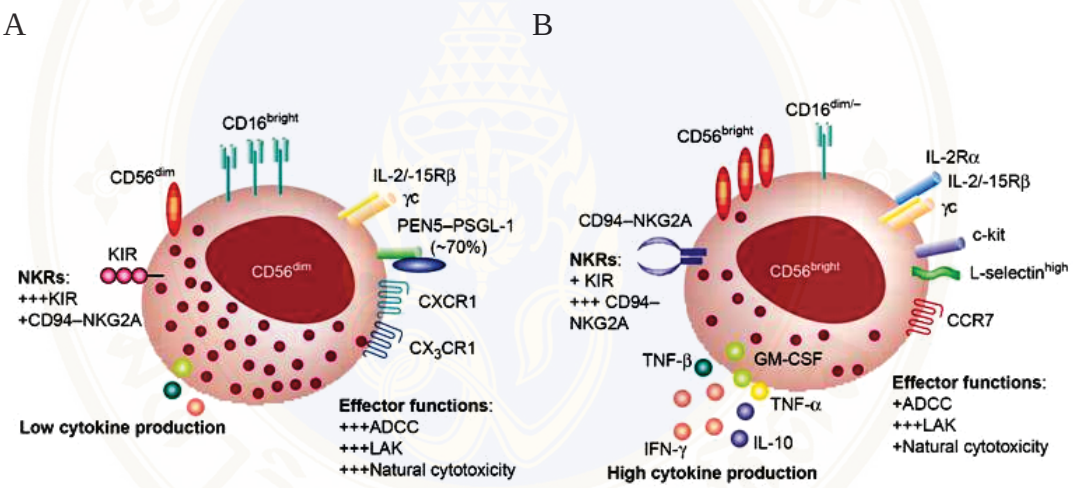

Cooper MA, et al. Trends Immunol. (2001)

Figure 3.1. Human NK cell subsets. NK cells are divided into 2 subsets based the expression of $CD3^{-}CD16^{bright}CD56^{dim}$ (A) and $CD3^{-}CD16^{dim}CD56^{bright}$ (B). The $CD16^{bright}$ NK cells produce low levels of NK-derived cytokines but are potent mediators of antibody-dependent cell-mediated cytotoxicity (ADCC), lymphokine-activated killer (LAK) activity and natural cytotoxicity, and have a more granular morphology than $CD56^{bright}$ NK cells. By contrast, $CD56^{bright}$ NK cells produce high levels of cytokines following stimulation with monokines. This subset has low-density expression of CD16 and exhibits low natural cytotoxicity and ADCC, but potent LAK activity (15).

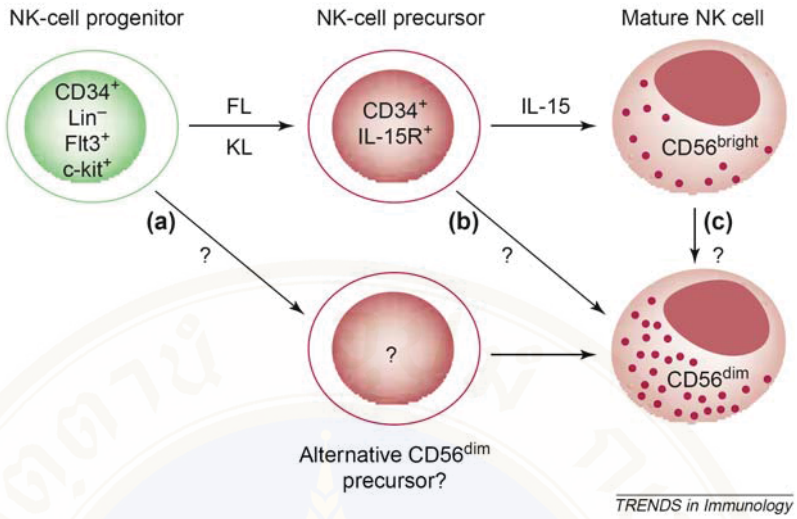

Cooper MA, et al. Trends Immunol. (2001)

Figure 3.2. Human NK cell subset development. NK-cell development can be divided into three discrete stages based on in vitro models. The negative lineage markers (Lin^-) $CD34^+$NK-cell progenitor cell expresses the receptor tyrosine kinases flt3 and c-kit that are responsive to flt3 ligand (FL) and c-kit ligand (KL), respectively. This progenitor cell differentiates into a precursor cell ($CD34^+IL\text{-}15R^+$, interleukin 15 receptor) that is responsive to IL-15 for maturation into a functionally mature $CD56^{bright}$ NK cell. The developmental relationship between $CD56^{bright}$ and $CD56^{dim}$ NK cells has never been established definitively, and $CD56^{dim}$ NK cells have not been generated in vitro. Potential hypothesis for the development of $CD56^{dim}$ NK cells includes: (a) the existence of a unique $CD56^{dim}$ NK-cell precursor; (b) an alternate signal (e.g. a novel cytokine) that could induce the differentiation of $CD56^{dim}$ cells from a common NK-cell precursor; or (c) maturation of $CD56^{bright}$ cells into $CD56^{dim}$ NK cells (15).

3.1.2. NK cell receptors

Two major superfamilies of NK receptors have been described in humans and RMs: (i) the iNKRs including KIR superfamily which primarily recognizes MHC class I and the C-type lectin superfamily includes CD94 and NKG2 receptors recognizing HLA-E; and (ii) the NCRs including NK cell protein 30 (NKp30), NKp44, and NKp46 (Figure 3.3) (1, 18), provide the ‘on signal” for stimulation of NK cells during their interaction with target cells. NK group 2-member D (NKG2D) is another activating receptor that binds to the endogenous ligand cytomegalovirus-UL16-binding protein (ULBP), MHC-class-I-polypeptide-related sequence A (MICA), MICB, and mediates lysis of target cells (15). NK cells have several accessory receptors that regulate their behaviors in response to various targets that lack of MHC class I molecules. These include NKp80, NK-cell receptor protein 1A (NKR-P1A; also known as CD161), CD96, and 2B4 (also known as CD244) (Figure 3.4) (19).

3.1.3. The ‘missing-self’ hypothesis

NK cells undergo a process of negative or positive selection termed ‘licensing’ or ‘arming’ that regulate NK cell activity by the balance of interactions between several families of activating and inhibitory NK cell receptors and their cognate ligands on the target cells (20). Early studies indicated that NK-cell responses are induced by loss of expression of MHC class I renders targets more susceptible to NK cell mediated killing due to the loss of the inhibitory signals via self-MHC-recognizing receptors as described by the missing-self hypothesis (Figure 1.1) (20). This hypothesis states that under normal conditions, the inhibitory signals are dominant, preventing the destruction of normal cells by NK cells. However, if a target cell fails to express MHC class I molecules, then NK cells kill this cell. The missing-self hypothesis is supported by the findings that tumour cells or virally infected cells that have decreased expression of MHC class I molecules become susceptible to NK-cell killing (21, 22).

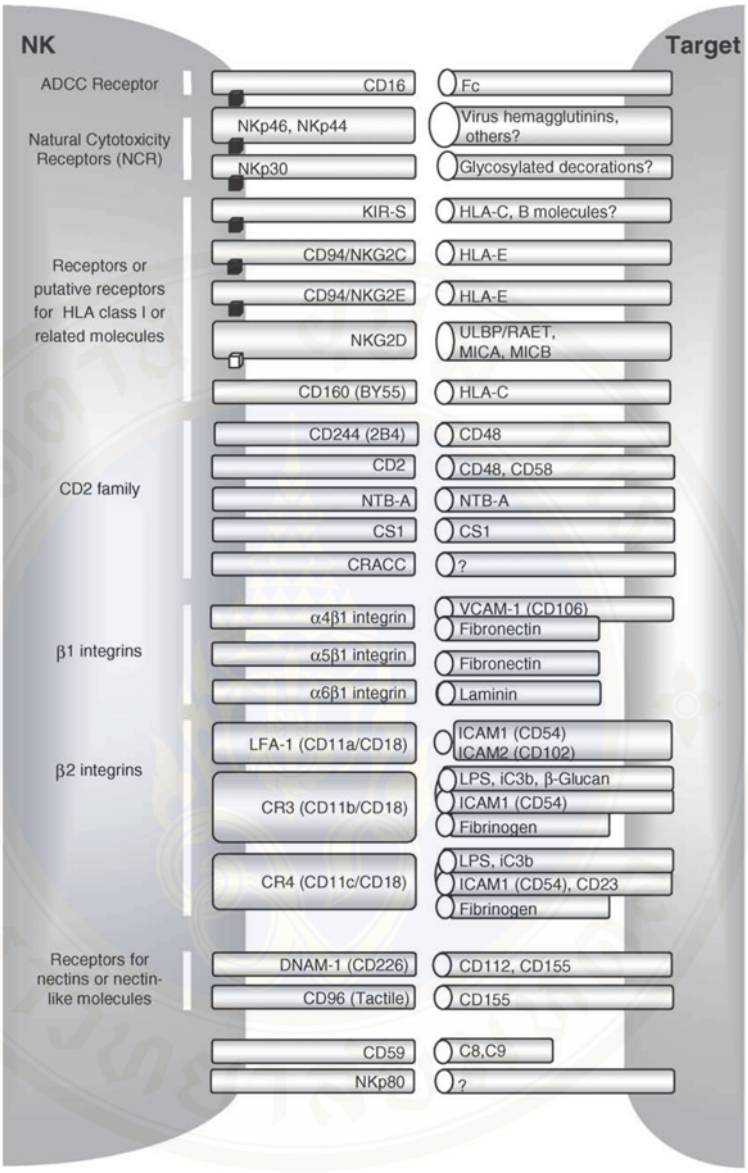

Chiesa S, et al. Mol Immunol. (2005)

Figure 3.3. Human NK cell receptors and their ligands (23).

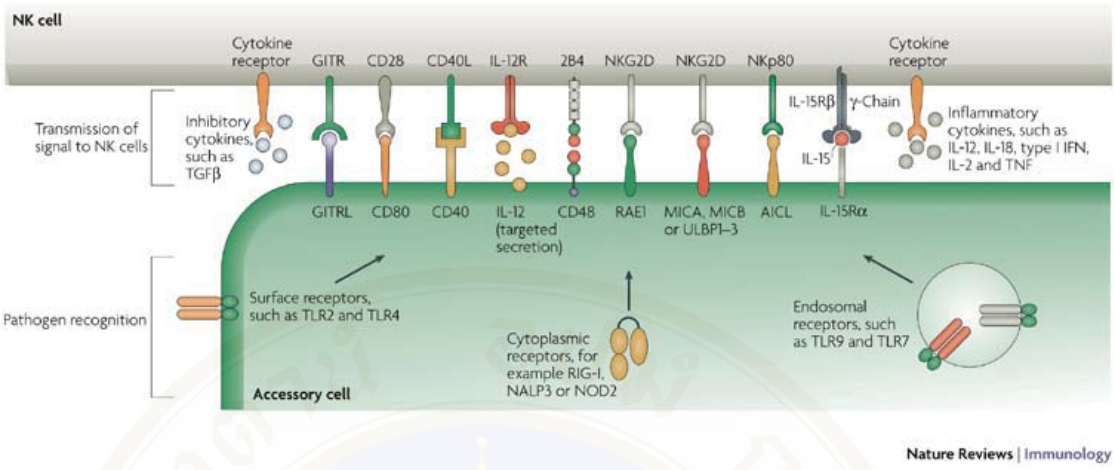

Newman KC, et al. Nat Rev Immunol. (2007)

Figure 3.4. Accessory NK cell receptors. Activation of NK cells by some virus requires the presence of accessory cells such as monocytes, macrophages, and dendritic cells. The accessory cells sense pathogenic ligands through receptors located on their surface and transmit signals to NK cells through various soluble or membrane-bound molecules. The degree to which each signal contributes to NK cell activation in response to different pathogens remains to be clearly established. For example, the interactions between GITRL and GITR, between IL-12 and IL-12R, between CD48 and 2B4, between MICA/MICB and NKG2D, and between AICL and NKp80 have supporting data obtained from human cells. Interactions between CD80 and CD28, between CD40 and CD40L and between RAE1 and NKG2D were obtained using a mouse model (19).

Abbreviations; Activation-induced C-type lectin, AICL; CD40L, CD40 ligand; interleukin-12, IL-12; interleukin-12 receptor, IL-12R; the major histocompatibility complex, MHC; MHC-class-I-polypeptide-related sequence A, MICA; MHC-class-I-polypeptide-related sequence B, MICB; retinoic acid early inducible 1, RAE1; tumor-necrosis factor, TNF; and glucocorticoid-induced TNF-receptor-related protein ligand, GITRL.

3.2. Killer immunoglobulin-like receptors

The key families of receptors used by NK cells are the KIRs, the Ly49 receptors and the CD94/NKG2 receptors. The Ly49 are C-type lectin-like and are crucial to NK cell recognition in the mouse, but appear to be of less importance to NK cell recognition in primates. Humans have one Ly49 gene that is likely to be a pseudogene, although it is expressed in baboons (*Papio hamadryas*) (13). The major NK recognition to function in primates results from expression of *KIR* genes. The *KIR* genes are immunoglobulin superfamily members located in the leukocyte receptor complex (LRC) on human chromosome 19q13.4 that modulate NK cell function upon recognition of MHC class I molecules (Figure 3.5A) (13, 20). KIR molecules are classified into KIR2D and KIR3D groups according to the presence of 2-3 Ig-like domains in their extracellular region. The three extracellular domains of KIR3D are named D0 (membrane-distal), D1 (middle), and D2 (membrane-proximal), and they are encoded by exons 3, 4, and 5, respectively (Figure 1.2). Comparision of cDNA sequences of KIR2D with those of KIR3D shows that the former lack either the region coding for the distal D0 domain or that encoding the middle D1 domain. The first group of KIR2D, with a D1-D2 configuration, comprises the majority of human KIR and called type I KIR2D, whereas the type II group, with a D0-D2 structure, includes KIR2DL4 and the recently identified as KIR2DL5 (24). There are two types of intracellular domain of KIR molecules, one it a long-, another is a short-cytoplasmic tail, for example KIR3DL1/KIR3DS1 as shown in Figure 3.6A. Long-cytoplasmic tail bears ITIMs that permit the transduction of inhibitory signals of KIR molecules. All iNKRs have employed negative regulators bearing ITIMs which mediate recruitment and activation of the intracellular tyrosine phosphatases SRC-homology-2-domain-containing protein tyrosine phosphatase 1 (SHP1) and SHP2 (Figure 3.7) (1). The short-cytoplasmic tail has positive charged arginine amino acid residue in the TM (25). Unlike other activating KIRs, KIR2DL4 locus contains an AGG sequence in TM which codes for a positively charged arginine that facilitate binding to the corresponding negatively charged TM residues of the ITAM-encoding adaptor proteins, such as DAP-12 (Figure 3.6B), which could contribute to the activation. KIR2DL4 molecule also has a functional ITIM in its cytoplasmic tail (4).

A

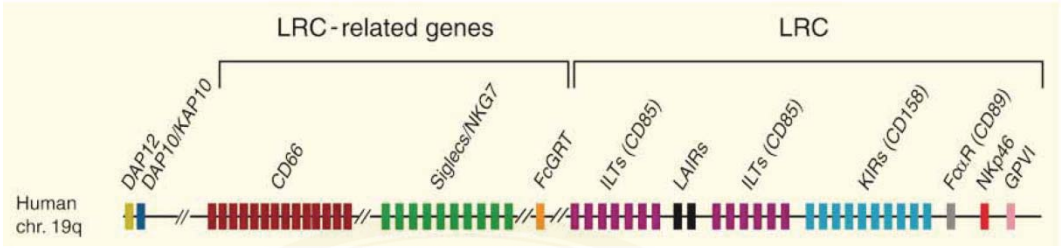

Trowsdale J, et al. Immunol Rev. (2001)

B

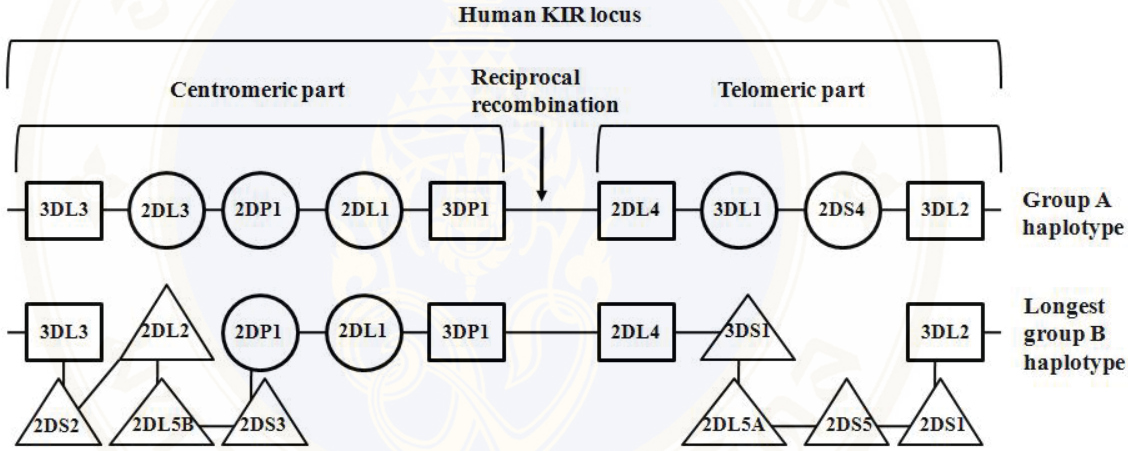

Modified from Parham P, et al. Nat Rev Immunol. (2005)

Figure 3.5. Human KIR genes. KIR loci are located on human chromosome 19q13.4 at the leukocyte receptor complex (A) (26). On KIR loci contain conserved genes (square, ☐) that are in both "group A" and "group B" KIR haplotypes (circle, ○), and genes and/or alleles that are specific to "group B" KIR haplotype (diamond, △) (B) (27).

A

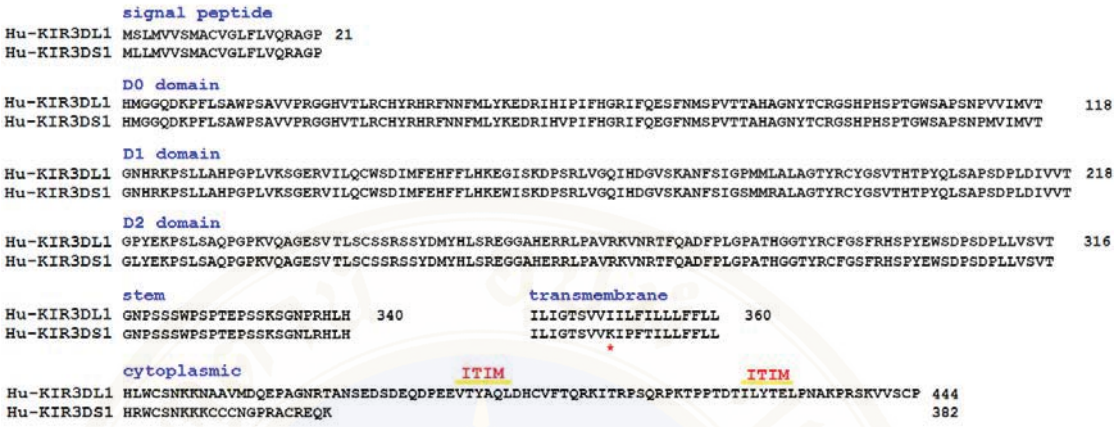

B

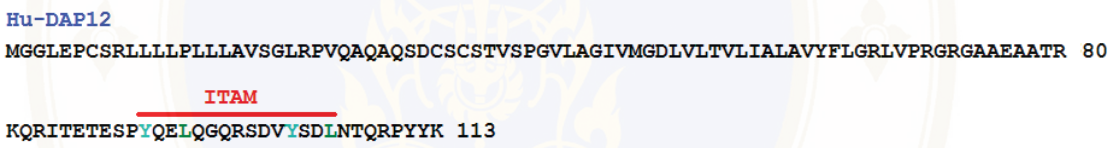

Figure 3.6. ITIM/ITAM motifs. (A) The long cytoplasmic tail of Hu-KIR3DL1 contains the immunoreceptor tyrosine-based inhibitory motifs (ITIMs; protein consensus: S/I/V/L-X-Y-XX-I/V/L). In contrast, Hu-KIR3DS1 molecule is the short cytoplasmic tail because of no ITIM expression, however, this molecule has the lysine (K) in their transmembrane domin (TM) that can bind to DAP-12 (B). DAP-12 molecule contains the immunoreceptor tyrosine-based activation motifs (ITAMs; protein consensus: Y-XX-I/L-$X_{(6–12)}$Y-XX-I/L) that regulate the activating NK cell activity. Modified by using Multiple aligment analysis refer to the numbering of GenBank accession number NP_037421, NP_001077008, AAD09436 for Hu-KIR3DL1, Hu-KIR3DS1, and DAP-12, respectively.

A B

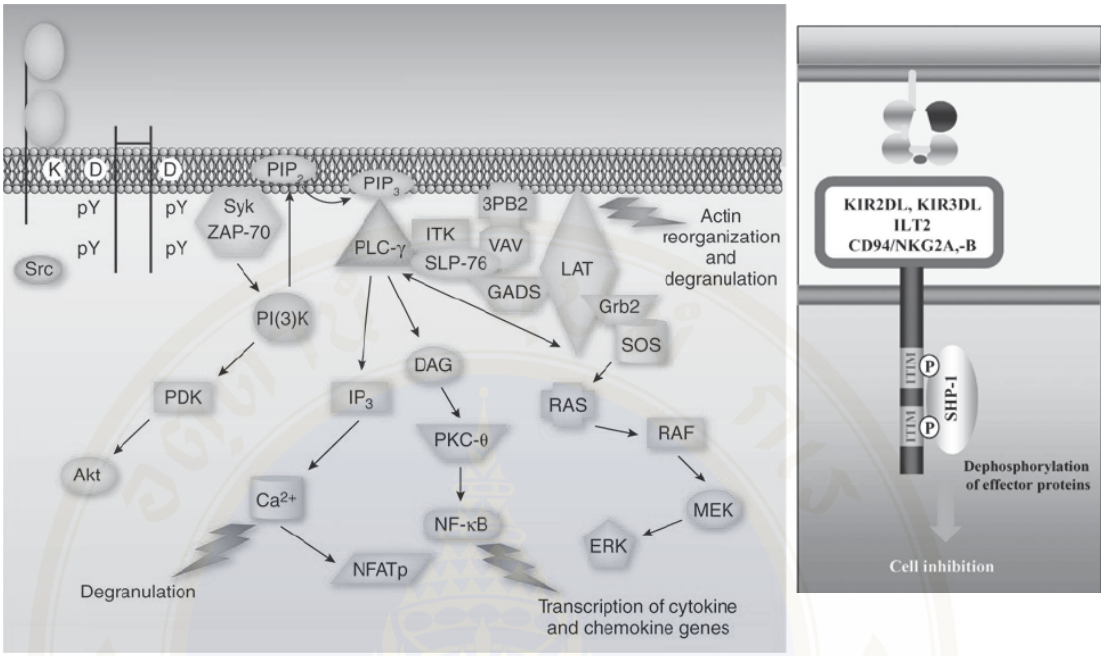

Borrego F, et al. Mol Immunol. (2002)

Figure 3.7. Signal transduction of the activating and the inhibitory KIR molecules on NK cells. After interaction between KIRs and their ligands, signal transduction is occurred either activation or inhibition due to these KIRs which have either short or long cytoplasmic tail. (A) The KIRs which a short cytoplasmic tail have a positive charge lysine (K) or arginine (R) that bind to a negative charge aspartic acid (D) in an adaptor molecule which contains a short cytoplasmic domains containing immunoreceptor tyrosine-based activation motifs (ITAMs). The ITAM-bearing signaling subunits are phosphorylated by Src family kinases that lead to NK cell activation. In contrast, (B) the inhibitory KIRs contain the immunoreceptor tyrosine-based inhibitory motifs (ITIMs) on their cytoplasmic tail (called long cytoplasmic tail) can phosphorylate the SHP-1 molecule that leads to the dephosphorylation of proteins whose phosphorylation is necessary for conveying activating signals, thus result in the inhibition of NK cell activity (28).

3.2.1. The nomenclature of KIRs

The fact that organisms inherit traits via discrete units of inheritance that obtained from their parents which are now called genes (http://www.ncbi.nlm.nih.gov/). Gene is normally a stretch of DNA. The total complement of genes in an organism or cell is known as its genome that includes both the genes (exon) and the non-coding sequences (intron) of the DNA. In addition, pseudogenes are DNA sequences, related to known genes, which have lost their protein-coding ability or no longer expressed in the cell. Pseudogenes arise from retrotransposition or genomic duplication of functional genes that are non-fucntional due to mutations that prevent the transcription of the gene such as within the gene promoter region or fatally alter the translation of the gene such as premature stop codons (29).

Genome projects are scientific endeavours that ultimately aim to determine the complete genome sequence of an organism such as the human genome project was organized to map and to sequence the human genome. The development of new technologies has dramatically decreased the difficulty and cost of sequencing, and the number of complete genome sequences is rising rapidly. Among many genome database sites, the one maintained by the United State National Institutes of Health is inclusive (http://www.ncbi.nlm.nih.gov/sites/entrez?db=Genome&itool=toolbar). Whereas a genome sequence lists the order of every DNA base in a genome, a genome map identifies the landmarks and is less detailed than a genome sequence and aids in navigating around the genome (http://en.wikipedia.org/).

In the fields of genetics and evolutionary computation, a locus is the specific location of a gene on a chromosome. A variant of the DNA sequence at a given locus is called an allele (http://en.wikipedia.org/). Alleles are now understood to be alternative DNA sequences at the same physical locus, which may or may not result in different phenotypic traits. In any particular diploid organism, with two copies of each chromosome, the genotype for each gene comprises the pair of alleles present at that locus, which are the same in homozygotes and different in heterozygotes. A species of organisms typically includes multiple alleles at each locus among various individuals. Allelic variation at a locus is measurable as the number of alleles (polymorphism) present, or the proportion of heterozygotes in the population. A haplotype is a combination of alleles at multiple loci that are transmitted together

on the same chromosome. Haplotype may refer to as few as one locus or to an entire chromosome depending on the number of recombination events that have occurred between a given set of loci.

In a second meaning, haplotype is a set of SNPs on a single chromatid that is statistically associated. It is thought that these associations, and the identification of a few alleles of a haplotype block, can unambiguously identify all other polymorphic sites in its region. Such information is very valuable for investigating the genetics behind common diseases, and has been investigated in the human species by the International HapMap Project (http://en.wikipedia.org/).

The naming of KIR genes is the responsibility of the HUGO Genome Nomenclature Committee (HGNC) based on the structures of the encoded molecules. The first digit following the KIR acronym corresponds to the number of Ig-like domains in the molecule and the 'D' denotes 'domain'. The D is followed by either an 'L' indicating a 'long' cytoplasmic tail, an 'S' indicating a 'short' cytoplasmic tail or a 'P' for pseudogenes. The final digit indicates the number of the gene encoding a protein with this structure. For example, KIR2DL1, KIR2DL2 and KIR2DL3 all encode receptors having two extracellular Ig-like domains and a long cytoplasmic tail (30). In KIR allele nomenclature, it was decided to name KIR allele sequences in an analogous fashion likes HLA alleles. After the gene name, an asterisk is a separator before a numerical allele designation. The first three digits of the numerical designation indicate the alleles that differ in the sequences of their encoded proteins. The next two digits are used to distinguish alleles that only differ by synonymous (non-coding) differences within the coding sequence. The final two digits are used to distinguish alleles that only differ by substitutions in either an intron or promoter or other non-coding region of the sequence. A complete listing of human KIR alleles is assigned official names can be found in website http://www.ebi.ac.uk/.

3.2.2. KIR haplotypes

Human KIR haplotypes are defined in the further diversified through allelic polymorphisms at the individual KIR loci that splited into two basic groups (haplotype 'A' and 'B'), based on gene content, that contain a total of 14 *KIR* genes and 2 pseudogenes (Figure 3.5B). Human *KIR* genes were named according to

convention with the prefix ‘Hu’. A new *Hu-KIR1D* was found but it is still unclear and does not include in haplotypic grouping. The most common haplotype ‘A’ contains two activating *KIR* genes; *Hu-KIR2DL4* and *Hu-KIR2DS4* and five inhibitory *KIR* genes; *Hu-KIR2DL1*, *Hu-KIR2DL3*, *Hu-KIR3DL1*, *Hu-KIR3DL2*, and *Hu-KIR3DL3*. By contrast, the haplotype ‘B’ contains the remaining *KIR* genes that are five activating *KIR* genes (*Hu-KIR2DS1*, *S2*, *S3*, *S5*, and *Hu-KIR3DS1*), two inhibitory *KIR* genes (*Hu-KIR2DL2* and *Hu-KIR2DL5*) and two pseudogenes (*Hu-KIR2DP1* and *Hu-KIR3DP1*) (31). The basic *KIR* gene make-up of ‘A’ and ‘B’ haplotypes, there is also the functional contribution of allelic polymorphisms at each locus to consider (13).

3.2.3. Diversity of KIR genes

The genetic diversity of *KIR* loci differ in the frequency and the amount of KIR expression in the individual subjects. Figure 3.8 illustates a donor ‘A’ has expressed *Hu-KIR3DL1* on only 5% of NK cells while a donor ‘B’ expresses it on 50% of NK cells (32). One factor that contributes to these observations is allelic variation at a locus, for example, the particular alleles of *Hu-KIR3DL1* (*002 and *01502) are expressed in higher amounts on NK cells with high percentage of NK cells within the donors (33). Additionally, KIR gene is a recognized ‘gene-dose’ effect that means if an individual subject has two copies of a gene, it will express in high frequencies when compared to other subjects who have just one copy of a gene (34). Once KIR receptor expression on NK cells has occurred during development, it appears to be a fixed trait within an individual. Both the percentage and level of expression of a given receptor remain stable within an individual over time (32, 35, 36).

3.2.4. Rhesus KIR family

The rhesus macaque (*Macaca mulatta*, often called the rhesus monkey, RM) is one of the best known species of Old World monkeys or *Cercopithecidae*. The species is native to northern India, Bangladesh, Pakistan, Burma, Thailand, Afghanistan, Southern China, and some neighboring areas (http://en.wikipedia.org/). The nonhuman primate animals have been critically important in developing medical

advances that have saved human lives. Work on the genome of RM completed in 2007 has lead RM to the second nonhuman primate model (37).

Like human KIRs, five distinctive subtypes of KIR in RM have been identified. Rhesus *KIR* genes were named according to convention with the prefix 'Mamu'. There are *Mamu-KIR1D, Mamu-KIR2DL4, Mamu-KIR2DL5, Mamu-KIR3DL, and Mamu-KIR3DH* genes based on their structure and homology to *Hu-KIRs* (Figure 3.9) (10).

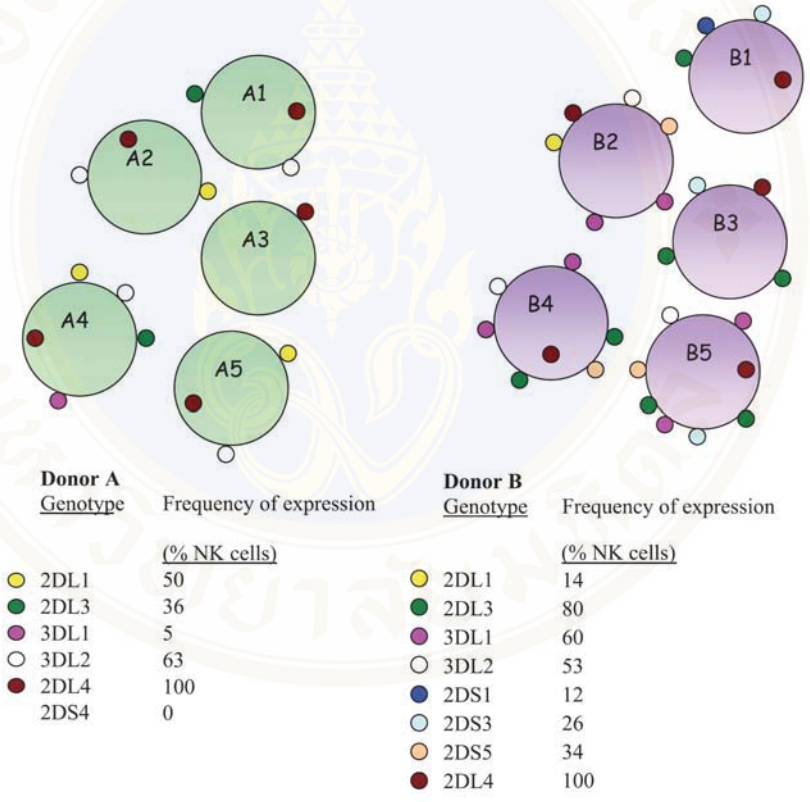

Gardiner CM. Int J Immunogenet. (2008)

Figure 3.8. Diversity of KIR expression. Individual NK cells from donor A (A1–A5) and from donor B (B1–B5) have diverse patterns of KIR expression. Donor A has a KIR haplotype AA. By contrast, donor B has a KIR haplotype AB. The frequency of NK cells expressing any given KIR in the two donors varies e.g. KIR2DL1 is expressed on 50% of NK cells from donor A but is present on only 14% of NK cells from donor B. This results in NK cell subsets co-expressing random combinations of KIR receptors which vary in complexity e.g. in donor A, NK cell A3 expresses only *KIR2DL4* whereas A4 expresses five *KIR* genes (36).

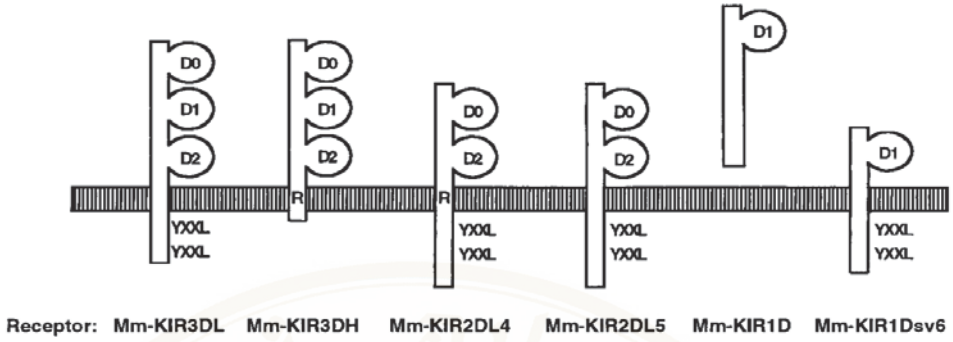

Hershberger KL, et al. J Immunol. (2001)

Figure 3.9. Rhesus monkey killer immunoglobulin-like receptor models. YXXL denotes an ITIM and 'R' indicates an arginine in the transmembrane domain (10).

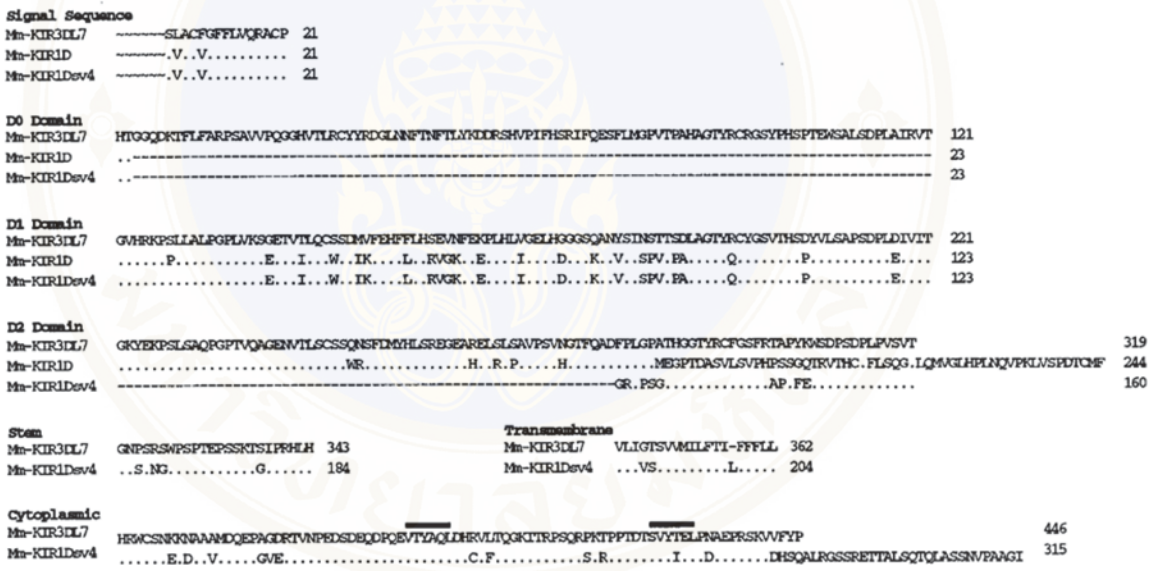

Hershberger KL, et al. J Immunol. (2001)

Figure 3.10. The novel Mamu-KIR1D amino acid sequences. Hershberger *et al* proposed the alignment of the amino acid sequences of *Mamu-KIR1D* and *Mamu-KIR1Dsv4* with *Mamu-KIR3DL7*. Periods (.) indicate identity with *Mamu-KIR3DL7*, dashes (-) indicate absence of amino acids, and tildes (;) indicate amino acids encoded by the PCR primer used to amplify the cDNA. The immunoreceptor tyrosine-based inhibitory motifs (ITIMs) are indicated by bars above the motifs. The amino acid sequence for *Mamu-KIR1D* does not have a recognizable stem, transmembrane, or cytoplasmic domain. *Mamu-KIR1Dsv4* is a splice variant of *Mamu-KIR1D* with a deletion in the D2 domain (10).

Mamu-KIR loci have been shown in some sequence data proposed by Hershberger *et al* (10). *Mamu-KIR1D* nucleotide sequence appears to encode a molecule with signal peptide, D1-Ig domain (some *Mamu-KIR1D* encoding molecules have part of D2-Ig domain, but not full length of this domain), stem, TM and a cytoplasmic tail that is similar in length to *Mamu-KIR2DL4* but their translated protein D1 and first two-thirds of the D2 domain is similar to *Mamu-KIR3DL*. The reason is due to frame shift translation at amino acid residue 55 that leads to the *Mamu-KIR1D* termination at a final length of 244 amino acids. However, *Mamu-KIR1D* has multiple splice variants such as *Mamu-KIR1D* splice variant 4 (*Mamu-KIR1D sv 4*). Interestingly, this variant has a deletion of nucleotide residue 176 in D2 that results in a 2-nucleotide frame shift. The predicted *Mamu-KIR1D sv 4* has the D1 domain, the one-thirds of the end of the D2 domain, stem, TM, and cytoplasmic tail containing ITIMs which similar to *Mamu-KIR3DL7* (Figure 3.10) (10). Although *Mamu-KIR1D* sequences have been published, 11 alleles/splice variants refer to the numbering of GenBank ac. no. AY728181, AF334635 through AF334643, FJ217804, and FJ217805 on NCBI databases, the understanding of genomic expression of *Mamu-KIR1D* locus is still unclear in the topic of genetic polymorphisms of the alleles/variants including the relation between genotypes/ phenotypes and disease's stages because these published sequences were determined in PBMCs isolated from only one or two animal models.

Hershberger *et al* also identified *Mamu-KIR2DL4* gene obtained from cDNA sequences (n = 1) which encode molecules of 84% homology to *Hu-KIR2DL4* by amino acid analysis. The structure of *Mamu-KIR2DL4* consists of signal peptide, D0, D2 domain, stem, TM with 'R' domain, and cytoplasmic tail with ITIMs (10). There are distinct sequence variants that differentiate two subtypes within this family of molecules that are *Mamu-KIR2DL4.1* and *Mamu-KIR2DL4.*2 (ac. no. AF334644 and AF334645, respectively). Interestingly, this frame shift is always associated with two amino acid changes, valine to threonine change (V238T) in the stem and alanine to isoleucine change (A262I) in the TM (10). They were also identified cDNA sequences that encode for *Mamu-KIR2DL5*. This rhesus molecule has ~80% amino acid (aa) identity to Hu-KIR2DL5 molecule. Although the encoding protein of *Mamu-KIR2DL5* contains signal peptide, D0, D2 domain, stem, TM, and cytoplasmic tail

with ITIMs as found in *Mamu-KIR2DL4* but KIR2DL5 molecule lacks arginine residue in the TM. *Mamu-KIR2DL5* locus had been characterized into two alleles that; *Mamu-KIR2DL5.1* and *Mamu-KIR2DL5.2* (ac. no. AF334646 and AF334647, respectively) (38).

Mamu-KIR3DL alleles encode KIR molecules with three Ig-like domains and long cytoplasmic tail as found in human. Members of Mm-KIR3DL family were classified into distinct types based on predicted amino acid sequence homology that Hershberger et al characterized the different alleles by 98% homology. Although only two KIR3DL molecules have been defined in humans, eleven distinct molecules were identified by Hershberger et al criterion in PBMC of five unrelated RMs (10). The Mm-KIR3DL molecules have 74–77% aa identity to Hu-KIR3DL1 and KIR3DL2. However, the cysteines in the D2 and stem domains that are thought to be important for homodimerization of Hu-KIR3DL2 are not present in the Mm-KIR3DL molecules. In addition, the cytoplasmic tails of Mm-KIR3DL molecules are the same length as the cytoplasmic tail of human KIR3DL1.

Mamu-KIR3DH molecules have been designated as a hybrid nature between Mamu-KIR3DL and Mamu-KIR2DL4.2 molecules (10). The scattered nucleotide changes occur in all three of the Ig-like domains that are distinct from any *Mm-KIR3DL* alleles. Although *Mamu-KIR3DH* locus have three Ig domains, portions of the stem/TM/cytoplasmic domains encoded by exon 7 that are similar in sequence to the homologous region of *Mm-KIR2DL4.2*. In particular, the TM of a novel Mamu-KIR3DH molecule includes an arginine as well as the threonine in the stem and isoleucine in the TM that are characteristic of Mm-KIR2DL4.2 molecule (10). Additionally, the nucleotide sequence of *Mamu-KIR3DH* at exon 8 had deletion of 53 nucleotids that led to a frame shift and terminate the molecule after encoding only two further amino acids in cytoplasmic tail. This early termination occurs before the ITIMs seen in the Mm-KIR3DL and Mm-KIR2DL4 molecules (10).

3.2.5. Evolutionary insights of KIR loci in Rhesus macaques

Interestingly, as a consequence of the synergy between these two components of KIR diversity, the likelihood that two unrelated individuals have identical KIR type is less than 0.01. Comparison of ethnic populations among

Australian aboriginals, Africans, Indians, Caucasians, and Japanese shows the divergence and population- specificity in KIR haplotypes and genotypes (39). Evidence for rapid KIR evolution is further reinforced by comparison of the human KIR system with that of other primate species: chimpanzee (*Pan troglodytes*, Pt) (40), bonobo or pygmy chimpanzee (*Pan paniscus*, Pp) (41), gorilla (*Gorilla gorilla*, Gg) (42), orangutan (*Pongo pygmaeus*, Popy) (43), and RM (Figure 3.11) (10). The analysis of complementary deoxyribonucleic acid (cDNA) from chimpanzees identified 10 Pt-KIR molecules that 4 of which have 95% nucleotide identity to their human homologues. Other six of these Pt-KIRs, although more divergent, have the same structural configuration as Hu-KIRs. It is not surprising that all of the Pt-KIRs are similar to the HuKIRs because humans and chimpanzees are very phylogenetically resemble (approximately 6 million year ago, Mya) (10, 40). However, the chimpanzee data have major limitations because the alignable sequences are only 1 to 2% different from that of the human. There is no informative 'signal' to distinguish conserved elements from the overall high background level of conservation. This is exacerbated by the fact that the chimpanzee genome is an incomplete draft, containing sequence errors that could potentially mask true divergence. Additionally, the differences that are found between human and chimpanzee are difficult to assign as specific to either the chimpanzee or the human. The results from chimpanzee model were provided relatively few answers to the fundamental question of the nature of the specific molecular changes that make us human. Thus, RMs exhibit greater similarity to human physiology, neurobiology, and susceptibility to infectious and metabolic diseases (44).

The studies showed that human and RM shared about 93% of their deoxyribonucleic acid (DNA) sequence and shared a common ancestor roughly 25 Mya. The availability of this genome sequence will enable new and better experiments that will speed up the pace of research and reduce the number of animals needed for biomedical research in the long run. There have been several reports that proposed the relationship between human and RM genes-related to immune response. Importantly, the National Human Genome Research Institute (NHGRI), National Institutes of Health (NIH) funds for the sequence characterization of the RM genome

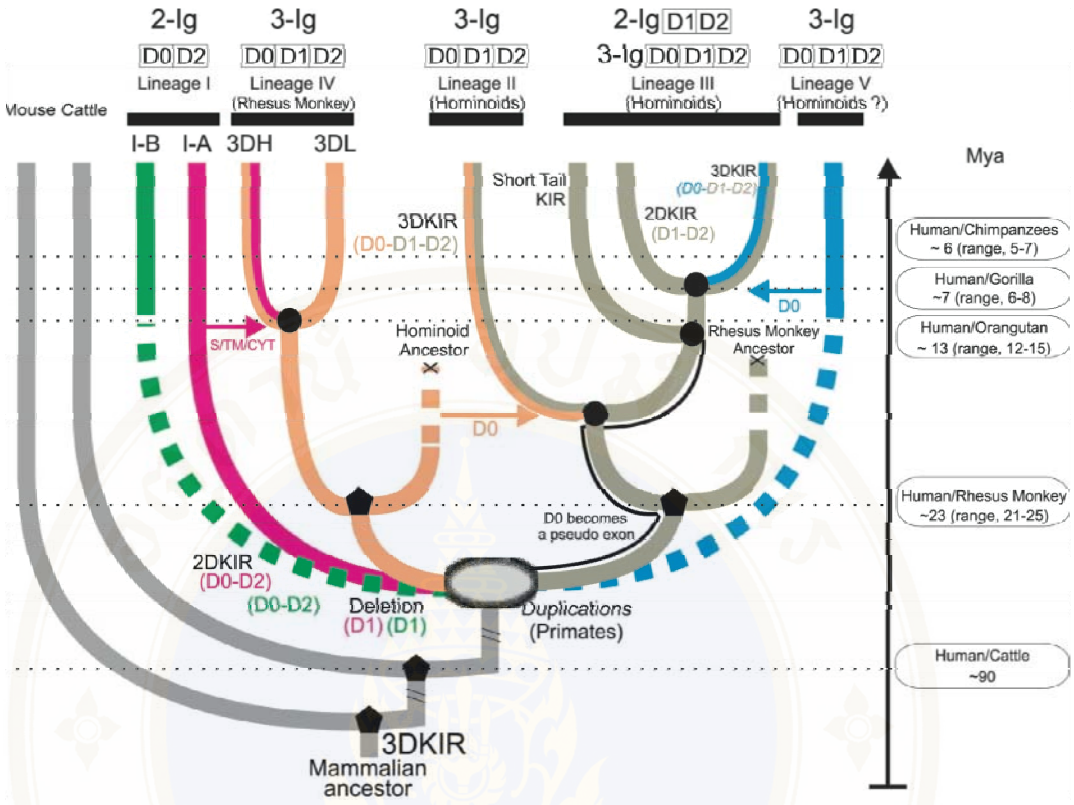

Rajalingam R, et al. J Immunol. (2004)

Figure 3.11. Model for the emergence of the KIR lineages in primates. Rajalingam et al proposed the mammalian KIR lineages that were reconstructed by using the information obtained from the domain-by-domain. Particularly, the reconstruction of the chronology of the events that gave rise to the different KIR structures as well as their relative positions comparing to speciation events are based on the presence/absence of these structures in the different species, and their phylogenetic relationships (42). Six species KIRs are divided into 5 lineages (lineage I to V); lineage I is characterized by KIR genes encoding D0 and D2 domains, lineage II contains genes encoding for 3 Ig-domains with having HLA-A and HLA-B specificity, and lineage III includes KIR genes with either 2- or 3-Ig domains. In humans, lineage III contains different KIR receptors that specific to HLA-C alleles. Lineage IV genes are specific to RM and, finally, lineage V encodes KIR receptors that are lacking the stem region (20). The divergence between the RM-KIR3DL and RM-KIR3DH sequences was roughly estimated based on the stem, transmembrane, and cytoplasmic domain (the S/TM/CYT domain) analysis. Divergence times between the species are indicated on the right side of the figure; the scale is not proportional. These estimations are from Glazko and Nej (45); the divergence time between human and cattle was used as a calibration in their analysis and corresponds to the paleontological data (42).

by using a combined whole genome shotgun plasmid, fosmid and Bacterial Artificial Chromosome (BAC) end sequences methods (44). The RM genome project resources are the followings:

1) The RM global resources from National Center for Biotechnology Information (NCBI) webpage including RM and RM-related resources, taxonomy, map viewer, update news, blasts, and reference sequences (http://www.ncbi.nlm.nih.gov/).
2) The genome center of Washington University focuses on the large scale generation and analysis of DNA sequences (http://genome.wustl.edu/).
3) The RM genome sequencing consortium is led by the Baylor College of Medicine (BCM), Human Genome Sequencing Center (HGSC), and in collaboration with the J. Craig Venter Institute Joint Technology Center, and the Genome Sequencing Center at Washington University, St. Louis (http://www.hgsc.bcm.tmc.edu/).
4) The MamuSNP web site from UC Davis University of California, their tools are including an alignment from a 454 sequence identifier or from the RM chromosome and location and a local copy of primer 3 (http://mamusnp.ucdavis.edu/).
5) The CHORI-250 Rhesus macaque BAC library has been constructed at the Children's Hospital Oakland Research Institute, BACPAC Resources, by Dr. Baoli Zhu using the cloning techniques developed in their laboratory (http://bacpac.chori.org/).
6) Pooled Genomic Indexing (PGI) is a method for mapping collections of BAC clones across species using a combination of clone pooling and DNA sequencing. PGI has been used to map a total of 16,495 unique RM-BAC clones. This project is done in collaboration with the Baylor HGSC (http://brl.bcm.tmc.edu/).

Critical progress in biomedicine attributed to RM includes the identification of the "rhesus factor" blood groups and advances in neuroanatomy and neurophysiology. Most importantly, their response to infectious agents related to human pathogens, including SIV and influenza, has made RM the preferred model for vaccine development (44). The polymorphism, genomic organization, and alternative

messenger ribonucleic acid (mRNA) splicing of KIR molecules have been characterized by using rhesus cDNA sequences. The number of KIR genes varies among individuals, and additional KIR genotypic diversity occurs due to allelic polymorphisms (2, 10). However, there is a few report on completely rhesus KIR sequences, as described at above, and genomic loci coding for these receptors are localized on rhesus chromosome 19 (46). Additionally, the sequence data available for *Mamu-KIR* genes obtained from healthy individual animals and therefore do not compile a database large enough to identify sequence patterns or alleles. Moreover, the expression of KIR molecules have been changed to be associated with disease severity in SIV infection (2).

3.3. Effect of HIV/SIV viremia on NK cells

HIV and SIV are obligate parasites in genus *Lentivirus*, family *Retroviridae*. The most common route of HIV infection is across mucosal barriers as a result of sexual exposure. The first infected cells detected in the resting memory $CD4^+$T cells of humans and monkeys at day 3 or 4 in the mucosa after infection. In the mucosal lymph nodes, virus interacts with the tissue dendritic cells and the Langerhans cells, and then, these cells carry virus on their surface to lymph nodes within a week after infection. The production of virus is increased in draining lymph nodes where dendritic cells and perhaps monocytes interact with viral antigen-specific $CD4^+$T cells resulting in amplification of infection through $CD4^+$T cells. At the same time, virus spreads to gut-associated lymphoid tissue that resulting in an increased viral infection into the effector memory $CD4^+$T cells and their rapid depletion coincides with peak plasma viral production around 21 days post-infection (47).

The natural SIV infection of African nonhuman primates is asymptomatic and usually does not induce significant T cell depletion despite high levels of viral replication (47). While the exact mechanisms by which natural SIV hosts remain healthy are still relatively poorly understood, a number of key observations have been made over the past few years that have clarified several important immunological and virological aspects of these infections. The phases of infection are divided into acute and chronic infection; in acute infection, the phase is characterized by a peak of viral replication occurring between one and two weeks post-inoculation. This peak is

followed by a relatively rapid decline to levels ranging around $10^5 – 10^7$ viral copies per ml. While set-point viremia in SIVmac239- or SIVmac251-infected RMs is usually higher than in sooty mangabeys (SM, a paradigmatic model of natural SIV infection) (48), relatively lower levels of viremia are observed in RMs infected with uncloned SIVsmm who can still progress to AIDS. In addition, several studies have shown that there is no tendency to develop AIDS even in the SMs with highest VL. Interestingly, in both SMs and RMs the transition from the acute to the chronic phase of infection results in a steady state of viral replication and $CD4^+$T cell homeostasis, however, $CD4^+$T cell counts are progressively decline overtime in the vast majority of RMs but only in a small minority of SMs (48). In human and RM, the fraction of $CCR5^+CD4^+$T cells is approximately 10-20% in blood and >50% in mucosal tissue (49). The effect of $CD8^+$T cell depletion seems to be more dramatic in RMs, however, the mechanisms by which $CD8^+$T cell depletion is followed by increased VL are complex and not well understood. Interestingly, the level of SIV-specific $CD8^+$T cell responses in RMs was measured by using intracellular cytokine staining in response to *ex vivo* stimulation with SIV peptide appears to be lower than in HIV-1-infected humans (50).

HIV is known to down-regulate HLA class I expression and thus would indeed be expected to mark infected cells for NK cell lysis. However, it became clear that the virus could down-regulate HLA-A and B while sparing HLA-C, thus helping to evade NK cell recognition (Figure 3.12) (13). However, several studies on the effects of virus to the expression of both NK cell receptors and their ligands remain largely unknown. Interestingly, there have been several articles investigated the different viral types and their strains of disease's stages, drug treatments, and genetic individuals that could affect NK cell functions. More recent studies demonstrated the association between HIV-1 disease's progression and KIR expression on NK cells including their putative ligands (Figure 3.13) (1, 2, 8, 9, 16, 18, 31). The genetic differences within species play an important role in viral infection and regulating disease severity. There have been several reports that proposed HLA/MHC class I alleles linked to delayed or rapid disease progression in HIV/SIV infection via two mainly mechanisms of MHC class I system that control viral replication. First, viral peptide-binding-HLA class I molecule present viral antigen to cytotoxic T cells

(CTLs) and generate their responsibility. Second, the interaction between MHC class I molecule and KIR receptor play a role in the NK-mediated activity (47). Subsequently, MHC class I alleles including *Mamu-A.01, Mamu-B.01, Mamu-B.08* and *Mamu-B.17* are associated with slow disease progression in SIV-infected RMs (51).

Martin *et al* reported that the activation of *Hu-KIR3DS1*, in combination with *HLA-B Bw4* allotypes presenting an isoleucine (I) at position 80 (*HLA-B Bw4*80I*), is associated with delayed progression to AIDS in patients with HIV-1 infection (7). In contrast, the various distinct allelic combinations of the *Hu-KIR3DL1* and *HLA-B Bw4*80I* that showed a significant and strong influence on both AIDS progression and plasma VL in a consistent manner (9). The hallmark of the relationship between KIR genetic individuals and disease's stages, has been shown by Alter et al, who proposed that the elevated activating or inhibitory KIR expression on NK cells were related to HIV-1 infection at acute and chronic phases (8). The results showed 32-fold higher in *Hu-KIR3DS1* levels from acute HIV-1 infected patients with *HLA-B Bw4*80I* positive individuals compared to HIV-1 serotype negative individuals with *HLA-B Bw4*80I* positive (p = 0.01). Moreover, there was a trend towards increased levels of *Hu-KIR3DL1* transcript levels in acutely infected individuals that encoded for at least one copy of *HLA-B Bw4*80I* compared to *HLA-B Bw6* positive individuals (KIR3DL1 mRNA levels were 6-fold higher in *HLA-B Bw4*80I* positive individuals, p = 0.07, and *Hu-KIR3DL1* transcript levels were 5-fold higher in *HLA-B Bw4*80I* positive with acute infection to *HLA-B Bw4*80I* positive HIV-1 negative controls). Both *Hu-KIR3DS1* and *Hu-KIR3DL1* expression were different in chronic HIV-1 infected patients with *HLA-B Bw4*80I* positive individuals when compared to acutely infected individuals. The expression of *Hu-KIR3DS1* locus in chronic infected individuals with *HLA-B Bw4*80I* was higher than patients with *HLA-B Bw6* but was lower than HIV-1 negative individuals. In contrast, *Hu-KIR3DL1* expression was substantially increased in chronically infected subjects with *HLA-B Bw4*80I* when compared with acutely infected individuals and HIV-1 negative individuals (8). This argued that carrying an 'activatory' NK cell programme was beneficial in limiting disease (13). Bostik *et al* investigated the *Mamu-KIR3DL* allelic and genetic relationship between fast progressive and LTNP SIV-infected

RMs. They found new 14 alleles and a variant of *Mamu-KIR3DL* locus in their cohort. Twelve alleles including their variant had the expression of histidine (H) at amino acid residue 159 while allele-13 and allele-14 had glutamine (Q) at the same position. It is important to note that they found that higher frequency of *Mamu-KIR3DL* allele-13 and 14 were associated with animals that exhibited high plasma VL. This data for the first time defined multiple alleles of *Mamu-KIR3DL* and showed association between virus control, NK cell function and genetic polymorphisms of KIR receptors (2).

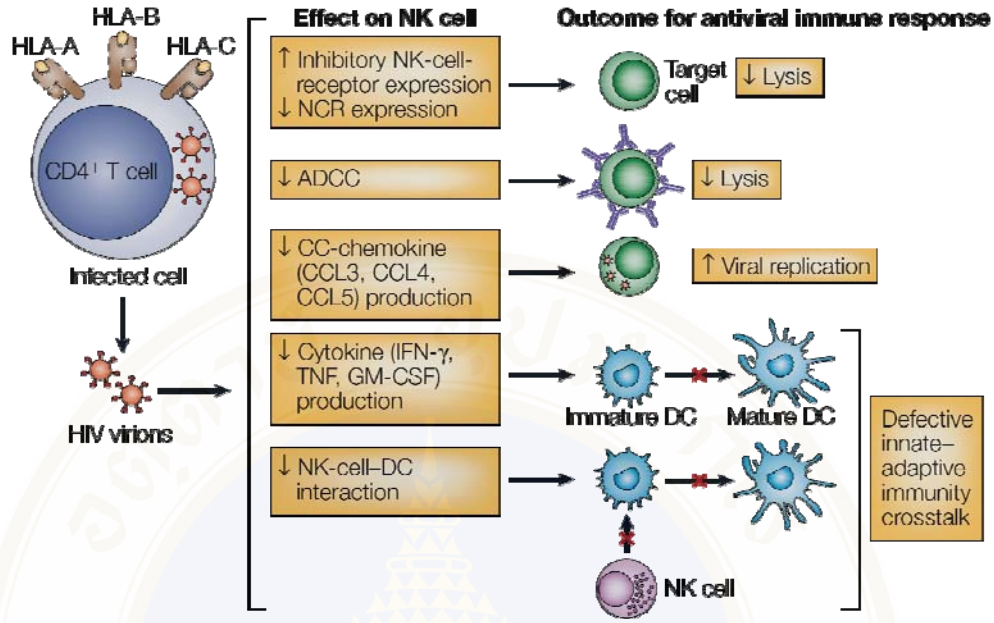

Fauci AS, et al. Nat Rev Immunol. (2005)

Figure 3.12. Effect of HIV viremia on NK-cell function. HIV viremia influences interactions of NK cells and other immune effector cells that are important for the initiation and maintenance of immune responses. Viruses reduce the expression of natural cytotoxicity receptors (NCRs) at the surface of NK cells while they increase the expression of inhibitory NK-cell receptors (iNKRs). The net result of this dichotomous effect on NK cell receptor expression is a reduced ability to lyse infected cells. HIV also inhibits the secretion of CC-chemokines by NK cells, which reduces the ability of NK cells to suppress HIV entry by blocking CC-chemokine-receptor binding of HIV. The secretion of pro-inflammatory cytokines such as interferon-γ (IFN-γ) and tumournecrosis factor (TNF) and granulocyte/macrophage colony-stimulating factor (GM-CSF) by NK cells are also reduced. This impairs the interaction of NK cells with other cellular components of the adaptive immune system, including dendritic cells (DCs). HIV-envelope-specific antibody-dependent cell-mediated cytotoxicity (ADCC) is impaired in HIV-infected individuals at later stages of disease (1).

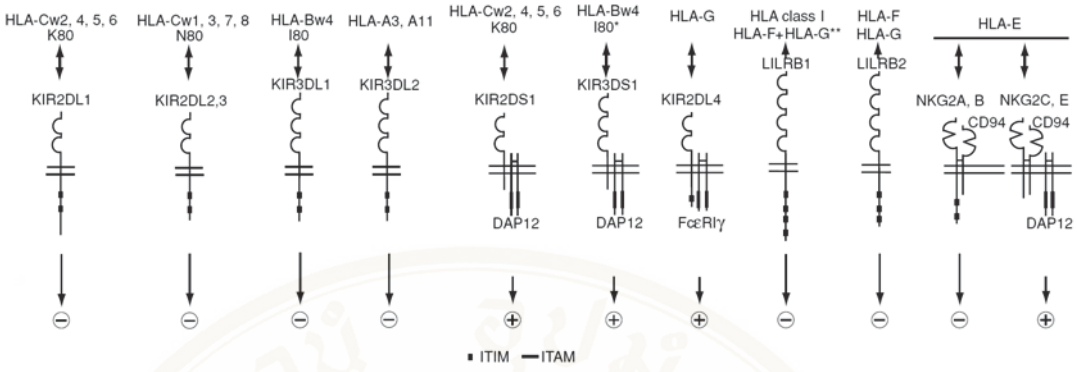

Biassoni R. Curr Protoc Immunol. (2009)

Figure 3.13. Human KIR receptors and their ligands. Human *KIR* alleles specifically interact with amino acid residues present in the α1 domain of the MHC heavy chain. KIR2DS1/KIR2DS1 receptors recognize HLA-Cw4 and other HLA-C molecules sharing lysine (K) 80;KIR2DS2/3 is specific for HLA-Cw3 and related molecules sharing asparagine (N) 80; KIR3DL1 and KIR3DL2 bind to HLA-Bw4 (I: isoleucine-80) of HLA-A3-A11, respectively.The unique exception is KIR2DL4. Although it is characterized by a single immunoreceptor tyrosine-based inhibitory motif (ITIM), it transduces activating signals by associating with immunoreceptor tyrosine-based activating motif bearing signal transducing FcεRIγ molecules. KIR2DL4 is specific for the HLA-G. Some LILR molecules display specificity for HLA-G, HLA-F, and inhibitory functions. Finally, CD94/NKG2A-B and CD94/NKG2C-E belong to the C-type lectin family of receptors and display HLA-E specificity or transduce inhibitory and activating signals, respectively. The minus sign (−) indicates that the receptor transduces inhibitory signaling, while the plus sign (+) indicates that the receptor transduces activating signaling (20).

CHAPTER IV
MATERIALS AND METHODS

4.1. Experimental animals

The heparinized peripheral blood samples were obtained from 38 SIV-infected RMs (*Macaca mulatta*) that were divided into two groups: high viral load (RM-HVL cohort, > 10^6 viral copies/ml of plasma, n = 20) and low viral load (RM-LVL cohort, < 10^4 viral copies/ml of plasma, n = 18). All animals were housed at the Yerkes Regional Primate Research Center of Emory University and were maintained according to the guidelines of the Committee on the Care and Use of Laboratory Animals of the Institute of Laboratory Animal Resources, National Research Council and the Health and Human Services guidelines Guide for the Care and Use of Laboratory Animals. MHC class I (Mamu) typing for *Mamu-A.01, -B.01, -B.08,* and *-B.17* was performed as described in Bostik *et al* (2). Some animals in cohort had PMPA treatmented as shown in Table A.1. in the section of Appendix. The antiviral drug treatement was not interfere to the genetic variations of *KIR* gene (11, 12).

4.2. Natural killer cell isolation

Peripheral blood mononuclear cells (PBMCs) were isolated from heparinized blood in individual animals by using Ficoll-hypaque density gradient centrifugation technique and were storage in liquid nitrogen. The frozen PBMCs were gently thawed and purified NK cells were obtained by using CELLection™ Pan Mouse IgG Kit, Invitrogen Corporation, CA, USA (catalog number (cat. #) 115.31D). Briefly, pelleted PBMCs (1×10^7 cells/ml) were resuspended in 10% fetal calf serum (FCS) in RPMI 1640 media (Gibco/Invitrogen Corporation, CA, USA) and were incubated with mouse anti-RM CD3 antibody (clone FN-18, Invitrogen Corporation, CA, USA) at a final concentration of 10 μg/ml, at the incubation time for 15 min in cold room on a shaker. Then, labeled cells were washed twice with phosphate buffered saline (PBS, pH 7.4, Gibco/Invitrogen Corporation, CA, USA) and were

resuspended with 0.1% bovine serum albumin (BSA) in PBS at a final concentration of 1×10^7 cells/ml. After that, the cells were added with CELLection Pan mouse IgG (anti-mouse IgG antibody) conjugated with magnetic beads at a final concentration of 1×10^7 beads/ml and then, the tubes were inverted in a couple of times to mix. Subsequently, cells were incubated with magnetic beads on the shaker in the cold room for 30 min. After that, the tubes containing cells and magnetic beads were placed on the magnet for 5 min at room temperature (RT, 20-25°C) and CD3 negative cells in supernatant were transfered into a new tube. Cells were washed with 0.1% BSA in PBS and were resuspended with a same buffer at a final concentration of 1×10^7 cells/ml. Mouse anti-RM NKG2A (CD159a) antibody (clone Z199, Beckman Coulter, Inc., CA, USA) (final concentration 10 μg/ml) was added into the sample and was incubated in cold room on the shaker for 15 min. After washing the cells with 0.1% BSA in PBS, cells were incubated with CELLection Pan mouse IgG conjugated with magnetic beads at a final concentration of 1×10^7 beads/ml on a gently shaker in the cold room for 30 min. NK cells were collected by placing the tube on the magnet and the supernatant was removed. NK cells conjugated with magnetic beads were incubated in Release buffer for 15 min at the RT on the shaker and the purified NK cells were finally harvested. Cells were kept either in 10% FCS in RPMI 1640 at 4°C for 1 week or at -20°C for 1 month.

4.3. Purification of total ribonucleic acid from animal cells

RNeasy® Mini Kit (Qiagen, CA, USA) (cat. # 74104) was used for ribonucleic acid (RNA) extraction in this study. Briefly, the equal volume of 70% ethanol was added into a tube containing lyzed cells in lysis buffer. Then, the lyzated solution was added into RNeasy spin column placed in a 2-ml-collection tube. After centrifugation (8,000 ×g for 15 sec), solution in a collection tube was discarded. RNA in column was washed with washing buffer and was eluted with RNase-free-water. The RNA concentration (μg/μl) was determined by using spectrophotometer (GeneQuant pro UV/Vis spectrophotometer, Biochrom Ltd, IN, USA) at a wavelength of 260 nm. One milliliter of solution with an A260 of 1 absorbance unit contains 40 μg of RNA. RNA should have an A260/A280 minimum ratio of 1.7 or higher. It is

very important to avoid exogenous ribonuclease contamination during the preparation, storage and handling of the RNA samples before cDNA synthesis.

4.4. Complementary deoxyribonucleic acid synthesis

Protoscript® First Strand cDNA Synthesis Kit (New Englang Biolabs Inc., MA, USA) (cat. # E6500L) is an easy technique to convert RNA to cDNA and get high amounts of cDNA. RNA samples reacted with 'Master mix 1' (Table 4.1) in a 0.5 ml microtube at 70°C for 5 min, 50 μl of mineral oil was overlay on the top of reaction. After that, 'Master mix 2' (Table 4.2) was added into the mixture and was incubated at 42°C for 1 h. The enzymes were inactivated at 95°C for 5 min. Then, the mixture was added with 1 μl (2 units) of RNase H and was incubated at 37°C for 20 min to degrade the RNA. Re-heat the mixture at 95°C for 5 min to enzyme inactivation. After that, cool down cDNA products were cooled down at 4°C and storaged at -20°C.

Table 4.1. Master mix 1 for complementary deoxyribonucleic acid synthesis.

Components	Volume /Reaction
1. Total RNA	5 μl (final conc. 1 ng- 2 μg)
2. Random Primer	2 μl
3. dNTPs mix	4 μl
4. Nuclease-free-water to a total volume of 16 μl	

Table 4.2. Master mix 2 for complementary deoxyribonucleic acid synthesis.

Components	Volume/Reaction
1. Mixture from Table M1	16 μl
2. 10× RT buffer	2 μl
3. RNase inhibitor	1 μl
4. M-MuLV reverse transcriptase	1 μl
Final volume	20 μl

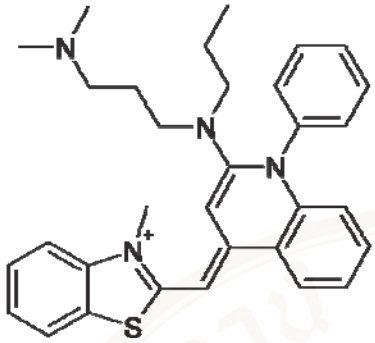

Figure 4.1. SYBR Green I.
Chemical structure of SYBR Green I dye.
(http://en.wikipedia.org/wiki/SYBR_Green)

4.5. Real time polymerase chain reaction

All cDNA samples were determined for their glyceraldehyde 3-phosphate dehydrogenase (GAPDH, housekeeping gene) with GAPDHKF1-GAPDHKR primer pair (Table 4.3) as measured by iQ™ SYBR® Green Supermix (Bio-Rad Laboratories, CA, USA, cat. # 170-8882) (Figure 4.1). Components in Table 4.4 were mixed in a 96 well-plate and were covered with plastic sticker before heated on iCycler Q5 qcPCR (Bio-Rad Laboratories, CA, USA). After real time polymerase chain reaction (qcPCR) step as show in Table 4.5, PCR quantification was analyzed by iCycler Q5 qcPCR. PCR products were determined by 1% agarose-ethidium bromide gel electrophoresis and were visualized and photographed by a long-wavelength UV lamp (Epi Chemi II Darkroom, UVP BioImaging System, UVP Inc., CA, USA). The 1 Kb plus DNA Ladder (Invitrogen Corporation, CA, USA) was used for markers.

Table 4.3. Primer pairs.

Primer name	Direction	Sequence 5' to 3'	length (bp)	Tm (°C)	%GC content
***GAPDH* gene:**					
GAPDHKF1	Forward	GCACCACCAACTGCTTAGCAC	21	56.57	57.14
GAPDHKR	Reverse	TCTTCTGGGTGGCAGTGATG	20	53.80	55.00
***KIR1D* gene:**					
KIR1DFL	Forward	TCATGGTCGTTAGCGTGGCGTGTG	24	67.98	58.33
KIR1DR	Reverse	CCTGCTGCTGGTACATTGGAACTG	24	66.28	54.17
***KIR2DL4* gene:**					
The extracellular domain					
KIR2DL4PSF7	Forward	CTGGCCTGTCTTGGGTTCTTCT	22	64.54	54.55
KIR2DL4PSR12	Reverse	GGTCCATTACAGCAGCATTCTT	22	60.81	45.45
The intracellular domain:					
KIR2D4FL	Forward	CAGTTCCCGGCGCTCCTTTGAC	22	68.26	63.64
KIR2DL4RL1	Reverse	CTAAGCAAAGGAGTGCGTTTTC	22	60.81	45.50
***KIR2DL5* gene:**					
KIR2D5FL2	Forward	ATGGCATGTGTTGGGTTCTTCTTG	24	66.35	45.83
KIR2D5RL1	Reverse	GCAGAGTCGCGCCTTCAGATTCCT	24	67.98	58.30

Table 4.4. Reaction set up for iQ™ SYBR® Green Supermix.

Components	Volume/Reaction	Final concentration
1. 2× iQ SYBR Green Supermix*	10 µl	1 ×
2. Forward Primer	1 µl	100 – 500 nM
3. Reverse Primer	1 µl	100 – 500 nM
4. Nuclease-free water	7 µl	
5. cDNA template	1 µl	
Final volume	20 µl	

*2× iQ SYBR Green Supermix containing 100 mM KCl, 40 mM Tris-HCI, pH 8.4, 0.4 mM of each dNTP (dATP, dCTP, dGTP, and dTTP), 50 units/ml iTaq DNA polymerase, 6 mM $MgCl_2$, SYBR Green I, 20 nM fluoresein, and stabilizers.

Table 4.5. Real time PCR cycles.

Cycle 1:	(1×)		
	Step 1:	95 °C	for 3 min
Cycle 2:	(45×)		
	Step 1:	95 °C	for 20 sec
	Step 2:	50-60 °C	for 20 sec
	When Row; A = 60.0ºC; B = 59.3ºC; C = 58.1ºC; D = 56.2ºC; E = 53.7ºC; F: 52.0ºC; G = 50.8ºC; and H = 50.0ºC.		
	Step 3:	60 °C	for 50 sec
	Data collection and real-time analysis enabled.		
Cycle 3:	(1×)		
	Step 1:	95 °C	for 1 min
Cycle 4:	(1×)		
	Step 1:	52 °C	for 1 min
Cycle 5:	(80×)		
	Step 1:	55 °C	for 10 sec
	Increase setpoint temperature after cycle 2 by 0.5ºC.		

Table 4.6. PCR reaction.

Components	**Volume/Reaction**
1. 10× GoTaq® Flexi Buffer	5.00 µl
2. $MgCl_2$ (25 mM)	5.00 µl
3. dNTPs (4 mM)	10.00 µl
4. Forward Primer (5 µM)	1.00 µl
5. Reverse Primer (5 µM)	1.00 µl
6. GoTaq® DNA polymerase (5 units/µl)	0.25 µl
7. DNA template	2.00 µl
8. Nuclease-free water	25.75 µl
Final volume	50.00 µl

4.6. Polymerase chain reaction amplification

The cDNA samples were amplified for *Mamu-KIR1D*, *Mamu-KIR2DL4*, and *Mamu-KIR2DL5* by using the specific primer as described in Table 4.3 (Operon Biotechnologies, Inc., Huntsville, AL, USA). The primers were designed to amplify the full-length of the *Mamu-KIR1D* from the signal sequence to the complete cytoplasmic tail (~1,100 base pair (bp)). The predicted *Mamu-KIR1D* amplification is in a coding region from nucleotide 8 to 1,117 (amino acid residues 4 to 365) based on the numbering used in GenBank for *Mamu-KIR1D* mRNA, ac. no. AY728181. Amplification of 2 μl of cDNA were performed in 50 μl of PCR reaction containing 1× PCR buffer, 2.5 mM of $MgCl_2$, 0.2 mM of each dNTPs, 5 mM of each primer, and 2.5 U of Gotaq Polymerase (Promega, Madison, WI, USA) (Table 4.6). PCR cycling conditions were as follows: the initial denaturation at 95°C for 5 min followed by 40 cycles of denaturation at 95°C for 30s, annealing at 58°C for 30s, extension at 72°C for 60s, and final extension at 72°C for 10 min.

For *Mamu-KIR2DL4* gene, KIR2DL4PSF7-KIR2DL4PSR12 primer pair was used to amplify *Mamu-KIR2DL4* that covered the signal peptide, D0, D2 domains, stem, TM and part of cytoplasmic tail (802 bp) based on GenBank ac. no. AY728182 and that amplified nucleotide at position 23 to 824 (amino acid residues 8 to 275). The PCR reaction of this primer pair were used as described in *Mamu-KIR1D* amplification (Table 4.6), and then, the cycling conditions were performed as follows: the initial denaturation at 95°C for 5 min, followed by 40 cycles of denaturation at 95°C for 30s, annealing at 56°C for 30s, extension at 72°C for 60s, and final extension at 72°C for 10 min. Additional *Mamu-KIR2DL4* tail sequences were amplified by using KIR2D4FL-KIR2DL4RL1 primer pair. The predicted PCR size is approximately ~819 bp with a coding region from nucleotide 433 to 1252 (amino acid residues 145 to 416) based on the numbering used in GeneBank for *Mamu-KIR2DL4* (ac. no. AY728182). PCR reaction and cycling were performed as described for *Mamu-KIR1D* amplification (Table 4.6).

For *Mamu-KIR2DL5* gene, *Mamu-KIR2DL5* gene was amplified by using KIR2D5FL2-KIR2D5RL1 primer pair (~ 1,279 bp). The predicted PCR product is in the coding region from nucleotide 13 to 1,279 (amino acid residues 5 to 426) based on

GenBank ac. no. AF334646 and AF334647. Amplification of 2 μl of cDNA were performed in 50 μl of PCR reaction containing 1× PCR buffer, 1.5 mM of $MgCl_2$, 0.2 mM of each dNTPs, 5 mM of each primer, and 2.5 U of Gotaq Polymerase (Promega, Madison, WI, USA). PCR cycling was performed as described for *Mamu-KIR2DL4* extracellular domain amplification.

All PCR reactions were overlaid with 50 μl of mineral oil and were amplified by using Perkin-Elmer Cetus DNA thermal cycler (Perkin-Elmer, Fremont, CA, USA). PCR products were determined by 1% agarose-ethidium bromide gel electrophoresis and were visualized and photographed by a long-wavelength UV lamp (Epi Chemi II Darkroom, UVP BioImaging System, UVP Inc., CA, USA). The 1 Kb plus DNA Ladder (Invitrogen Corporation, CA, USA) was used for markers.

4.7. DNA purification by using Wizard® SV gel and PCR clean-up system

Target DNA band was cut under UV visualization. After that, the gel slice was transferred into a new 1.5 ml microtube with known the weight of the empty tube. The tube containing the gel slice had to record for a new weight and calculated the corrected weight of the gel slice (this gel may be stored at 4°C or at -20 °C for up to a week in a tightly closed tube under nuclease-free condition before purification). The membrane binding buffer solution was added into the gel slice at a ratio of 10 μl of solution per 10 mg of agarose gel slice. After mixing by vortex, the sliced gel mixture was incubated at 50-65 °C for 10 min or until the gel slice was completely dissolved. Samples were transferred into SV minicolumn placed on a collection tube. Then, samples were incubated at RT for 1 min. Next, the samples were centrifuged at 16,000 × g for 1 min. Solution in a collection tube was discarded, after that, the SV column was returned to the collection tube. The column was washed by using 700 μl of membrane washing solution and centrifuged at 16,000 × g for 1 min. The washing step was repeated once (in this step, we used 500 μl of membrane washing solution). After that the column was placed on a new 1.5 ml microtube. DNA was eluted by using 50 μl of nuclease-free water and centrifuged at 16,000 × g for 1 min. DNA in a 1.5 ml microtube was kept at -20 °C.

4.8. Ligation between DNA target and pGEM®-T vector

The pGEM®-T vector (Promega, Madison, WI, USA, Figure 4.2) was used as a convenient system for the cloning of PCR products. Briefly, DNA product was added into ligation reaction contained in the 0.5 ml microtube (Table 4.7). The reactions were mixed by pipetting. Then, the reactions were incubated at RT for an hour or at 4°C for overnight (~14-16 hours).

A B

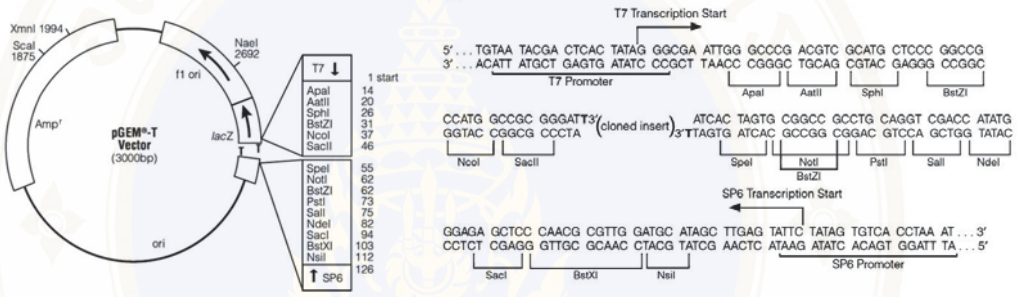

Figure 4.2. pGEM® T-vector. The vector circle map and sequence reference points (A). The promoter and multiple cloning sequence of the pGEM®-T vector (B). The top strand of the sequence shown corresponds to the RNA synthesized by T7 RNA polymerase. The bottom strand corresponds to the RNA synthesized by SP6 RNA polymerase (Promega, Madison, WI, USA).

Table 4.7. Ligation reaction.

Components	Volume/Reaction
1. 2× Rapid Ligation Buffe	5 µl
2. pGEM®-T vector (50 ng)	1 µl
3. PCR product	1 µl
4. T4 DNA Ligase (3 Weiss units/µl)	1 µl
5. Deionized water	2 µl
Final volume	10 µl

4.9. Transformation of inserted plasmid into JM109 competent cells

In the steps of transformation, 2 μl of each ligation reaction were added into a sterile 1.5 ml microtube, then, 50 μl of JM109 cells were added. Gently flicked the tubes to mix and then, placed the transformation cells on ice for 20 min. After that, heat-shock the cells for 45 sec in a water bath at exactly 42°C. Immediately returned the tubes to ice for 2 min and added 950 μl of LB medium into the tubes. Then, the transformation cells were incubated at 37°C for 1.5 h in incubator with shaking (~150 rpm). After the incubation time, 100 μl of transformation culture were placed onto duplicate LB plate containing 100 μg/ml of ampicillin, 0.5 mM of IPTG, and 80 μg/ml of X-Gal. The plates were incubated overnight at 37°C. White colonies were generally inserted target gene into host cells. In contrast, the blue colonies did not contain interested gene in the host cells. A single white colony was picked and inoculated into 3 ml of LB broth containing antibiotics. After that, the cells were incubated at 37°C for overnight. Cells were harvested by centrifugation at 10,000 × g for 5 min in RT. Pelleted cells were used in the step of plasmid purification. The bacterial cells were kept at 4°C for 1 week before pelleted cell collection.

4.10. Purification of plasmid by using Wizard® plus SV Minipreps DNA purification system

Bacterial culture from transformation step were harvested by centrifugation at 10,000×g for 5 min. Pelleted cells were lyzed by adding 250 μl of cell resuspension solution and then adding equal volume of cell lysis solution. After inverting, 10 μl of alkaline protease solution were added in the mixture and incubated at RT for 5 min. Then, mixture was added by 350 μl of neutralization solution and centrifugation at 14,000×g for 10 min. Supernatant solution was transferred into column placed on a 2 ml-collection tube and was centrifuged at 14,000×g for 1 min. After removal of solution in flow-through, 750 μl of column washing solution were added into the column and centrifuged at 14,000×g for 1 min. The washing step was repeated again by added 500 μl of column wash solution and centrifuged at 14,000×g for 5 min. All of the washing solutions were removed by centrifugation at 14,000×g

for 1 min. Then, the column was placed on a new 1.5 ml-microtube and was added 100 μl of nuclease-free water for elution. DNA was stored at -20°C.

4.11. DNA sequencing

DNA sequence obtained from each purified plasmid sample were analyzed and sequenced by using T7 and SP6 primers (Promega, Madison, WI, USA) and using the genomic solutions sequencing services (Agencourt Bioscience Corporation, Beverly, MA, USA). Sequences were analyzed by using the DNASTAR Lasergene analysis package (DNASTAR, Inc., Madison, MA, USA).

4.12. Statistical analysis

Statistical analysis was performed using the odds ratio (OR), the chi-square (χ^2), and the multiple logistic regression analysis (the forward stepwise-likelihood ratio and the enter methods). Values of $p < 0.05$ were considered as significant difference. The odds are the ratio of the probability that the event of interest occurs to the probability of the event of interest that does not. This is often estimated by the ratio of the number of times that the event of interest occurs to the number of times that does not (52). For example, the association between viral load (A) and *KIR* genotypes (B) as shown in Table 4.8.

Table 4.8. Frequency table for 2×2 data

	B_1	B_2	Total
A_1	f_{11}	f_{12}	f_{10}
A_2	f_{21}	f_{22}	f_{20}
Total	f_{01}	f_{02}	f_{00}

Where;

A_i, B_j defined to the categories of variables in the dichotomous study. A_1 is high viral load; A_2 is low viral load; B_1 is KIR-B_1 gene; and B_2 is KIR-B_2 gene.

f_{ij} defined to the observed frequency of the respondents which fall into the category (A_i, B_j).

Mathematically:

$$f_{00} = \sum_i f_{i0} = \sum_j f_{0j} = \sum_i \sum_j f_{ij}$$

When:

$$f_{i0} = \sum_{i} f_{ij} \qquad \text{and} \qquad f_{0j} = \sum_{i} f_{ij}$$

Whether *KIR-B1* genotype is associated with viral load, the proportion of *B1* genotype is f_{11}/f_{01} and the odd is f_{11}/f_{21}. Additional, the proportion of *B2* genotype is f_{12}/f_{02} and the odd is f_{12}/f_{22}. Comparing the proportions this way, the difference is $(f_{11}/f_{01})-(f_{12}/f_{02})$; the ratio (relative risk) is $(f_{11}/f_{01})/(f_{12}/f_{02})$; and the odds ratio is $(f_{11}/f_{21})/(f_{12}/f_{22})$ which can rearranged to give:

$$\text{The odds ratio (OR)} = \frac{f_{11}f_{22}}{f_{12}f_{21}}$$

The sample odds ratio itself seems to be a rather awkward function to work with, partly because of the problems that can arise with a zero observed cell frequency, for example f_{11}, and it is better to work with:

$$\text{The odds ratio (OR)} = \frac{(f_{11}+0.5)(f_{22}+0.5)}{(f_{12}-0.5)(f_{21}-0.5)}$$

CHAPTER V
RESULTS

5.1. *Mamu-KIR1D* gene

NK cells were isolated from 38 SIV-infected RMs (20 RM-HVL and 18 RM-LVL cohorts). The mRNA was extracted from these cells and cDNA created. Subsequently, *Mamu-KIR1D* gene was amplified by primer pair as described in Metherials and Methods (Table 4.3).

5.1.1. *Mamu-KIR1D* gene amplification and cloning

The full-length of cDNA of *Mamu-KIR1D* was amplified, from the signal sequence to the complete cytoplasmic tail based on GenBank ac. no. AY728181 (as defined *Mamu-KIR1D* mRNA, complete cds) could span nucleotide 8 to 1,117 (amplicon size 1,110 bp). PCR products from 38 ansimals were loaded into 1% agarose-ethidium bromind gel electrophoresis as shown in the Figure 5.1.

Thirty-one of 38 animals (18 RM-HVL and 13 RM-LVL cohorts) represented the amplicon (Figure 5.1) in addition some samples had non-specific band(s) at position 850 and/or 1,500 bp when compared to the 1 Kb DNA plus Ladder marker (Invitrogen, CA, USA). Six of these 31 animals were cut either two or three bands from the agarose gel and were purified for DNA samples. Subsequently, DNA samples were cloned into pGEM®-T vector and were transformed into JM109 cells. Five isolated white colonies (per animal) were picked and purified for plasmid. Plasmids were sequenced and analyzed as shown in Table 5.1. Two of 6 animals (sample ID mm 3 and 9) were negatively amplified for their *Mamu-KIR1D* gene when using this technique. The predicted size at position 1,100 bp was a strongly positive to clone *Mamu-KIR1D*, although, the position 850 bp was also positive for *Mamu-KIR1D* amplification, the yield was not a full sequence in length.

A

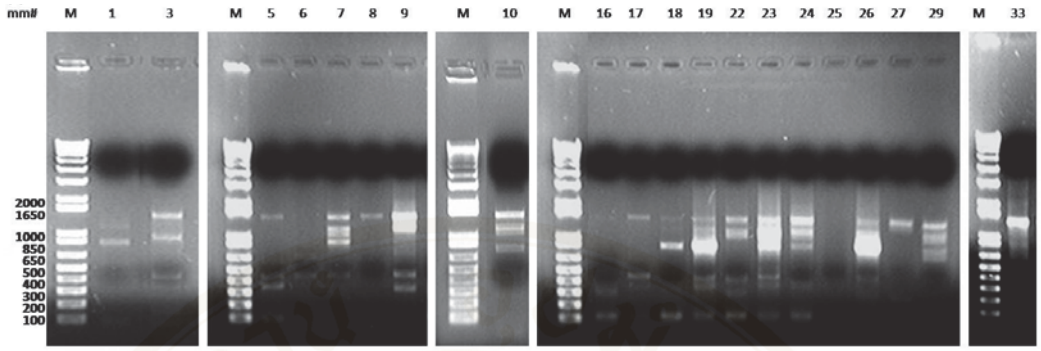

B

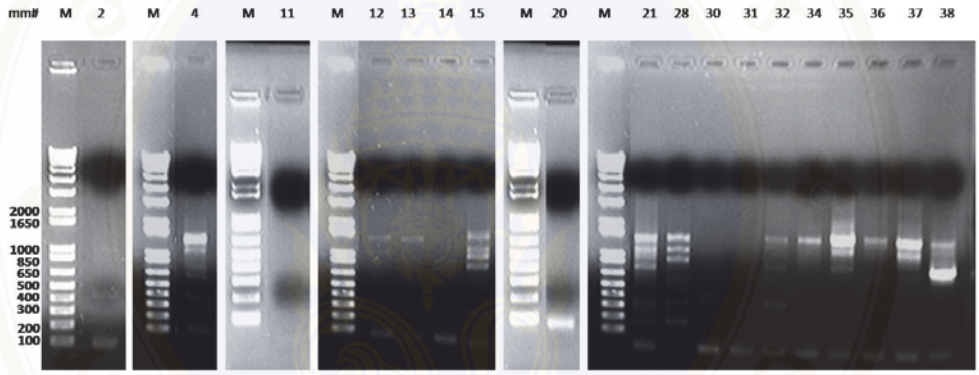

Figure 5.1. The amplified *Mamu-KIR1D* products on gel electrophoresis. cDNA samples were amplified for their full length of *Mamu-KIR1D* gene from 20 RM-HVL cohort (A) and 18 RM-LVL cohort (B) by using KIR1DFL-KIR1DR primer pair. The predicted amplicon size was approximately 1,110 bp where 'M' is the 1 Kb plus DNA Ladder marker.

Table 5.1. The blastn analysis of the predicted *Mamu-KIR1D* gene.

Sample ID	Position 1,500 bp	Position 1,100 bp	Position 850 bp
3	*Mamu-KIR3DL*	*Mamu-KIR3DH*	N/A*
7	*Mamu-KIR3DH*	*Mamu-KIR1D* and *Mamu-KIR3DH*	*Mamu-KIR1D* and *Mamu-KIR3DL*
9	*Mamu-KIR3DL* and *Mamu-KIR3DH*	*Mamu-KIR3DL* and *Mamu-KIR3DH*	N/A*
10	*Mamu-KIR1D*, *Mamu-KIR3DL*, and *Mamu-KIR3DH*	*Mamu-KIR1D* and *Mamu-KIR3DL*	*Mamu-KIR1D*
15	*Mamu-KIR3DL* and *Mamu-KIR3DH*	*Mamu-KIR1D*	*Mamu-KIR1D*
28	*Mamu-KIR3DL* and *Mamu-KIR3DH*	*Mamu-KIR1D*	N/A*

*Not available.

Table 5.2. *Mamu-KIR1D*-related clones.

A. RM-HVL cohort

Sample ID	Clone 1	Clone 2	Clone 3	Clone 4	Clone 5
mm01	allele 1	allele 1	allele 1	allele 1	allele 6
mm07	allele 2	allele 2	allele 10Bsv1	allele 2	allele 2
mm10	allele 3	allele 1	allele 3	N/A*	allele 1
mm18	allele 11	N/A*	allele 7	allele 7	allele 7
mm19	allele 8	allele9A	allele 8	allele 7	allele 9B
mm22	allele 1	allele 1	allele 10B	allele 10B	allele 3
mm23	allele 1	allele 2	allele 2	allele 1	allele 1
mm26	N/A*	N/A*	allele 11	allele 8	allele 8
mm29	allele 3	allele 3	allele 3	N/A*	allele 5

B. RM-LVL cohort

Sample ID	Clone 1	Clone 2	Clone 3	Clone 4	Clone 5
mm15	allele 6	allele 1	allele 5	allele 1	allele 5
mm20	N/A*	allele 1	allele 2	allele 5	allele 5
mm21	allele 1	allele 1	N/A*	allele 1	allele 10A
mm28	allele 1	allele 4	allele 1	N/A*	allele 4
mm37	allele 1	N/A*	allele 3	allele 3	allele 1
mm38	allele 8	allele 7	allele 8	allele 11sv1	N/A*

*DNA sample sequence which was encoded as the early truncated protein.

5.1.2. *Mamu-KIR1D* polymorphisms

Five *Mamu-KIR1D* positive clones were chosen from each animal. Only fifteen animals in the cohort (9 RM-HVL and 6 RM-LVL cohorts) were positive for *Mamu-KIR1D* expression as measured by this set of primer pair (Table 5.2). No *Mamu-KIR1D* clone was found for the other 23 of the 38 animals. A total of 75 DNA samples were sequenced by using T7 and SP6 analysis. The length of a contig was approximately 700-800 bp. Subsequently, the couple of the contigs was aligned and merged by using the SeqMan software (the length of the overlap part was approximately 300–500 bp). All of these 75 sample sequences were proofed by analysis of the electropherogram to insure changes seen (insertions, deletions, and base pair changes) were real and not just due to poor sequence quality. Subsequently, sample sequences were blasted and the results showed the *Mamu-KIR1D* gene was the first hit as measured by the blastn analysis (NCBI databases). The approach begins with the translation of DNA sample sequences into protein sequences based on sorted the frame shift translation, which were performed by using MegAlign software for ultimately looking at the functional differences of the receptors, not the genomic variations and “silent” SNPs that do not translate into amino acid change. Analysis of the sequences in MegAlign software showed that 65 sample sequences were considerated into 11 alleles (*Mamu-KIR1D* allele-1 to allele-11) by phylogenetic tree and multiple alignment analysis (Figure 5.2). Ten sample sequences were nonsense sequences which would create truncated proteins, each having a stop codon directly after either the signal peptide or D1 domain and the extremely mismatch sequences (Figure 5.3). All samples in each allelic grouping had >98% homology in both DNA and protein alignment analysis, and then, alleles were identified to finding the similarity to previously published *Mamu-KIR1D* sequences from NCBI databases as known in the named *Mamu-KIR1D* (ac. no. AY728181) and 11 *Mamu-KIR1D splice variants (sv)-1* to *sv-11* (ac. no. AF334635 to AF334643, FJ217804, and FJ217805, respectively). Phylogenetic tree and multiple alignment analysis showed our created *Mamu-KIR1D allele-1* to *allele-8* had closely to previously published *Mamu-KIR1D, Mamu-KIR1Dsv-1, sv-2, sv-4, sv-6, sv-9, sv-10, and sv-11,* respectively, at >98% identity of DNA and protein analysis. Additionally, none of the animals in our cohort expressed four of the previously described *Mamu-KIR1Dsv-3, sv-5, sv-7,* and *sv-8*

(ac.no. AF334637, AF334639, AF334641, and AF334642, respectively). As described in the previous study, Hershberger *et al* (10), a novel *Mamu-KIR1D* gene was identified that the encoding Mamu-KIR1D molecule with D1 domain, and the first two-thirds of the D2 domain of Mamu-KIR3DL molecule (Figure 5.4), because of a frame shift, the predicted amino acid sequence then changes to a novel domain of 55 aa, and the molecule terminates at a final length of 244 aa (refer to *allele-1*, *2*, and *10*, Figure 5.5B) (10).

In addition, there were 3 new alleles identified *Mamu-KIR1D allele-9* (*variant A* and *variant B*), *allele-10* (*variant A, variant B,* and *variant B-sv-1*), and *allele-11* (wide type and *sv-1*) refer to ac. no. GU564169 through GU564175, respectively. The previously published *Mamu-KIR3DL7* (ac. no. AF334622) was utilized as a consensus sequence for the analysis of the *Mamu-KIR1D* alleles. As seen in Figure 5.5, the 11 *Mamu-KIR1D* alleles were considerated to Cluster I and Cluster II based on the presence or absence of ITIM(s). Thus, while the members of *Mamu-KIR1D* Cluster I had ITIM(s) expression in their cytoplasmic tail and included *alleles-3, 4, 5, 7, 8, 9,* and *11*, those belonging to Cluster II showed no ITIM expression and consists of *alleles-1, 2, 6,* and *10*. Interestingly, Cluster I was found in ~1.7 folds more animals from the RM-HVL cohort than the RM-LVL cohort; thus, animals in the RM-HVL cohort tended to express the inhibitory KIR molecules (ITIMs in the cytoplasmic region) (Table 5.3). There was no significant difference between HVL and LVL groups in macaques expressing Cluster II (no ITIMs) (Table 5.3).

Mamu-KIR1D allele-9 showed 99% DNA homology to *allele-8*, however, a base deletion was found upstream of the secondary ITIM, resulting in a frame-shift. This allele was identified as two variants (*variant A* and *B*) based on different clones from the same RM-HVL animal. In *allele-9A*, the thymine at position 623 was deleted (623delT) and in *allele-9B*, the adenine at position 662 was deleted (662delA); *allele-8* was used as the consensus sequence (Figure 5.6). These deletions result in a reading frame mutation within the cytoplasmic tail which causes the loss of an ITIM (Figure 5.5).

Mamu-KIR1D allele-10 had two variants (*A* and *B*) and a splice variant - *variant Bsv-1*- that were each defined by four independent clones from three different animals (Table 5.3 and Table 5.4). *Allele-10A* was identical to *allele-10B* and *10Bsv-1* at 86.5% and 87.7% homology in protein level, respectively. Additionally, *allele-10A* showed difference before the stop codon in few amino acids. *Allele-10B* and *allele-10Bsv-1* showed 99.1% homology at protein level, interestingly, *allele-10Bsv-1* seems to have 36 nucleotides' deletion upfront at D1 domain (Figure 5.6).

Furthermore, *Mamu-KIR1D allele-11* was found to be closely related to allele-8 with 99.2% amino acid (aa) homology, however, there were 18 aa motif in the ending shown the difference. *Mamu-KIR1D allele-11 sv-1* had 96% homology to *allele-8* and 93.9% homology to *allele-11*, at protein level. *Allele-11 sv-1* expressed an ITIM but lost part of the TM with 35 aa were deleted, similar to *Mamu-KIR1D allele-3*. Whether these proteins (no TM domain) are still function remain unknown.

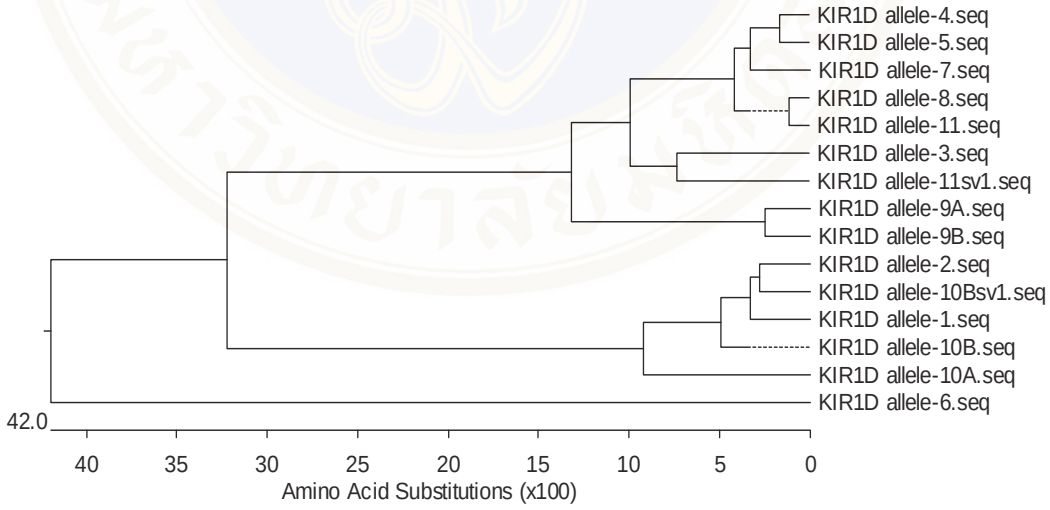

Figure 5.2. Phylogenetic tree of *Mamu-KIR1D* gene at the protein level. The consensus sequences of *Mamu-KIR1D* alleles and their variants were generated and compared between the individual sequences based on the phylogenetic relationship.

Table 5.3. Association of the *Mamu-KIR1D* alleles in SIV-infected RMs according to plasma VLs.

Cluster	Allele	HVL (n)	LVL (n)	Total (n)
I	3	3	1	4
	4	0	1	1
	5	1	2	3
	7	2	1	3
	8	2	1	3
	9A	1	0	1
	9B	1	0	1
	11	2	0	2
	11sv1	0	1	1
	Total (n)	12 (60%)*	7 (39%)*	19 (50%)**
II	1	4	5	9
	2	2	1	3
	6	1	1	2
	10A	0	1	1
	10B	1	0	1
	10Bsv1	1	0	1
	Total (n)	9 (45%)	8 (44%)	17 (45%)

* % of total monkey in group. HVL total = 20, LVL total = 18

** % of total of all 38 monkeys

Table 5.4. The lists of the animals, which express each particular allele of *Mamu-KIR1D* gene.

Allele	Sample ID	
	HVL	LVL
1	1, 10, 22, and 23	15, 20, 21, 28, and 37
2	7 and 23	20
3	10, 22, and 29	37
4	none	28
5	29	15 and 20
6	1	15
7	18 and 19	38
8	19 and 26	38
9A	19	none
9B	19	none
10A	none	21
10B	22	none
10Bsv1	7	none
11	18 and 26	none
11sv1	none	38

```
                          Signal peptide      D1 domain
Mamu-KIR1D allele-4       MVVSVACVGFFLVQRACPHTGVHRKPSLLALPGPLVKSEETVILQCWSDIKFEHFLLHRV 60
Mamu-KIR1D allele-1       MVVSVACVGFFLVQRACPHTGVHRKPSLLALPGPLVKSEETVILQCWSDIKFEHFLLHRV 60
KIR1D_mm10_clone4.seq     MVVSVACVGFFLVQRACPHTGESFPKP*GVISPPERIFLKQEGSPVQESLIN*EEGALGY 60
KIR1D_mm18_clone2.seq     --VSVACVGFFLLQRAWPHTGVHRKPSLLALPGPLVKSEETVILQCWSDIKFEHFLLTEW 58
KIR1D_mm26_clone1.seq     ------------------------------------------------------------ 1
KIR1D_mm26_clone2.seq     MVVSVACVGFFLVQRACPHTGESFPKP*GVISPPERIFLKQEGSPVQESLIN*EEGALGY 60
KIR1D_mm29_clone4.seq     MVVSVACVGFFLVQRACPHTGVHRKPSLLALPGPLVKSEETVILQCWSDIKFEHFLLHRV 60
KIR1D_mm20_clone1.seq     MVVSVACVGFFLVQRACPHAEVHRKPSLLALPGPLVKSEETVILQCWSDIKFEHFLLHRV 60
KIR1D_mm21_clone3.seq     MVVSVACVGFFLVQRACPHTGVHRKPSLLALPGPLVKSEETVILQCWSDIKFEHFLLHRV 60
KIR1D_mm28_clone4.seq     MVVIVACVGFFLVQRACPHMGVHRKPSLLALPGPLVKSEETVILQCWSDIKLEHFLLH*V 60
KIR1D_mm37_clone2.seq     MVVSVACVGFFLVQRACPHTGVHRKPSLPALPGPLVKSEETVILQCWSDIKFEHFLLHRV 60
KIR1D_mm38_clone5.seq     MVVSVACVGFFLLQRAWPHTGVHRKPSLLALPGPLVKSEETVTLQCWSDIKFEHFLLHRV 60

Mamu-KIR1D allele-4       GKFEEPLHLIGELHDGGSKANVSISPVTPALAGTYQCYGSVTHSPYVLSAPSDPLEIVIT 120
Mamu-KIR1D allele-1       GKFEEPLHLIGELHDGGSKANVSISPVTPALAGTYQCYGSVTHSPYVLSAPSDPLEIVIT 120
KIR1D_mm10_clone4.seq     STHSSDLALPSLSFPWQSQVLWGPGSPQKTFSPGPPRSPGEIRRDGHPAVLVRYQV*ALP 120
KIR1D_mm18_clone2.seq     GSLRSPCISSESSMMGAPRPMSPSVQ*HLPWQGPTNATVLSLTPPMCCQLPVTPWRS*SQ 118
KIR1D_mm26_clone1.seq     GEV*GALASHRRAP*WGSKANVSISPVTPALAGTYQCYGSVTHSPYVLSAPSDPLEIVIT 60
KIR1D_mm26_clone2.seq     STHSPDLALPSLSFPWQSQVLWGPGSPGEIRRDGHPAVLVRYQV*ALPSAPSGEV*GALA 120
KIR1D_mm29_clone4.seq     GKFEEPLHLIGELHDGGSKANVSISPVTPALAGTYQCYGSVTHSPYVLSAPSDPWRS*SQ 120
KIR1D_mm20_clone1.seq     GKFEEPLHLIGELHDGGSKANVSISPVTPALAGTYQCYGSVTHSPYVLSAPSDPLEIVIT 120
KIR1D_mm21_clone3.seq     GKFEEPLHLIGELHDGGSKANVSISPVTPALAGTYQCYGSVTHSPYVLSAPSDPLEIVIT 120
KIR1D_mm28_clone4.seq     GKFEEPLHLIGELHDGGSKANVSISPVTPALAGTYQCYGSVTHSLYVLSAPSDPLEIVIT 120
KIR1D_mm37_clone2.seq     GKFEEPLHLIGELHDGGSKANVSISPVTPALAGTYQCYGSVTHSPYVLSAPSDPLEIVIT 120
KIR1D_mm38_clone5.seq     GKFEEPLHLIGELHDGGSKANVSISPVTPALQGPTNATVLSLTPPMCCQLPVTPWRS*SQ 120

                                                          Stem
Mamu-KIR1D allele-4       GRLPSGTHGGTYRCFGSFRAPPFEWSDPSDPLPVSVTGNSSNGWPSPTEPSSKTGIPRHL 180
Mamu-KIR1D allele-1       GKYEKPSLSAQPGPTVQAGENVTLSCSSWRSFDMYHLSREGEAHELRLPAVPSVHGTFQA 180
KIR1D_mm10_clone4.seq     SAPSGEV*GALASHRRAP*WGLQGQCLHQSSDTCPGRDLPMLRFCHSLPLCVVSSQ*SPG 180
KIR1D_mm18_clone2.seq     GTLQMVGLHPLNQVPKLVSPDTCMF*LCPQWS*SSSPSPSSFSCIAGAPTKRMLL*WTKS 178
KIR1D_mm26_clone1.seq     GNPSNGWPSPTEPSSKTGIPRHLHVLIVSSVVMILFTILFFFLLHRWCSNKKDAAVMDQE 120
KIR1D_mm26_clone2.seq     SHRRAP*WGLQGQCLHQSSDTCPGRDLPMLRFCHSLPLCVVSSQ*PPGDRDHREPFKWLA 180
KIR1D_mm29_clone4.seq     VNMRNLLSQPSRAPRFRQERT*PCPAAPGAPLTCTIYPGRGRPMNLGSLQCPVSMERSRP 180
KIR1D_mm20_clone1.seq     GRLPSGTHGGTYRCFGSFRAPPFEWSDPSDPLPVSITGNPSRTWPSPSEPSSKTSIPRHL 180
KIR1D_mm21_clone3.seq     GEESPCLSHVLRS*SHS*GASC**WKEAWTDAERRRGLGNSSNGWPSPTEPSSKTERMFH 180
KIR1D_mm28_clone4.seq     GKYEKPSLSAQPGPTVQAGENATLSCSSWRSFDMYHLSREGEAHELRLPAVPSVHGTFQA 180
KIR1D_mm37_clone2.seq     GKYEKPSLSAQPGPTVQAGENVTLSCSSWRSFDMYHLSREGEAHELRLPAVPSVHGTFQA 180
KIR1D_mm38_clone5.seq     GTLQMVGLHPLNQVPKLMLL*WTKSLEWKEQ*IRRTLMNKTLRR*HTHSWITAFSHREKS 180

                           Transmembrane       Cytoplasmic tail
Mamu-KIR1D allele-4       HVLIVSSVVMILFTILFFFLLHRWCSNEKDAAVMDQEPGVERTVNPEDSDEQDPQEVTYA 240
Mamu-KIR1D allele-1       DFPLGPMEGPTDASVLSVPHPSSGQTRVTHCPFLSQGTLQMVGLHPLNQVPKLVSPDTCM 240
KIR1D_mm10_clone4.seq     DRDHR*I*ETFSLSPAGPHGSGRRERDLVLQLLALL*HVPSIQGGGGP*T*APCSAQCPW 240
KIR1D_mm18_clone2.seq     LEWKEQ*IRRTLMNKTLRR*HMHSWITAFSRREKSLALLRGPRDPQQIPACT*NFQMLSP 238
KIR1D_mm26_clone1.seq     PGVERTVNPEDSDEQDPQEVTYAQLDHCVFTQGKITCPSQRSKRPPTDTSVYIELPDAEP 180
KIR1D_mm26_clone2.seq     FTH*TKFQNWMLL*WTKSLEWKEQ*IRRTLMNKTLRR*HTHSWITALSHREKSLALLRGP 240
KIR1D_mm29_clone4.seq     TSLWDPWRDLQMLRFFPCPTLRVVRPE*PTARFCHRELFKWLAFTH*TKFQNWMLL*WTK 240
KIR1D_mm20_clone1.seq     HVLIGTSVVTILFTIFFFLLHLWCSNKKNAAAMDQEPAGDRTVNPEDSDEQDPQEVTYAQ 240
KIR1D_mm21_clone3.seq     HVGQACLKLPTSSDLTISASQSTGITGIPRHLHVLIVSSVVMILFTILFFFLLHRWCSNE 240
KIR1D_mm28_clone4.seq     DFPLGPMEGPTDASVLSVPHPSSGQTRVTHCPFLSQGTLQMVGLHPLNQVPKLVSPDTCM 240
KIR1D_mm37_clone2.seq     DFPLGPTEEPTDASVLSVPHPTSGQTRVTHCPFLSQETLHVLGLHPLNQAANPVSPDTCL 240
KIR1D_mm38_clone5.seq     LALLRGPRDPQQIPACT*SFQMLSPDRKLTTVRP*GGPPGRQQPCLKPSLPVPMYQQQ   238

Mamu-KIR1D allele-4       QLDHCVFTQGKITRPSQRSKRPPTDTSVYIELPDAEPRSKVDHSQALRGSSRETTALSQT 300
Mamu-KIR1D allele-1       F*LCPQWS*FSSPSSSSFSCIAGAPMKRMLL*WTKSLEWKEQ*IRRTLMNKTLRR*HTHS 300
KIR1D_mm10_clone4.seq     NVPGRLPSGTHGGTYRCFGSFRAPPFEWSDPSDPLPVSVTGNSSNGWPSPTEPSSKTGIP 300
KIR1D_mm18_clone2.seq     DRKLTTVRPRGGPPGRQQPCLKPSLPVPMYQQQ                             271
KIR1D_mm26_clone1.seq     RSKVDHSQALRGSSRETTALSQTQLASSNDQQQN                            214
KIR1D_mm26_clone2.seq     RDPQQIPACT*SFQMLSPDRKLTTVRP*GGPPGRQQPCLKPSLPVPMYQQQ          291
KIR1D_mm29_clone4.seq     SLEWKEQ*IRRTLMNKTLRR*HTHSWITAFSHREKSLALLRGPRDPQQIPACT*SFQMLS 300
KIR1D_mm20_clone1.seq     LDHRVLTQGKITRPSQRPKTPPTDTSVYTELPNAEPRSKVVFYP*APPSGLEGVF*GDNS 300
KIR1D_mm21_clone3.seq     KDAAVMDQEPGVERTVNPEDSDEQDPQEVAYAQLDHCVFTQGKITRPSQRSKRPPTDTSV 300
KIR1D_mm28_clone4.seq     F*LCPQWS*FSSPSSSSFSCIAGAPMKRMLL*WTKSLEWKEQ*IRRTLMNKTLRR*HTHS 300
KIR1D_mm37_clone2.seq     L*LGTRWPPSSSPSSSSFSFVVGAPTKRDSEEQDPQEVTYAQLGHCAFTRGKITRPSQRP 300
KIR1D_mm38_clone5.seq                                                                   238
```

Figure 5.3. *Mamu-KIR1D* nonsense sample sequences. The early truncated proteins and the extremely mismatch sample sequences were excluded in the analysis where star (*) is a stop codon; *Mamu-KIR1D allele-1* and *allele-4* refer to GenBank ac. no. AY728181 and AF334638, respectively.

Figure 5.4. A novel *Mamu-KIR1D* structure. The encoded Mamu-KIR1D alleles and their alternatively spliced variants compared to Mamu-KIR3DL7 molecule. The diagonal lines were an ITIM motif.

A

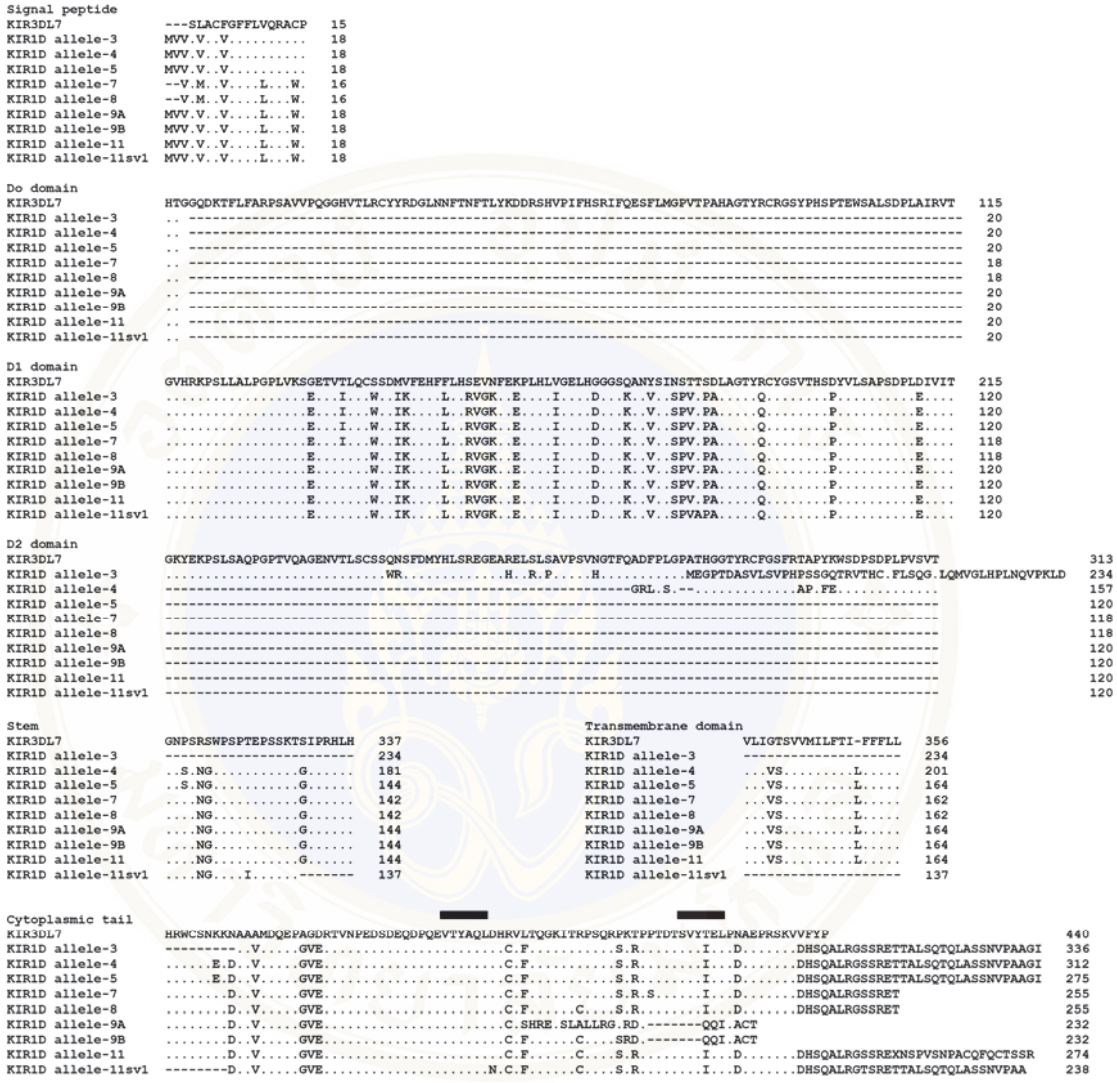

Figure 5.5. *Mamu-KIR1D* Cluster I and Cluster II. (A) Cluster I contains *Mamu-KIR1D alleles* which had the ITIMs in their cytoplasmic tail. These motifs regulate the inhibitory function of NK cells. (B) Cluster II contains other four *Mamu-KIR1D alleles*, this cluster was believed in a null phenotype because of no TM and ITIM expression.

B

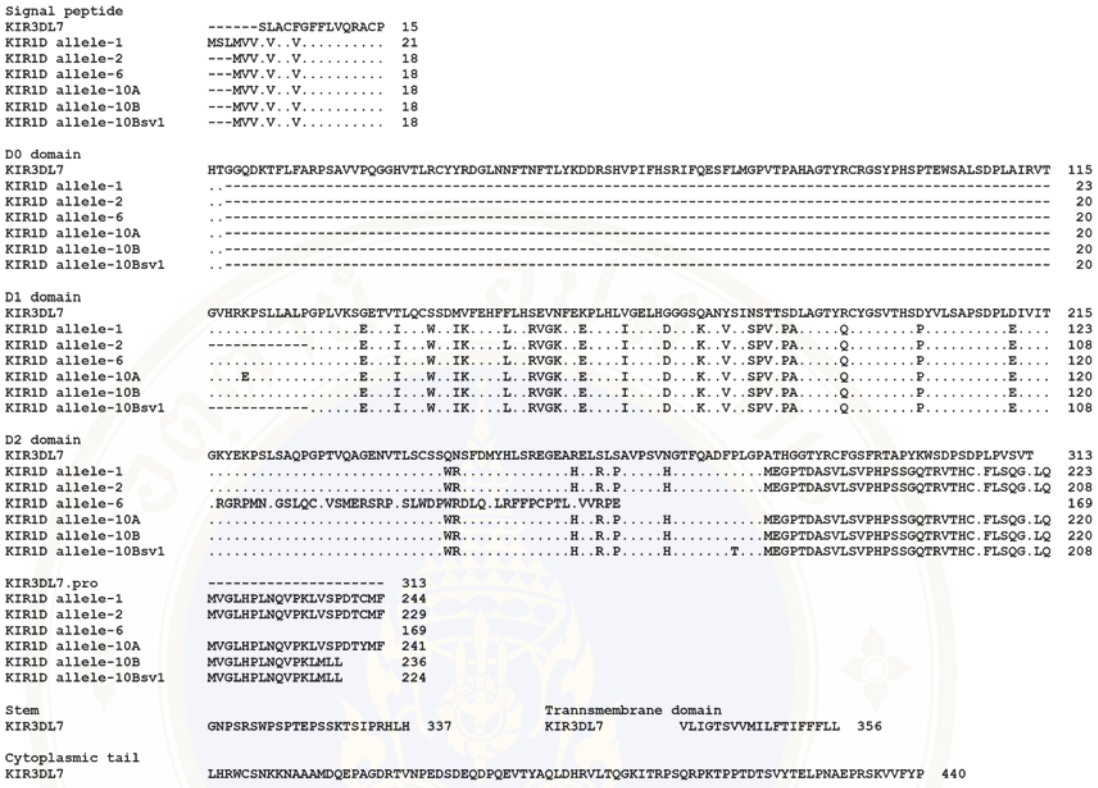

Figure 5.5. *Mamu-KIR1D* Cluster I and Cluster II (continued.).

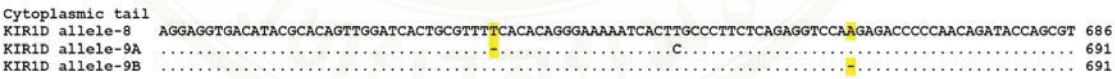

Figure 5.6. Base deletion of *Mamu-KIR1D allele-9 variants.* The deletion at nucleotide 623 in *allele-9 variant A* or at nucleotide 662 in *allele-9 variant B* result in a reading frame mutation within the cytoplasmic tail which causes the loss of an ITIM.

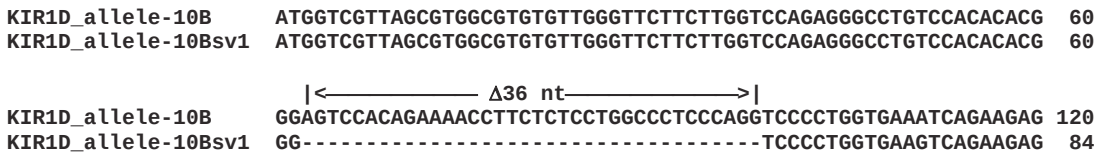

Figure 5.7. *Mamu-KIR1D allele-10 variants.* The 36 nucleotides of *variant Bsv-1* deleted at D1 domain when compared to *variant B* where dash is no base.

5.2. *Mamu-KIR2DL4* gene

Previous studies showed that *Mamu-KIR2DL4* gene from the same animal had two different allelic groups (*allele-1* and *allele-2*) by using Ig3Up-Ig3Down primer pair (10). Following the previous observation, we could not amplify the full length of the other alleles by using the same primers and PCR conditions. Therefore, our laboratory designed two sets of primer pairs for amplification of the extracellular and the intracellular regions of this gene (Figure 5.8). The overlapping section of the predicted products from the extracellular and the intracellular domains in the same sample was aligned to ensure complete coverage of the cDNA.

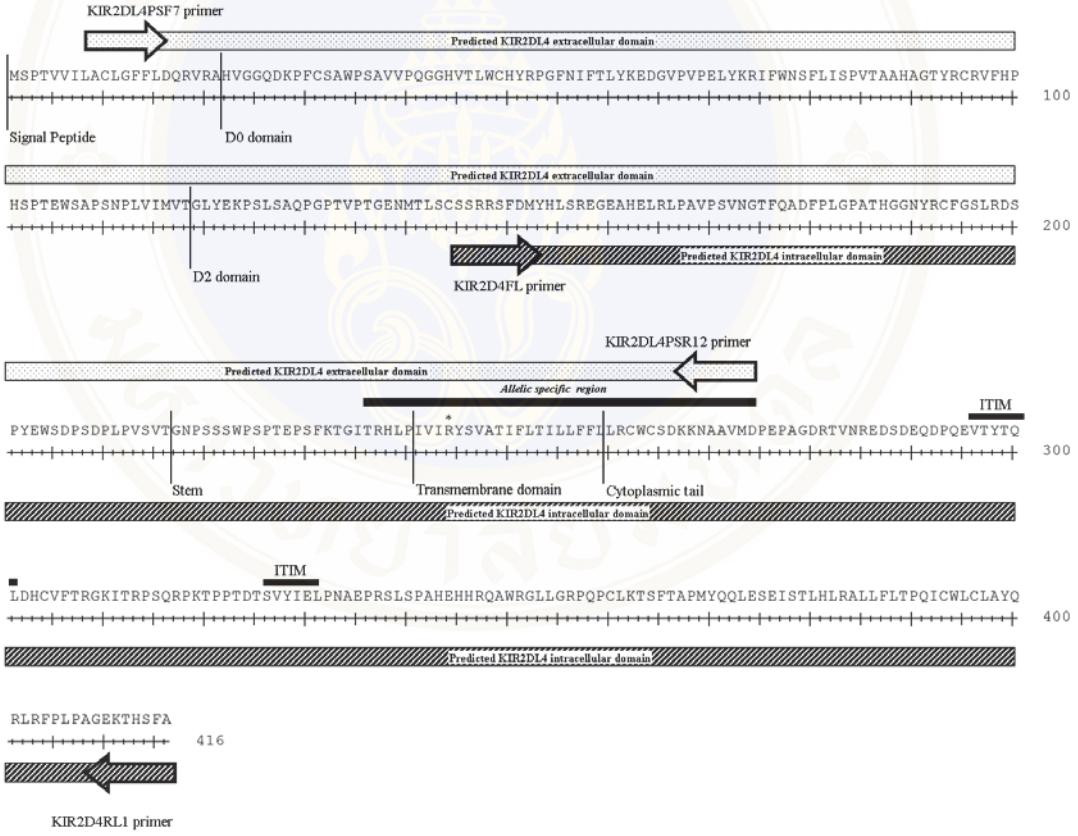

Figure 5.8. The predicted extracellular and intracellular domains of *Mamu-KIR2DL4* gene. *Mamu-KIR2DL4* extracellular and intracellular regions were amplified by using KIR2DL4PSF7 - KIR2DL4PSR12 and KIR2D4FL - KIR2D4RL1 primer pairs, respectively. The overlapping between the predicted KIR2DL4 extracellular and intracellular domains was 392 bp in length. The encoding sequence was translated from *Mamu-KIR2DL4 allele-2* based on reference numbering AY728182.

5.2.1. *Mamu-KIR2DL4* extracellular domain

The KIR2DL4PSF7-KIR2DL4PSR12 primer pair was utilized for amplifying the extracellular region of *Mamu-KIR2DL4* locus covers the signal sequence, D0 and D2 domains, stem, TM, and part of cytoplasmic tail (Figure 5.8). The predicted PCR product based on the sequence of ac. no. AY728182 (as defined by *Mamu-KIR2DL4* mRNA, complete cds) that could span nucleotide from 23 to 824 (amplicon size 802 bp).

5.2.1.1. Extracellular *Mamu-KIR2DL4* amplification and cloning

The cDNA samples from 38 animals in the cohort were used to amplify the *Mamu-KIR2DL4*-extracellular domain, the gel electrophoresis as shown in the Figure 5.9. Thirty-six of 38 animals showed positive PCR products by using this technique. The PCR products which located at position 802 bp (the estimated size) were cut and purified for the cloning step.

5.2.1.2. Extracellular *Mamu-KIR2DL4* polymorphisms

This primer pair was successfully amplified and cloned from 27 of 38 animals (15 RM-HVL and 12 RM-LVL cohorts), five clones per animal (Table 5.5). Total of 135 sample sequences were analyzed, 12 of these 135 sequences showed an early stop codon (truncated protein) which were not utilized for further analysis (Figure 5.10). As described in the section of *Mamu-KIR1D* gene, all individual sequences with ‘silent’ SNPs that did not translate into amino acid change were disregarded. The protein sequences were subsequently grouped based on the phylogenetic distance in a stepwise fashion. Figure 5.11 illustrates the phylogenetic tree of the 7 alleles encoded by the *Mamu-KIR2DL4* locus. Once the protein analysis was completed, a reverse analysis was performed using the corresponding DNA sequences. Such analysis led to the assignment of the sequences to a total of 7 *Mamu-KIR2DL4 alleles* which included two previously identified alleles (*allele-1* and *allele-2* refer to GenBank ac. no EU702486 and AY728182, respectively) and five new alleles (*allele-3* to *allele-7,* ac. no. GU564176 to GU564181) (Figure 5.12).

Mamu-KIR2DL4 allele-1 to *allele-4* containing an AGG sequence in their TM which codes for a positively charged arginine (R) (at position 244, Figure 5.12), this arginine residue facilitates the binding to the corresponding negatively charged TM residues of the ITAM-encoding adaptor proteins, such as DAP-12, which could contribute to the activation of the KIR2DL4 molecule (3). Other of these four alleles, *allele-5* to *allele-7* had the point mulation, single base insertion or deletion which led to premature translation in addition the stop codon showed either stem or TM. However, these alleles had longer enough to understand the fully extracellular region sequences (Figure 5.13). It is still not known that the premature proteins expressed on the cell surface which had no arginine and ITIM expression play any role on their function(s).

The extracellular domain of *Mamu-KIR2DL4 alleles-1* and *allele-2* were found to be the two most dominant alleles in these cohorts with each of 27 animals expressing either *allele-1*, *allele-2* or both in addition to the other alleles identified (Table 5.5). Thus, 17 of 27 animals (12 RM-HVL and 5 RM-LVL cohorts) expressed *Mamu-KIR2DL4 allele-1* sequences and 13 of 27 animals (5 RM-HVL and 8 RM-LVL cohorts) were found to express *Mamu-KIR2DL4 allele-2*. Three or more clones of each macaque expressed *allele-1* in 15 of 17 animals (11 RM-HVL and 4 RM-LVL cohorts) and *allele-2* in 10 of 13 animals (3 RM-HVL and 7 RM-LVL cohorts). High *allele-1* to *allele-2* ratio was found in RM-HVL cohort (2.40 fold) when compared with RM-LVL cohort (0.63 fold) whereas highly expression of *allele-2* was found in RM-LVL cohort (*allele-2* to *allele-1* ratio was ~1.6 fold) (Table 5.6). The expression of the allelic homozygous was considerated in the identity of all five clones from the same animal; therefore, 6 animals (3 RM-HVL and 3 RM-LVL cohorts) were homozygous *Mamu-KIR2DL4 allele-1*. Meanwhile 7 different animals expressed only *allele-2* in all five clones tested, however, 6 of these 7 animals were from the RM-LVL cohort and only 1 animal was from the RM-HVL cohort. The segregation of genetic *Mamu-KIR2DL4* expression in HVL and LVL was great that could be definitely a good candidate to try for the TaqMan probe. This is our goal to characterize KIR genetic variation and its variation to viral control in SIV-infected RMs. Additionally, the specific motif localized between the stem and TM appeared to be a signature motif for *allele-1* or *allele-2* associated with

Mamu-KIR2DL4 gene as previously described (10). Whereas *allele-1* showed a 'VT-X_3-A-X_{18}-H-X_5-D' motif, the *allele-2* showed either a 'TR-X_3-I-X_{18}-L-X_5-D' or 'VR-X_3-A-X_{18}-L-X_5-D' motifs at aa residue 236 to 266 (Figure 5.12).

Other *Mamu-KIR2DL4 alleles* which were identified in this study (*allele 3-7*), were expressed at a much lower frequency, thus, they were found in only one or two clones (Table 5.6). *Mamu-KIR2DL4 allele-3* (803 bp or 252 aa) and *allele-4* (802 bp or 252 aa) coded for a full length extracellular region and that were different from *alleles-1* and *2* in the D0 and D2 domains. *Alleles-3* and *4* were close by related to *allele-1* at 96.3% and 97% aa homology, respectively, and were also close by related to allele-2 at 94.8% and 95.5% aa homology, respectively. The amino acids within the extracellular region were distinctive from those expressed by *alleles-1* and were also containing a 'VT-X_3-A-X_{18}-H-X_5-D' motif as found in *allele-1*. Interestingly, these alleles (*allele-3-4*) were expressed in RM-HVL cohort and not found in RM-LVL cohort. *Mamu-KIR2DL4 alleles-5* was found to be closely related to *allele-2* with 98.1% aa and 99.3% DNA homology. *Allele-5* was 802 bp long and had a nonsense mutation causing the adenine to be replaced with thymine at position 673 yielding TAA (673A>T) in the cDNA sequence (Figure 5.13) and since TAA is a stop codon, it would result in a truncated protein product at stem in the early 'VR-X_3-A-X_{18}-L-X_5-D' motif. *Mamu-KIR2DL4 allele-6* (803 bp or 236 aa) had one adenine base insertion within the cDNA sequence at position 676 (676-677insA) that led to a frameshift translation (a shift in the reading frame) resulting in a truncated protein at TM. *Mamu-KIR2DL4 allele-7* was identified from two clones which appear to encode closely related proteins (96.3% aa and 99.5% DNA homology). However, these clones had different deleted bases and were designated as two variants; *variant A* which lacks a guanine at position 591 (591delG) and *variant B* which lacks a cytosine at position 608 (608delC) that led to the same stop codon at aa residue 235 (Figure 5.12). These proteins, although truncated, were included in this analysis and assigned to alleles (allele-5 through allele-7) since all three codes for the full length extracellular region of *Mamu-KIR2DL4*. If these proteins were expressed on the cell surface, they could still bind their ligands resulting in an inhibitory signal to the NK cells. There have been several reports that have identified HLA-G as the ligand for *Hu-KIR2DL4* (53, 54). However, the precise sequence that is involved in recognition

of the HLA-G molecule by KIR2DL4 receptor remains unknown at present. It is possible that the Ig-like domains of KIR2DL4 molecule might function in ligand-receptor interactions similar to the interaction previously described for the HLA-B Bw4-KIR3DL binding (5, 6, 55). Interestingly, four animals in the RM-HVL cohort expressed the low frequency of *alleles-5, 6,* and *7,* while only one animal in the RM-LVL cohort expressed *allele-7*.

Additionally, the truncated proteins of *allele-5*, samples from six animals (4 RM-HVL and 2 RM-LVL cohorts), resulted in clones which coded for an early stop codon within either the D0 or D2 domain (Figure 5.14). These clones had a high degree of sequence homology at both the DNA and protein level with *allele-5* (Table 5.7). They were thus termed '*predicted Mamu-KIR2DL4 allele-5*' (*p-allele-5*) in this study (Table 5.5). A preponderance of animals in RM-HVL cohort (8 of 15 RMs) appeared to express truncated KIR2DL4 proteins if one takes into account all of the truncated KIR2DL4 proteins (which include *alleles-5, 6,* and *7* and the *predicted allele-5*). In contrast, 3 of 12 RMs in RM-LVL cohort had these truncated proteins.

A

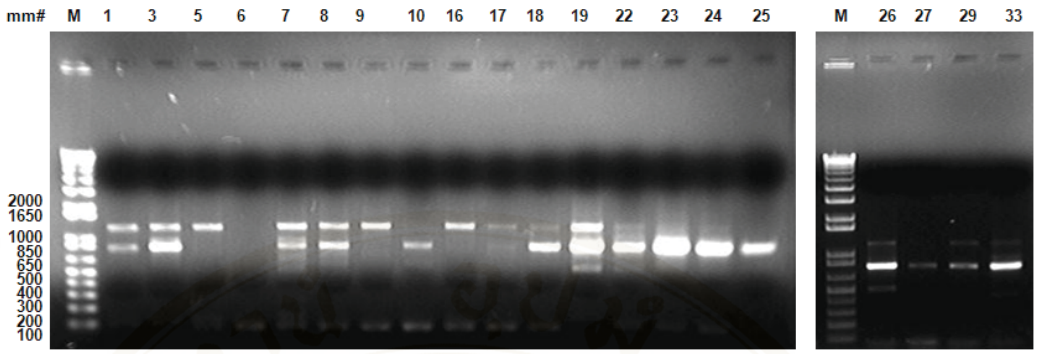

B

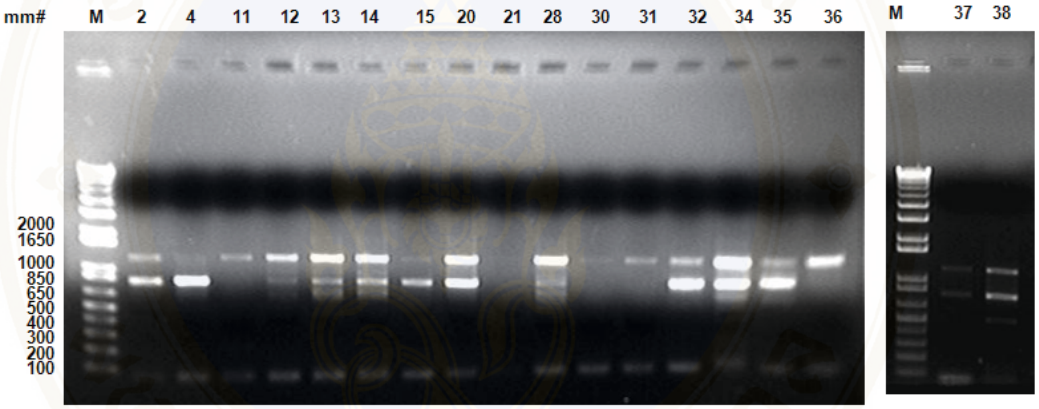

Figure 5.9. The amplified products of *Mamu-KIR2DL4*-extracellular domain on gel electrophoresis. Thirty-eight cDNA samples were amplified for *KIR2DL4* extracellular domain from 20 RM-HVL cohort (A) and 18 RM-LVL cohort (B) by using KIR2DL4PSF7-KIR2DL4PSR12 primer pair. The predicted amplicon size was 802 bp. Where M is the 1 Kb plus DNA Ladder marker.

Table 5.5. The clones which are related the extracellular domain of *Mamu-KIR2DL4* gene

Cohort	Sample ID	Clone 1	Clone 2	Clone 3	Clone 4	Clone 5
HVL	mm01	allele-1	allele-1	allele-1	allele-1	allele-1
	mm03	allele-1	allele-1	allele-3	N/A**	allele-1
	mm07	allele-1	N/A**	allele-5	allele-1	allele-1
	mm08	allele-2	allele-5	allele-2	allele-2	allele-2
	mm10	allele-1	allele-1	allele-1	allele-1	N/A**
	mm18	allele-6	allele-7B	allele-1	allele-1	allele-1
	mm19	N/A**	allele-2	allele-1	allele-1	allele-1
	mm22	N/A**	N/A**	allele-1	allele-1	p-allele-5*
	mm23	allele-1	allele-1	N/A**	allele-1	allele-6
	mm24	N/A**	allele-2	allele-2	allele-2	allele-2
	mm25	allele-2	p-allele-5*	allele-1	allele-1	allele-1
	mm26	p-allele-5*	allele-1	allele-1	allele-1	allele-1
	mm27	allele-1	allele-1	allele-1	allele-4	allele-1
	mm29	allele-1	allele-1	allele-1	allele-1	allele-1
	mm33	allele-2	allele-2	allele-2	p-allele-5*	allele-2
LVL	mm02	allele-2	allele-2	allele-2	allele-2	allele-2
	mm04	allele-2	p-allele-5*	allele-2	allele-2	allele-2
	mm14	allele-1	allele-1	allele-1	allele-1	allele-7A
	mm15	allele-1	allele-1	N/A**	allele-1	allele-1
	mm20	p-allele-5*	allele-1	allele-2	allele-2	allele-1
	mm21	allele-1	allele-1	N/A**	allele-1	allele-1
	mm28	allele-2	allele-2	allele-2	allele-2	N/A**
	mm32	allele-2	allele-2	allele-2	allele-2	allele-2
	mm34	allele-2	allele-2	N/A**	allele-2	allele-2
	mm35	allele-2	allele-2	allele-2	allele-2	allele-2
	mm37	allele-2	allele-2	allele-2	allele-2	allele-2
	mm38	allele-1	allele-1	allele-1	allele-1	allele-1

*p-allele-5, *predicted Mamu-KIR2DL4 allele-5.*

**Not available.

Table 5.6. Association of the Mamu-KIR2DL4 alleles in SIV-infected RMs according to plasma VLs.

Allele	HVL (n)	LVL (n)	Total (n)
1	12	5	17
2	5	8	13
3	1	0	1
4	1	0	1
5	2	0	2
6	2	0	2
7A	0	1	1
7B	1	0	1
Predicted allele-5	4	2	6
allele-1/allele-2 ratio	2.40	0.63	1.31

```
                          Signal peptide D0 domain
2DL4_mm_03_clone_4.seq  LACLGFFLDQRVRAHVGGQDKPFCSAWLSAVVPQGGHVTLWCHYRPGFNIFTLYKEDGVP 60
2DL4_mm_07_clone_2.seq  ............................P............................... 60
2DL4_mm_10_clone_5.seq  ................S.........P............................... 60
2DL4_mm_15_clone_3.seq  ---------...................P............................... 51
2DL4_mm_19_clone_1.seq  ............................P............................... 60
2DL4_mm_21_clone_3.seq  ............................P............................... 60
2DL4_mm_22_clone_1.seq  ............................P............................... 60
2DL4_mm_22_clone_2.seq  ..........CGHTWVVRTS.SALPGPALWCLREDTRLFGVTIVL.LTSSRCTRKT.CL 60
2DL4_mm_23_clone_3.seq  ................TSFSPRWSGQALLLCLAQRCGASGRT.DSLVSLSSWV*HLHA 60
2DL4_mm_24_clone_1.seq  ............................P............................... 60
2DL4_mm_28_clone_5.seq  ............Y............P............................... 60
2DL4_mm_34_clone_3.seq  ........V..ACP.T.....T.LF.RP...........R.Y..D.L.N......... 60

                                                                          D2 domain
2DL4_mm_03_clone_4.seq  VPELYKRIFWNSFLISPVTAAHAGTYRCRVFHPHSPTEWSAPSNPLVIMVTGQRAPVWAS 120
2DL4_mm_07_clone_2.seq  .S.......*TVSSLAL*LQHMQ.PTDVEF.IRTP.LSGRH.AT.W*SWSQVYMRNLLSQ 120
2DL4_mm_10_clone_5.seq  .........*TVSSLAL*LQHMQ.PTDVEF.IRTP.LSGRH.AT.W*SWSQVYMRNLLSQ 120
2DL4_mm_15_clone_3.seq  ....................................AT.W*SWSQVSMRNLLSQ 111
2DL4_mm_19_clone_1.seq  ..................................................LYEKPSL. 120
2DL4_mm_21_clone_3.seq  ..................T..........................LYEKPSL. 120
2DL4_mm_22_clone_1.seq  ..........S....AL*LQHMQ.PTDVEF.IRTP.VSGRH.AT.W*SWSQVYMRNLLSQ 120
2DL4_mm_22_clone_2.seq  SLSST.EYSGTVSS*PCDCSTCRDLQMSSFSSALPH*VVGTQQP.GDHGHRSI*ETFSL. 120
2DL4_mm_23_clone_3.seq  .QGRRGACP*ALQKNILEQFP.*PCDCSTCRDLQMSSFS..LPH*V.GTQQPPGDHGHR. 120
2DL4_mm_24_clone_1.seq  ..................................................LYEKPFSQ 120
2DL4_mm_28_clone_5.seq  ........................................*SWSQVYMRNLLSQ 120
2DL4_mm_34_clone_3.seq  ....................................AT.W*SWSQVYMRNLLSQ 120

2DL4_mm_03_clone_4.seq  PCPTS*IPELLLGVSVRVPSSRP*LSLGSI*ETFSLSPAGPHGSHMREHDLVLQFPALL* 180
2DL4_mm_07_clone_2.seq  .SRAPRF.QERT*PCPA..GAPLTCTIYPGRGRPMNLGSLQCRAS.EHSR.TSLWALPPT 180
2DL4_mm_10_clone_5.seq  .SRAPRF.QERT*PCPA..GAPLTCTIYPGRGRPMNLGSLQCRASTEHFR.TSLWALPPT 180
2DL4_mm_15_clone_3.seq  .SRAPRF.QERT*PCPA..GAPLTCTIYPGRGRPMNLGSLQCRAS.EHSR.TSLWALPPT 171
2DL4_mm_19_clone_1.seq  AQ.GPTV.TGENMTLSCSSGAPLTCTIYPGRGRPMNLGSLQCRAS.EHSR.TSLWALPPT 180
2DL4_mm_21_clone_3.seq  AQ.GTTV.TGENMTLSCTSRRSFDMHHL.REGDAHELTLHGEAIVVDTSLADVPA*LKHP 180
2DL4_mm_22_clone_1.seq  .SRAPRF.QERT*PCPA..GAPLTCTIYPGRGRPMNLGSLQCRAS.EHSR.TSLWALPPT 180
2DL4_mm_22_clone_2.seq  .AGPHGSHRREHDLVLQF.ALL*HVPSIQGGGGP*T*APCSAERQWNIPG*LPSG.CHPR 180
2DL4_mm_23_clone_3.seq  I*E.FSLSPAGPHG.H.REHDLVLQFPALL*HVP.IQGG.GP*T*APCSAERQWNIPG*L 180
2DL4_mm_24_clone_1.seq  .SQAPRF.QERT*PCPA..GAPLTCTIYPGRGRPMNLGSLQCRAS.EHSR.TSLWALPPT 180
2DL4_mm_28_clone_5.seq  .SQAPRF.QERT*PCPA..GAPLTCTIYPGRGRPMNLGSLQCRAS.EHSR.TSLWALPPT 180
2DL4_mm_34_clone_3.seq  .SRAPRF.QERT*PCPA..GAPLACTIYPGRGRPTYLGSLQCRAS.EHSR.TPSG.CHPR 180

2DL4_mm_03_clone_4.seq  HVPSIQGGGGP*T*APCSAERQWNIPG*LPSGPCHPRRELQMLRLSP*LSLRVVRPK*PT 240
2DL4_mm_07_clone_2.seq  EGTTDASALSVTLPTSGQTQVTHCPFLSQETLQVVGLHP.NQASKLVSSHTCLL*LGTRW 240
2DL4_mm_10_clone_5.seq  EGTTDASAHSVTLPTSGQTQVTHCPFLSQETLQVVGLHP.NEASKLVSSHTCLL*LGTRW 240
2DL4_mm_15_clone_3.seq  EGTTDASALSVTLPTSGQTRVTHCPFLSQETLQVVGLHP.NQASKLVSPDTYLL*LGTRW 231
2DL4_mm_19_clone_1.seq  EGTTDASALSVTLPTSGQTRVTHCPFLSQETLQVVGLHP.NQASKLVSSDTYLL*LGTRW 240
2DL4_mm_21_clone_3.seq  SKD.RCARTHT*LIE*WVPTKRFSSL.DGQHSLHDVGLLRML.Y*TES.PPHFLS*TQIV 240
2DL4_mm_22_clone_1.seq  EGTTDASTLSVTLPTSGQTQVTHCPFLSQETLQVVGLHP.NQASKLVSSHTCLL*LGTRW 240
2DL4_mm_22_clone_2.seq  RELQMLRLSP*LSLRVVRPK*PTARFCHRKPFK*LAFTH*TK.QNWYRHTPACCD*VLGG 240
2DL4_mm_23_clone_3.seq  PSGPCHPRRELQMLRLSP*LSLRVVRPK*.TARFCH.KPFK*.AFTH*TK.QNWYRHT.A 240
2DL4_mm_24_clone_1.seq  EGTTDASALSVTLPTSGQTRVTHCPFLSQETLQVVGLHP.NQASKLVSSDTYLL*LGTRW 240
2DL4_mm_28_clone_5.seq  EGTTDASALSVTLPTSGQTRVTHCPFLSQETLQVVGLHP.NQASKLVSSDTYLL*LGTRW 240
2DL4_mm_34_clone_3.seq  RELQMLRLSP*LSLRVVRP.*PTARFCHRKPFK*LAFTR*TK.QNWYHQTPAYCD*VLGG 240

2DL4_mm_03_clone_4.seq  AHFCHRKPFK*LAFTH*TKLQNWYRHTPACCD*VLGGHLLPHHPPLPSPSLLVLRQKECCCNG 303
2DL4_mm_07_clone_2.seq  PPSSSPSSSSFSIVAGAPTKRMLL*W.                                  267
2DL4_mm_10_clone_5.seq  PPSSSPSSSSFSIVAGAPTKRMLL*W.                                  267
2DL4_mm_15_clone_3.seq  PPSSSPSSSSFSFVAGAPTKRMLL*W.                                  258
2DL4_mm_19_clone_1.seq  PPSSSPSSSSFSFVAGAPTKRMLL*W.                                  267
2DL4_mm_21_clone_3.seq  L.RQTTGSCPYPQ*VFTISVPFYPQ.V.ISQTVICRPTE                      279
2DL4_mm_22_clone_1.seq  PPSSSPSSSSFSIVAGAPTKRMLL*W.                                  267
2DL4_mm_22_clone_2.seq  H.LP.HP.LLSPSLLVLRQKECCCNG                                   266
2DL4_mm_23_clone_3.seq  CCD*VLGGHHLPHHPPLLSPSLLVLRQKE..CNG                           274
2DL4_mm_24_clone_1.seq  PPSSSPSSSSFSFVAGAPTKRMLL*W.                                  267
2DL4_mm_28_clone_5.seq  PPSSSPSSSSFSFVAGAPTKRMPL*W.                                  267
2DL4_mm_34_clone_3.seq  H.LP.HP.LLSPSLLVLRQKECCCNG                                   266
```

Figure 5.10. Twelve early truncated Mamu-KIR2DL4 molecules. Dash, no amino acid; dot, similar to mm 3 clone 4; and star (*), stop codon.

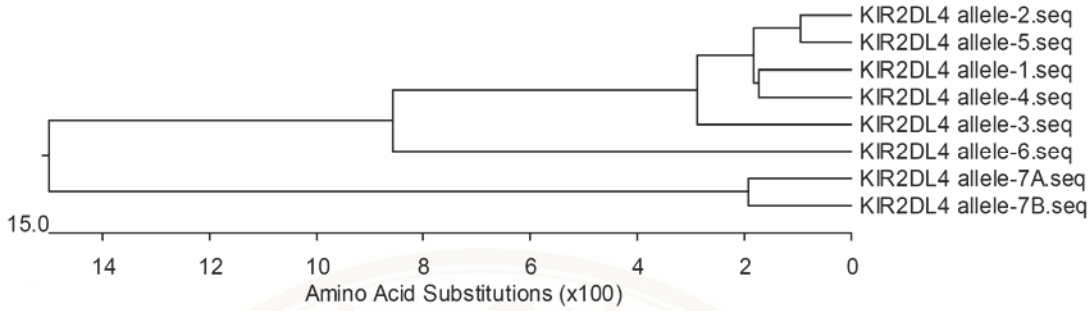

Figure 5.11. Phylogenetic tree of the *Mamu-KIR2DL4*-extracellular domain at the protein level.

```
Signal peptide
Consensus          -------LACLGFFLDQRVRA
KIR2DL4 allele-1   MSPTVVI.............   21
KIR2DL4 allele-2   MSPTVVI.............   21
KIR2DL4 allele-3   -------......C.......   14
KIR2DL4 allele-4   -------............Q.   14
KIR2DL4 allele-5   -------..............   14
KIR2DL4 allele-6   -------..............   14
KIR2DL4 allele-7A  -------..............   14
KIR2DL4 allele-7B  -------..............   14

Do domain
Consensus          HVGGQDKPFCSAWPSAVVPQGGHVTLWCHYRPGFNIFTLYKEDGVPVPELYKRIFWNSFLISPVTAAHAGTYRCRVFHPHSPTEWSAPSNPLVIMVT
KIR2DL4 allele-1   ..................................................................................................   118
KIR2DL4 allele-2   ..................................................................................................   118
KIR2DL4 allele-3   ..............G.....................................V.............................................   111
KIR2DL4 allele-4   .....AE.................A.............A.....................................................   111
KIR2DL4 allele-5   ..................................................................................................   111
KIR2DL4 allele-6   ..................................................................F.............................   111
KIR2DL4 allele-7A  ..................................................................................................   111
KIR2DL4 allele-7B  ..................................................................................................   111

D2 domain
Consensus          GLYEKPSLSAQPGPTVPTGENMTLSCSSRRSFDMYHLSREGEAHELRLPAVPSVNGTFQADFPLGPATHGGNYRCFGSLRDSPYEWSDPSDPLPVSVT
KIR2DL4 allele-1   ..................................................................................................   216
KIR2DL4 allele-2   ..................................................................................................   216
KIR2DL4 allele-3   ..................................................................................................   209
KIR2DL4 allele-4   ...G.....................L.....................................C.....................   209
KIR2DL4 allele-5   ....N.....................................................................................   209
KIR2DL4 allele-6   ..................................................................................................   209
KIR2DL4 allele-7A  ................H.................................................................CQTQVTHC.FLSQ   209
KIR2DL4 allele-7B  ..................................Y.................................................HC.FLSQ   209

Stem
Consensus          GNPSSSWPSPTEPSFKTGIVTHLP
KIR2DL4 allele-1   ........................   240
KIR2DL4 allele-2   ...................TR...   240
KIR2DL4 allele-3   ........................   233
KIR2DL4 allele-4   ........................   233
KIR2DL4 allele-5   .........A....*....R...   233
KIR2DL4 allele-6   .....G..........NWYRHTPA   233
KIR2DL4 allele-7A  ETLQVVGLH.LNQAS.LVSPHTCL   233
KIR2DL4 allele-7B  ETLQVVGLH.LNQAS.LVSSHTCL   233

Transmembrane domain
Consensus          AVIRYSVATIFLTILLFFL
KIR2DL4 allele-1   ...................   259
KIR2DL4 allele-2   I..................   259
KIR2DL4 allele-3   ...................   252
KIR2DL4 allele-4   ...................   252
KIR2DL4 allele-5   V..................   252
KIR2DL4 allele-6   CCD*VLGGHHLPHHPPLLS   252
KIR2DL4 allele-7A  L*LGTRWPPSSSPSSSS.S   252
KIR2DL4 allele-7B  L*LGTRWPPSSSPSSSS.S   252

Cytoplasmic tail
Consensus          HRCWCSDKKNAAVMD
KIR2DL4 allele-1   ...............   274
KIR2DL4 allele-2   L..............   274
KIR2DL4 allele-3   .........ECCCNG   267
KIR2DL4 allele-4   ...............   267
KIR2DL4 allele-5   L..............   267
KIR2DL4 allele-6   PSLLVLRQ.ECCCNG   267
KIR2DL4 allele-7A  IVAGAPT.RMLL*WT   267
KIR2DL4 allele-7B  IVAGAPT.RMLLSWT   267
```

Figure 5.12. The protein sequences of *Mamu-KIR2DL4*-extracellular domain. Dash, no amino acid; dot, similar to consensus sequence; and star (*), stop codon.

```
Signal peptide
Consensus           ---------------------CTGGCCTGTCTTGGGTTCTTCTTGGACCAGAGGGTGCGGGCA
KIR2DL4 allele-1    ATGTCGCCCACGGTCGTCATC.....................................   63
KIR2DL4 allele-2    ATGTCGCCCACGGTCGTCATC.....................................   63
KIR2DL4 allele-3    ---------------------.................G.....................   42
KIR2DL4 allele-4    ---------------------.....................................A....   42
KIR2DL4 allele-5    ---------------------.....................................   42
KIR2DL4 allele-6    ---------------------.....................................   42
KIR2DL4 allele-7A   ---------------------.....................................   42
KIR2DL4 allele-7B   ---------------------.....................................   42

Do domain
Consensus           CACGTGGGTGGTCAGGACAAGCCCTTCTGCTCTGCCTGGCCCAGCGCTGTGGTGCCTCAGGGAGGACACGTGACTCTTTG
KIR2DL4 allele-1    ..........................................................................   143
KIR2DL4 allele-2    ..........................................................................   143
KIR2DL4 allele-3    ........................................G.................................   122
KIR2DL4 allele-4    ..............C.G.....................................................C.....   122
KIR2DL4 allele-5    ..........................................................................   122
KIR2DL4 allele-6    ..........................................................................   122
KIR2DL4 allele-7A   ..........................................................................   122
KIR2DL4 allele-7B   ..........................................................................   122

Consensus           GTGTCACTATCGTCCTGGGTTTAACATCTTCACGCTGTACAAGGAAGACGGGGTGCCTGTCCCTGAGCTCTACAAAAGAA
KIR2DL4 allele-1    ..........................................................................   223
KIR2DL4 allele-2    ..........................................................................   223
KIR2DL4 allele-3    ..........................................................................G  202
KIR2DL4 allele-4    ............................G.............................................   202
KIR2DL4 allele-5    ..........................................................................   202
KIR2DL4 allele-6    ..........................................................................   202
KIR2DL4 allele-7A   ..........................................................................   202
KIR2DL4 allele-7B   ..........................................................................   202

Consensus           TATTCTGGAACAGTTTCCTCATTAGCCCTGTGACTGCAGCACATGCAGGGACCTACAGATGTCGAGTTTTTCATCCGCAC
KIR2DL4 allele-1    ..........................................................................   303
KIR2DL4 allele-2    ..........................................................................   303
KIR2DL4 allele-3    ..........................................................................   282
KIR2DL4 allele-4    ..........................................................................   282
KIR2DL4 allele-5    ..........................................................................   282
KIR2DL4 allele-6    ..................T.......................................................   282
KIR2DL4 allele-7A   ..........................................................................   282
KIR2DL4 allele-7B   ..........................................................................   282

Consensus           TCCCCCACTGAGTGGTCGGCACCCAGCAACCCCCTGGTGATCATGGTCACA
KIR2DL4 allele-1    .....................................................   354
KIR2DL4 allele-2    .....................................................   354
KIR2DL4 allele-3    .....................................................   333
KIR2DL4 allele-4    .....................................................   333
KIR2DL4 allele-5    .....................................................   333
KIR2DL4 allele-6    .....................................................   333
KIR2DL4 allele-7A   .....................................................   333
KIR2DL4 allele-7B   .....................................................   333
```

Figure 5.13. DNA sequences of *Mamu-KIR2DL4*-extracellular domain. Dash, no amino acid; dot, similar to consensus sequence; and star (*), stop codon.

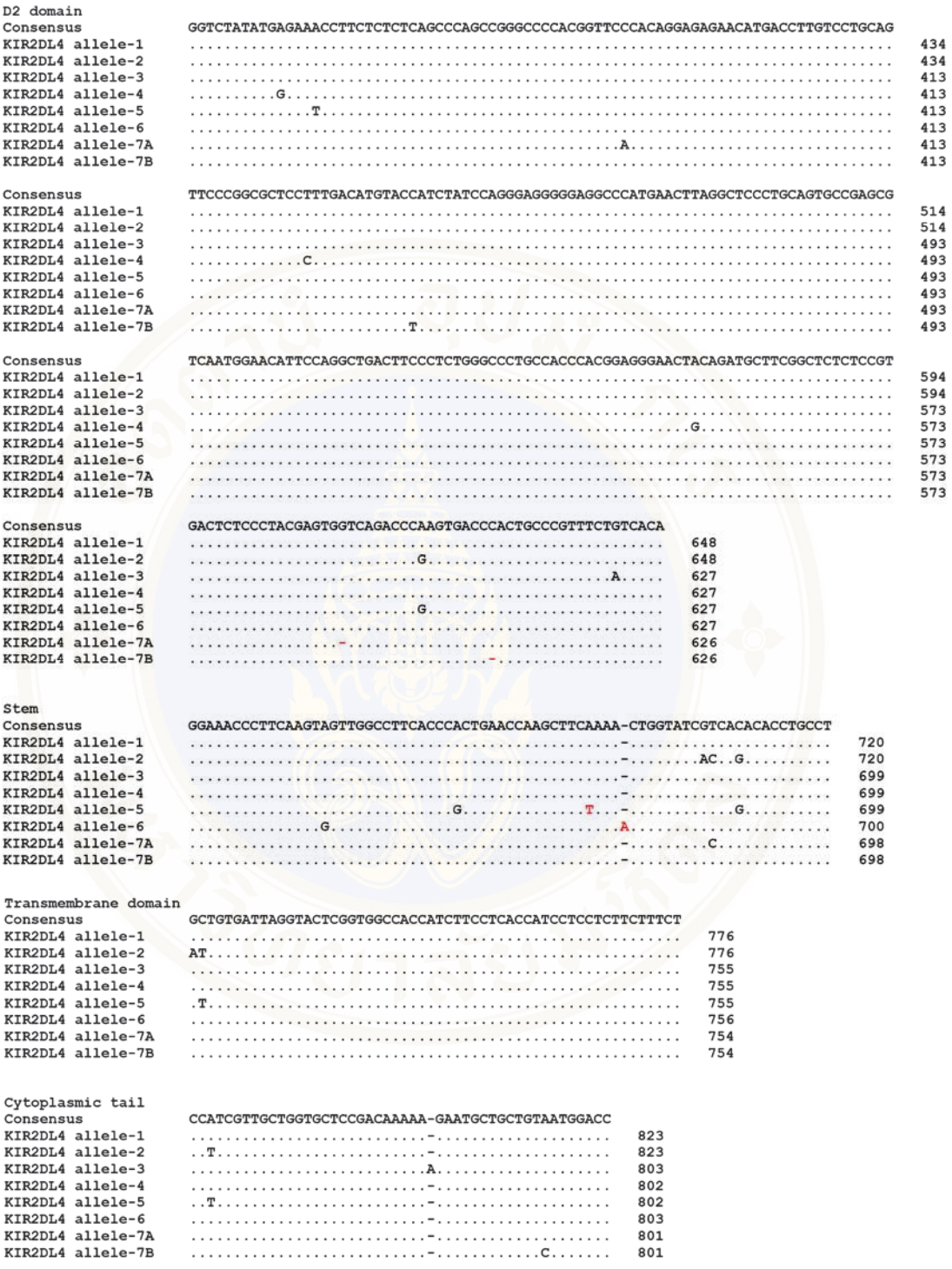

Figure 5.13. DNA sequences of *Mamu-KIR2DL4*-extracellular domain (continued.).

```
Signal peptide
KIR2DL4_allele-5        LACLGFFLDQRVRA  14
2DL4_mm_22_clone_5.seq  ..............
2DL4_mm_25_clone_2.seq  ..............
2DL4_mm_26_clone_1.seq  ..............
2DL4_mm_33_clone_4.seq  ..............
2DL4_mm_04_clone_2.seq  ..............
2DL4_mm_20_clone_1.seq  ..............

D0 domain
KIR2DL4_allele-5        HVGGQDKPFCSAWPSAVVPQGGHVTLWCHYRPGFNIFTLYKEDGVP  60
2DL4_mm_22_clone_5.seq  ............................................
2DL4_mm_25_clone_2.seq  ............................*................
2DL4_mm_26_clone_1.seq  ............................................
2DL4_mm_33_clone_4.seq  ......*.....................................
2DL4_mm_04_clone_2.seq  ............................................
2DL4_mm_20_clone_1.seq  .M..........................................

KIR2DL4_allele-5        VPELYKRIFWNSFLISPVTAAHAGTYRCRVFHPHSPTEWSAPSNPLVIMVT  111
2DL4_mm_22_clone_5.seq  ........................*...................
2DL4_mm_25_clone_2.seq  ...........I................................
2DL4_mm_26_clone_1.seq  ...................V.....*...................
2DL4_mm_33_clone_4.seq  ............................................
2DL4_mm_04_clone_2.seq  ............................................
2DL4_mm_20_clone_1.seq  ............................................

D2 domain
KIR2DL4_allele-5        GLYENPSLSAQPGPTVPTGENMTLSCSSRRSFDMYHLSREGEAHELRLPAV  162
2DL4_mm_22_clone_5.seq  ....K.......................................
2DL4_mm_25_clone_2.seq  ....K.......................................
2DL4_mm_26_clone_1.seq  ....K.......................................
2DL4_mm_33_clone_4.seq  ....K.......................................
2DL4_mm_04_clone_2.seq  ....K.......................................
2DL4_mm_20_clone_1.seq  ....K.....*.............................K.....

KIR2DL4_allele-5        PSVNGTFQADFPLGPATHGGNYRCFGSLRDSPYEWSDPSDPLPVSVT  209
2DL4_mm_22_clone_5.seq  ............................................
2DL4_mm_25_clone_2.seq  ............................................
2DL4_mm_26_clone_1.seq  ..................................L.........
2DL4_mm_33_clone_4.seq  ............................................
2DL4_mm_04_clone_2.seq  ..............................*...A.........
2DL4_mm_20_clone_1.seq  ............................................

                        Stem                TM
KIR2DL4_allele-5        GNPSSSWPSPAEPSF*TGIVRHLPVVIRYSV 240
2DL4_mm_22_clone_5.seq  ..........T....K....T...A......
2DL4_mm_25_clone_2.seq  ..........T....K....T...A......
2DL4_mm_26_clone_1.seq  ..........T....K....T...A......
2DL4_mm_33_clone_4.seq  ..........T....K........A......
2DL4_mm_04_clone_2.seq  ..........T....K...T....I......
2DL4_mm_20_clone_1.seq  ..........T....K..F.T...A......
```

Figure 5.14. Protein sequences of *predicted-Mamu-KIR2DL4 allele-5.* Dot, similar to *allele-5*; star (*), stop codon

Table 5.7. Percentage of *predicted Mamu-KIR2DL4 allele-5* to *allele-5*, at amino acid homology.

				% amino acid homology							
	Mamu-KIR2DL4 alleles			*Allele-5*		*Predicted allele-5*					
		Cohort		HVL						LVL	
			Sample ID	mm 07 clone 3	mm 08 clone 2	mm 22 clone 5	mm 25 clone 2	mm 26 clone 1	mm 33 clone 4	mm 04 clone 2	mm 20 clone 1
% DNA homology	*Allele-5*	HVL	mm 07 clone 3		95.5	98.1	97.8	97.4	97.4	96.3	97.0
			mm 08 clone 2	98.0		96.6	96.3	95.9	97.4	97.8	95.9
	Predicted allele-5		mm 22 clone 5	99.1	98.1		98.9	99.3	98.5	97.4	98.1
			mm 25 clone 2	99.1	98.1	99.3		98.1	98.1	97.0	97.8
			mm 26 clone 1	99.1	98.1	99.5	99.3		97.8	96.6	97.4
			mm 33 clone 4	98.6	98.4	98.8	98.8	98.8		98.1	97.4
		LVL	mm 04 clone 2	98.0	99.0	98.1	98.1	98.1	98.4		96.3
			mm 20 clone 1	98.9	97.9	99.0	99.0	99.0	98.5	97.9	

5.2.2. *Mamu-KIR2DL4* intracellular domain

5.2.2.1. Intracellular *Mamu-KIR2DL4* amplification and cloning

cDNA samples from 9 animals (5 RM-HVL and 4 RM-LVL cohorts), which showed positive *Mamu-KIR2DL4*-extracellular region amplification, were amplified for intracellular *Mamu-KIR2DL4* domain by using KIR2D4FL-KIR2D4RL1 primer pair. The predicted amplicon size was approximately 819 bp with a coding region from nucleotide 433 to 1,252 (from part of D2 domain to the end of the cytoplasmic tail) based on the numbering used in GeneBank for *Mamu-KIR2DL4* gene (ac. no. AY728182) (Figure 5.8). The PCR products were run on the 1% agarose-gel electrophoresis (Figure 5.15), and then, samples were cut and purified for cloning.

5.2.2.2. Intracellular *Mamu-KIR2DL4* polymorphisms

The stem, TM, and the cytoplasmic tail of the *Mamu-KIR2DL4*

sequences were also amplified from these 9 animals from our cohort. These sequences including the ITIMs were found to share >98% homology to previously published data and, surprisingly, each of these were associated with the extracellular domain of *allele-2* (Figure 5.16). Although the full-length protein could not be amplified, overlapping sections of the extracellular and the intracellular domains were aligned to ensure complete coverage of the cDNA.

A

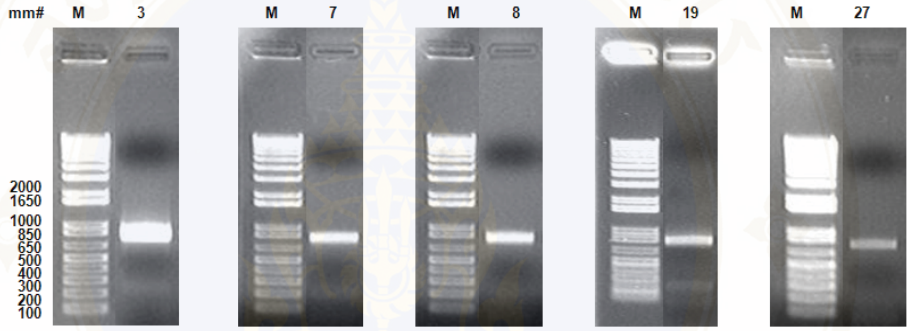

B

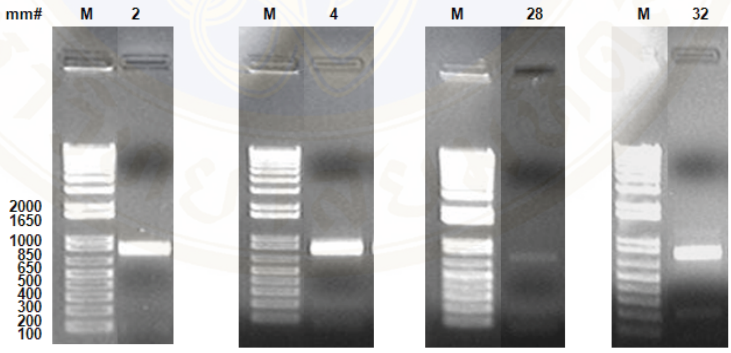

Figure 5.15. The amplified products of *Mamu-KIR2DL4* intracellular domain on gel electrophoresis. cDNA samples were amplified for their *Mamu-KIR2DL4* intracellular domain from 9 RMs which were positive *Mamu-KIR2DL4* extracelular domain clones. 5 RM-HVL cohort (A) and 4 RM-LVL cohort (B) were positive for *Mamu-KIR2DL4* intracelllar region cloned by using KIR2D4FL-KIR2D4RL1 primer pair. The predicted amplicon size was 819 bp. Where M is the 1 Kb plus DNA Ladder marker.

```
                    Signal peptide D0 domain
Extracellular region  LACLGFFLDQRVRA HVGGQDKPFCSAWPSAVVPQGGHVTLWCHYRPGFNIFTLYKEDGVP 60
Intracellular region  -------------- ---------------------------------------------- 1

                                                                          D2 domain
Extracellular region  VPELYKRIFWNSFLISPVTAAHAGTYRCRVFHPHSPTEWSAPSNPLVIMVT GLYEKPSLS 120
Intracellular region  ------------------------------------------------- --------- 1

Extracellular region  AQPGPTVPTGENMTLSCSSRRSFDMYHLSREGEAHELRLPAVPSVNGTFQADFPLGPATH  180
Intracellular region  -----------------...................H.............L.......  43

                                                Stem                      TM
Extracellular region  GGNYRCFGSLRDSPYEWSDPSDPPPVSVT GNPSSSWPSPTEPSFKTGITRHLP IVIRYSV240
Intracellular region  ........................... ......................... .......103

                      Cytoplasmic tail
Extracellular region  ATIFLTILLFFL LRCWCSDKKNAAVMD-------------------------------- 267
Intracellular region  ............ ...............PEPAGDRTVNREDSDEQDPQEVTYTQLDHCVFT 163

Extracellular region  ------------------------------------------------------------  267
Intracellular region  RGKITRPSLRPKTPPTDTSVYIELPNAEPRSLSPAHEHHRQAWRGLLGRQQPCLKTGFTA  223

Extracellular region  ---------------------------------------------               267
Intracellular region  PVPAAGISLDSASSIALPHTTNLLALSCLPMSVVPTACWRENALLCL               270
```

Figure 5.16. Merge protein sequences between the extracellular and the intracellular domains of *Mamu-KIR2DL4*. Pairwise alignment analysis were performed from translated protein sequences of mm4 clone 1 that were amplified by using KIR2DL4PSF7-KIE2DL4PSR12 and KIR2D4FL-KIR2D4RL1 primer pairs for Mamu-KIR2DL4 extracellular and for intracellular regions, respectively.

5.3. *Mamu-KIR2DL5* gene

5.3.1. *Mamu-KIR2DL5* gene amplification and cloning

Mamu-KIR2DL5 was amplified for the full-length of the cDNA, from the signal sequence to the complete cytoplasmic tail based on GenBank ac. no. AF334646 could span nucleotide from 13 to 1,133 (amplicon size 1,121 bp). PCR products from 16 animals (8 RM-HVL and 8 RM-LVL) were loaded into 1% agarose-ethidium bromind gel electrophoresis as shown in the Figure 5.17. Nine of these 16 animals (5 RM-HVL and 4 RM-LVL cohorts) were positive for *Mamu-KIR2DL5* amplification. Each band was cut and cloned into vector. Purified plasmids were sequenced and analyzed by using T7 and SP6 analysis.

5.3.2. *Mamu-KIR2DL5* gene polymorphisms

Only three different animals from these nine purified plasmids, five clones per animal, gave results with most of the sequences that have already been previously published for *Mamu-KIR2DL5 allele-1* (refer to GenBank ac. no. AF334646). The phylogenetic tree and multiple alignment analysis showed the identities scores of sample sequences to *allele*-1 and *2* (Figure 5.18). In addition, two different animals (sample ID; mm8 and mm21) had 98% aa homology to *allele-1* whereas sample ID mm 7 had 73% aa homology to *allele-1* (Figure 5.19). All five clones from mm 7 had D2 domain deletion. However they were not indicated into either new allele/variant or new KIR1D molecule. Because the amounts of samples generated the clones obtained from the same animal and the efficientcy of the primer pair used to generate the clones is too low. In addition, other seven animals were identified as *Mamu-KIR3DL20* (refer to GenBank ac no. NM_001104552) as described in previous study (38), *Mamu-KIR2DL5* gene was identical to *Mamu-KIR3DL20* and it is likely that these were alternatively spliced transcripts from the same locus because there has been speculated to represent an evolutionary intermediate between these two genes (38). Bimber *et al* hypothesized that *KIR2DL5* gene was the *KIR3DL* allele which lacks D1 domain and it was nonfunction. We were also attempted to amplify, clone and sequence alleles encoded by the *Mamu-KIR2DL5*

locus using the different sets of primer pairs (Table 5.8) in an attempt to generate sufficient data. Unfortunately, all of these primer pairs did not work (data not shown).

A

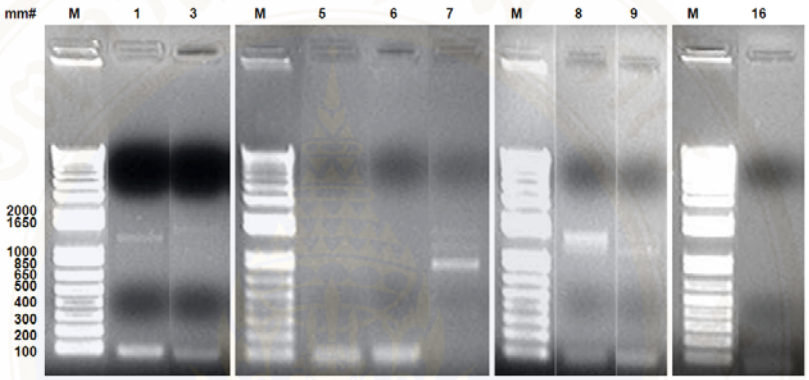

B

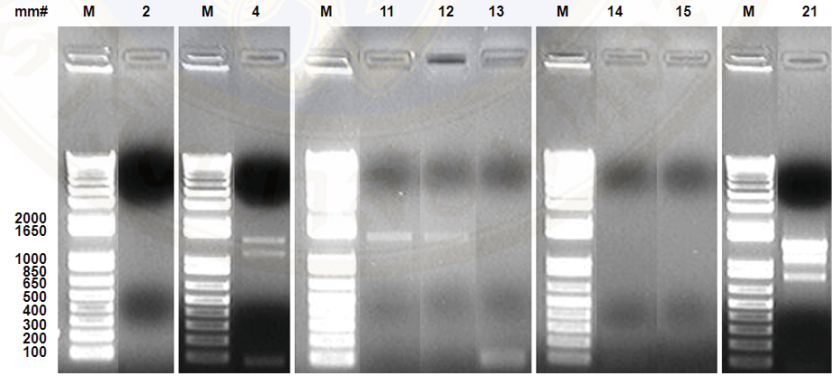

Figure 5.17. The amplified *Mamu-KIR2DL5* products on gel electrophoresis. cDNA samples were amplified for the full length of *Mamu-KIR2DL5* gene from 8 RM-HVL cohort (A) and 8 RM-LVL cohort (B) by using KIR2D5FL2-KIR2D5RL1 primer pair. The predicted amplicon size was 1,121 bp where M is the 1 Kb plus DNA Ladder marker.

Table 5.8. The primer pairs for Mamu-KIR2DL5 amplification.

Primer name	Direction	Sequence 5' to 3'	length (bp)
KIR2D5F	Forward	CCCCACGGTTCAGGCAGGAGAG	22
KIR2D5FL2	Forward	ATGGCATGTGTTGGGTTCTTCTTG	24
KIR2D5R	Reverse	ACATAGGGCAGGGCACGGAAAGAG	24
KIR2D5RL	Reverse	GGGCAGGGATCAAGTGAAGTGGAG	24
KIR2D5RL1	Reverse	GCAGAGTCGCGCCTTCAGATTCCT	24

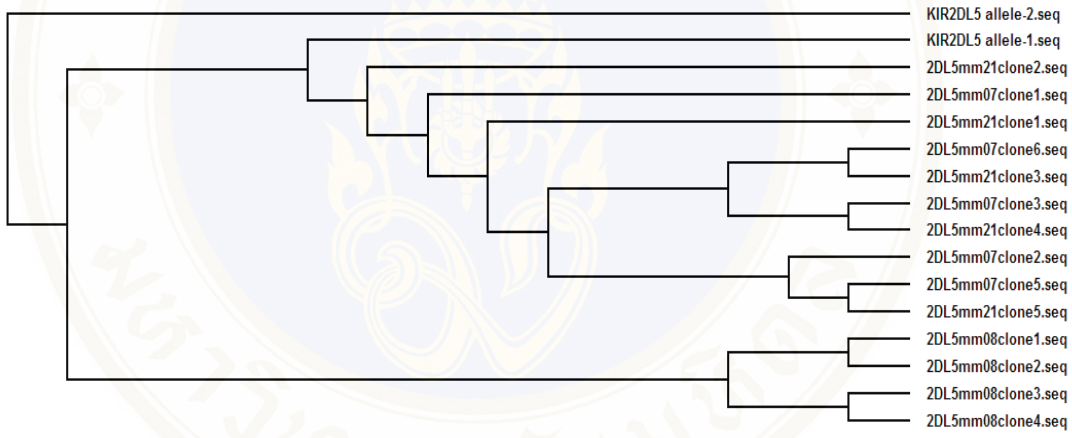

Figure 5.18. Phylogenetic tree of *Mamu-KIR2DL5* gene at the protein level. Rectangular cladogram was analyzed by using BioEdit software version 7.0.9, by Tom Hall, Ibis Therapeutics, Carlsbad, CA.

```
Signal peptide
KIR2DL5 allele-1  MVISMACVGFFLLQRAWS 18
KIR2DL5 allele-2  ..................  18
2DL5mm07clone1    -----GM...........  13
2DL5mm07clone2    ----..............  14
2DL5mm07clone3    ----..............  14
2DL5mm07clone5    ----..............  14
2DL5mm07clone6    ----.............P  14
2DL5mm08clone1    ----..............  14
2DL5mm08clone2    ----..............  14
2DL5mm08clone3    ----------------  1
2DL5mm08clone4    ----..............  14
2DL5mm21clone1    ----..............  14
2DL5mm21clone2    ----..............  14
2DL5mm21clone3    ----..............  14
2DL5mm21clone4    ----..............  14
2DL5mm21clone5    ----..............  14
D0 domain
KIR2DL5 allele-1  HVDGQDKPFLSAWPSAVVPQGEHVSLQCHSHLGFTIFSLYKEDGVPAPELYNRRFWKDILLGPVTPAHAGTYRCRGSHLHSPTEWSAPSNPLVITVT 115
KIR2DL5 allele-2  ..................................................................................................... 115
2DL5mm07clone1   ..................................................................................................... 110
2DL5mm07clone2   ..................................................................................................... 111
2DL5mm07clone3   ..................................................................................................... 111
2DL5mm07clone5   ..................................................................................................... 111
2DL5mm07clone6   ..................................................................................................... 111
2DL5mm08clone1   ..................................................................................................... 111
2DL5mm08clone2   ..................................................................................................... 111
2DL5mm08clone3   --.................................................................................................  95
2DL5mm08clone4   ..................................................................................................... 111
2DL5mm21clone1   ..................................................................................................... 111
2DL5mm21clone2   ..................................................................................N........ 111
2DL5mm21clone3   ..................................................................................................... 111
2DL5mm21clone4   ........P.............................................................................. 111
2DL5mm21clone5   ..................................................................................................... 111
D2 domain
KIR2DL5 allele-1  GLYGKPSLSAQPGPTVQAGENVTLSCSSQSSFDIYRLSRDGEAHGLRLPAVPRVSGTFKADFPLGPATHGGNYRCFGSFRALPYVWSHPSDPLPISVT 213
KIR2DL5 allele-2  .V.....................................................A..................... 213
2DL5mm07clone1   ----------------------------------------------------------------------------------- 111
2DL5mm07clone2   ----------------------------------------------------------------------------------- 111
2DL5mm07clone3   ----------------------------------------------------------------------------------- 111
2DL5mm07clone5   ----------------------------------------------------------------------------------- 111
2DL5mm07clone6   ----------------------------------------------------------------------------------- 111
2DL5mm08clone1   ..................................................................................F.. 209
2DL5mm08clone2   ..................................................................................F.. 209
2DL5mm08clone3   ..................................................................................... 193
2DL5mm08clone4   ..................................................................................... 209
2DL5mm21clone1   .V.............R.....................................................A..................... 209
2DL5mm21clone2   .V..........X.....................................................A..................... 209
2DL5mm21clone3   .V.........................L.....................................A..................... 209
2DL5mm21clone4   .V.............................C.....................S..........A..................... 209
2DL5mm21clone5   .V........R.....................................................................P.. 209

Stem                                                                  Transmembrane domain
KIR2DL5 allele-1  GNSSSTWSSPTEPSSNTGIPRHLH 237                       KIR2DL5 allele-1  VLIGTSVVIIPFTILFFFLL 257
KIR2DL5 allele-2  ......................... 237                       KIR2DL5 allele-2  ...VS..........L.... 257
2DL5mm07clone1    ......................... 134                       2DL5mm07clone1    ..................... 154
2DL5mm07clone2    ......................... 135                       2DL5mm07clone2    ..................... 155
2DL5mm07clone3    ......................... 135                       2DL5mm07clone3    ..................... 155
2DL5mm07clone5    ......................... 135                       2DL5mm07clone5    ...........Y......... 155
2DL5mm07clone6    ......................... 135                       2DL5mm07clone6    ..................... 155
2DL5mm08clone1    ......................... 233                       2DL5mm08clone1    ...VS..........L.... 253
2DL5mm08clone2    ......................... 233                       2DL5mm08clone2    ...VS..........L.... 253
2DL5mm08clone3    ......................... 217                       2DL5mm08clone3    ...VS..........L.... 237
2DL5mm08clone4    ......................... 233                       2DL5mm08clone4    ...VS..........L.... 253
2DL5mm21clone1    ......................... 233                       2DL5mm21clone1    ..................... 253
2DL5mm21clone2    ......................... 233                       2DL5mm21clone2    ..................... 253
2DL5mm21clone3    ......................... 233                       2DL5mm21clone3    ..................... 253
2DL5mm21clone4    ......................... 233                       2DL5mm21clone4    ..................... 253
2DL5mm21clone5    ......................... 233                       2DL5mm21clone5    ..................... 253
Cytoplasmic tail
KIR2DL5 allele-1  HRWCSNKKNAAVMDQEPAGDRTVNREDSDEPDPQEVTYAQLDHRVFTQRKITRPSQRPKRPPTDTSVYIELPNAEPRSLSPAR 340
KIR2DL5 allele-2  .C.............................QG...................A.............................. 340
2DL5mm07clone1    ..................................................................................... 237
2DL5mm07clone2    ..................................................................................... 238
2DL5mm07clone3    ..................................................................................... 238
2DL5mm07clone5    ..................................................................................... 238
2DL5mm07clone6    ..................................................................................... 238
2DL5mm08clone1    ..........................................I.......................................... 336
2DL5mm08clone2    ..........................................I.......................................... 336
2DL5mm08clone3    ..........................................I.......................................... 320
2DL5mm08clone4    ..........................................I.......................................... 336
2DL5mm21clone1    ..................................................................................... 336
2DL5mm21clone2    ..................................................................................... 336
2DL5mm21clone3    ..................................................................................... 336
2DL5mm21clone4    ..................................................................................... 336
2DL5mm21clone5    ......................D.............................................................. 336

KIR2DL5 allele-1  EHQSQALRGSSRETTALSQTQLASSNVPAAGIRRDSASDIALPHTTNLNVPLSCLPMSKV 400
KIR2DL5 allele-2  ....................................G..................... 400
2DL5mm07clone1    ..................................----------------------- 273
2DL5mm07clone2    ..................................----------------------- 274
2DL5mm07clone3    ..................................----------------------- 274
2DL5mm07clone5    ..................................----------------------- 274
2DL5mm07clone6    ..................................----------------------- 274
2DL5mm08clone1    ..................................----------------------- 372
2DL5mm08clone2    ..................................----------------------- 372
2DL5mm08clone3    ..................................----------------------- 356
2DL5mm08clone4    ..................................----------------------- 372
2DL5mm21clone1    ..................................----------------------- 372
2DL5mm21clone2    ..................................----------------------- 372
2DL5mm21clone3    ..................................INCGRLQVDHMES----SH---- 388
2DL5mm21clone4    ..................................----------------------- 372
2DL5mm21clone5    ..................................INCGRLQVDHMGE------NAX- 391
```

Figure 5.19. Multiple alignment analysis of amplified *Mamu-KIR2DL5* sample sequences. Clone from 3 animals were aligned for the translated protein sequences as compared with previously published for *Mamu-KIR2DL5 allele-1* and *2*.

```
Signal peptide
KIR3DL20          STMSLMVISMACVGFFLLQRAWS 23
KIR2DL5_allele-1  ----------.......... 18
KIR2DL5_allele-2  ----------.......... 18

D0 domain
KIR3DL20          HVDGQDKPFLSAWPSAVVPQGEHVSLQCHSHLGFTIFSLYKEDGVPAPELYNRRFWKDILLGPVTPAHAGTYRCRGSHLHSPTEWSAPSNPLVITVT 120
KIR2DL5_allele-1  ..................................................................................................... 115
KIR2DL5_allele-2  ..................................................................................................... 115

D1 domain
KIR3DL20          GVYRKPSLLAHPGPLVKSGEMVVLQCWSDMRFEHFLLHREGITEDPLHLTGQLHDGGSQANSSVGPMIPALAGTYRCFGSVAYSPYEWSAPSDPLDIVII 220
KIR2DL5_allele-1  ----------------------------------------------------------------------------------------------- 115
KIR2DL5_allele-2  ----------------------------------------------------------------------------------------------- 115


D2 domain
KIR3DL20          GLYGKPSLSAQPGPTVQAGENVTLSCSSQSSFDIYRLSRDGEAHGLRLPAMPRVSGTFKADFPLGPATHGGNYRCFGSFRALPYVWSHPSDPLPISVT 318
KIR2DL5_allele-1  ..................................................V..................................................... 213
KIR2DL5_allele-2  .V................................................V.................A.......................... 213

Stem                                                                Transmembrane domain
KIR3DL20          GNSSSTWSSPTEPSSNTGIPRHLH 3342                     KIR3DL20          VLIGTSVVIIPFTILFFFLL 362
KIR2DL5_allele-1  ......................... 237                     KIR2DL5_allele-1  ..................... 257
KIR2DL5_allele-2  ......................... 237                     KIR2DL5_allele-2  ...VS.........L.... 257

Cytoplasmic tail
KIR3DL20          HRWCSNKKNAAVMDQEPAGDRTVNREDSDEPDPQEVTYAQLDHRVFTQRKITRPSQRPKRPPTDTSVYIELPNAEPRSLSPAREHQSQALRGSSRETTA 461
KIR2DL5_allele-1  ..................................................................................................... 356
KIR2DL5_allele-2  .C............................QG..................A..................................................... 356

KIR3DL20         LSQTQLASSNVPAAGI 477
KIR2DL5_allele-1  ................ 372
KIR2DL5_allele-2  ................ 372
```

Figure 5.20. Multiple alignment analysis between *Mamu-KIR2DL5* and *Mamu-KIR3DL20*. The sequences illustrared *Mamu-KIR3DL20*, *Mamu-KIR2DL5 allele-1* and *allele-2* refer to GenBank ac no. NM_001104552, AF334646, and AF334647, respectively.

5.4. The evolution of KIR family

Study on the evolutionary biology of *KIR* genes and their association with SIV infection in macaques was characterized by using KIR cDNA clones from our cohort. The alleleles/variants of Mamu-KIRs were also aligned and analyzed for the phylogenetic tree to exchange of KIR genes between the Old World monkeys and hominoids by using the NCBI and the EBI databases.

5.4.1. The diversity of *Mamu-KIR* genes in SIV-infected RMs associated with plasma VLs.

Although the initial studies of KIR polymorphisms in RMs were carried out by Hershberger *et al* (10) who defined 5 different KIR genes, the degrees of KIR gene polymorphism associated with SIV infection unwire not clear. Our laboratory has previously described the association of genetic variation of *Mamu-KIR3DL* alleles that observed from purified NK cells in a cohort of SIV-infected RMs which were also utilized in this study (2). In the present study, we have succeed to observations of the additional *Mamu-KIR* genes including *Mamu-KIR1D, Mamu-KIR2DL4* and *Mamu-KIR3DH* (unpublished) to increase our knowledge in the KIR polymorphisms, the genetic linkage between genes, and the potential role of KIRs in influencing plasma VLs and SIV pathogenesis. KIR cDNA sequence analysis showed highly variable sites of *KIR* genes and polymorphisms. Individual allelic expressions of Mamu-KIR family from individual animals in our cohort were investigated and identified. These include 11 alleles from *Mamu-KIR1D* gene, 7 alleles from *Mamu-KIR2DL4* gene, 14 alleles from *Mamu-KIR3DH* gene, and 14 alleles from *Mamu-KIR3DL* gene (Table 5.9) (2). The cDNA sequences were encoded into protein sequences, subsequently; the consensus sequences were aligned and created into phylogenetic tree by using Protdist and Neighbor-Joining analysis, BioEdit software version 7.0.9, created by Tom Hall, Ibis Therapeutics, Carlsbad, CA, USA (Figure 5.21). A phylogram showed the branch lengths proportional to distance of *Mamu-KIR* genes that represented the relationship between alleles. *Mamu-KIR3DH* shared a internal node with *Mamu-KIR3DL* and closely related to *Mamu-KIR2DL4* as described in previous study (2), they have designated them as *3DH*, where H denotes a hybrid molecule.

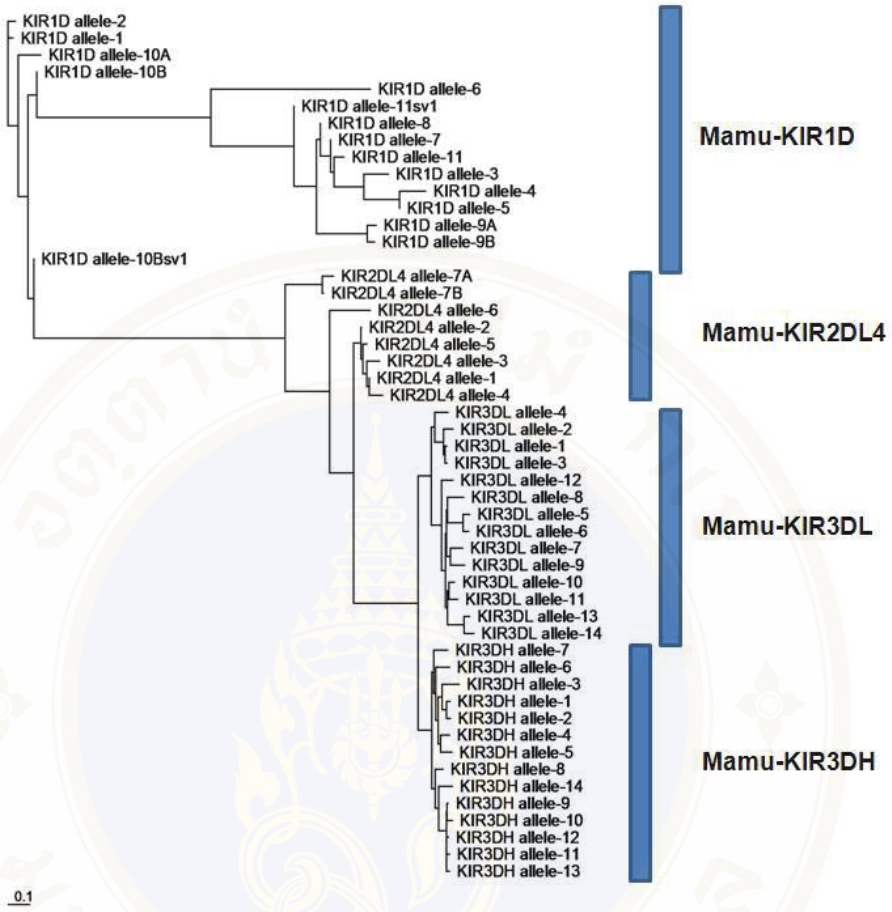

Figure 5.21. Phylogenetic tree of Mamu-KIR family at protein level. Vertical bars indicate phylogenetic groups. A phylogram was analyzed by using BioEdit software version 7.0.9 (by Tom Hall, Ibis Therapeutics, Carlsbad, CA) that showed the branch lengths of distance.

Table 5.9. Mamu-KIR genotypic expressions of SIV-infected RMs in our cohort (2).

Sample ID	Cohort	KIR allelic expression			
		KIR1D gene[a]	*KIR2DL4 gene*[b]	*KIR3DH gene*[c]	*KIR3DL gene*[d]
mm01	HVL	allele-1, 6	allele-1	allele-14	allele-6, 9
mm03	HVL		allele-1, 3	allele-6, 9	allele-2,13
mm05	HVL				
mm06	HVL				
mm07	HVL	allele-2, 10Bsv1	allele-1, 5	allele-1	
mm08	HVL		allele-2, 5	allele-2	allele-7, 11, 14
mm09	HVL			allele-8	allele-10, 12, vA[f]
mm10	HVL	allele-1, 3	allele-1	allele-11	allele-2, 5
mm16	HVL				allele-14
mm17	HVL				
mm18	HVL	allele-7, 11	allele-1, 6, 7B	allele-3, 10	allele-13
mm19	HVL	allele-7, 8, 9A, 9B	allele-1, 2	allele-8	allele-13
mm22	HVL	allele-1, 3, 10B	allele-1, p5[e]		
mm23	HVL	allele-1, 2	allele-1, 6		allele-5, 13
mm24	HVL		allele-2	allele-3, 13	allele-3, 8, 13,vA[f]
mm25	HVL		allele-1, 2, p5[e]		
mm26	HVL	allele-8, 11	allele-1, p5[e]		allele-5
mm27	HVL		allele-1, 4	allele-14	allele-13
mm29	HVL	allele-3, 5	allele-1	allele-10, 11	allele-1
mm33	HVL		allele-2, p5[e]	allele-7	allele-1, 8
mm02	LVL		allele-2	allele-1, 9	allele-1, 7
mm04	LVL		allele-2, p5[e]		allele-1, 10
mm11	LVL				allele-8
mm12	LVL			allele-4	allele-8
mm13	LVL				
mm14	LVL		allele-1, 7A		allele-12
mm15	LVL	allele-1, 5, 6	allele-1		
mm20	LVL	allele-1, 2, 5	allele-1, 2, p5[e]		allele-1, vA[f]
mm21	LVL	allele-1, 10A	allele-1		allele-4, 6
mm28	LVL	allele-1, 4	allele-2	allele-7	
mm30	LVL				allele-11
mm31	LVL				
mm32	LVL		allele-2	allelle-5	allele-13, vA[f]
mm34	LVL		allele-2	allele-14	allele-10, 13
mm35	LVL		allele-2	allele-7	allele-3, 8
mm36	LVL			allele-4, 8	allele-8, vA[f]
mm37	LVL	allele-1, 3	allele-2	allele-7, 9	allele-13
mm38	LVL	allele-7, 8, 11sv1	allele-1	allele-12	allele-8

[a]*Mamu-KIR1D allele-1* to *8, 9A, 9B, 10A, 10B, 10Bsv1, 11,* and *11sv1* refer to ac. no. AY728181, AF334635, AF334636, AF334638, AF334640, AF334643, FJ217804, FJ217805, GU564169 to GU564175; [b]*Mamu-KIR2DL4 extracellular domain allele-1* to *7A,* and *7B* refer to ac.no. EU702486, AY728182, GU564176 to GU564181; [c]*Mamu-KIR3DH allele-1, allele-4* to *14* refer to ac.no. GU564157, GU564158 to GU564168; [d]*Mamu-KIR3DL allele-1* to *14* refer to ac. no. FJ562108-FJ562121; [e]p5 means *predicted Mamu-KIR2DL4 allele-5*; and [f]vA means *Mamu-KIR3DL variant A.*

Table 5.10. Diversity of Mamu-KIR genes in the cohort.

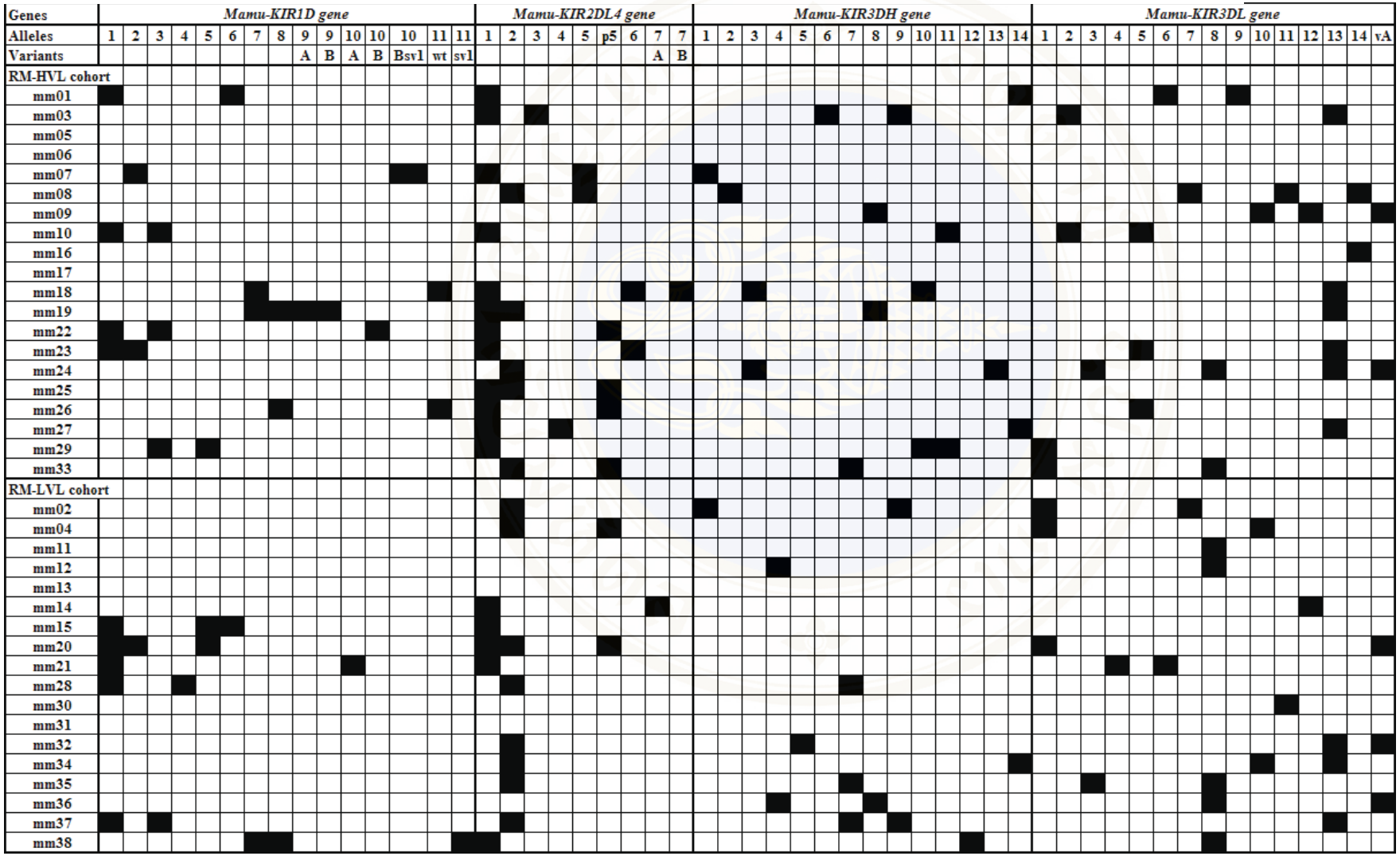

Diversity of Mamu-KIR allelic expressions in the individual animals (Table 5.10) from our cohort was characterized into clusters as described in the previous section.Briefly, Mamu-KIR1D-Cluster I (denoted *1D*i* genotype containing *allele-3, 4, 5, 7, 8, 9,* and *11*) and Cluster-II (denoted *1D*n* genotype containing *allele-1, 2, 6,* and *10*); *Mamu-KIR2DL4 allele-1, 2, 3, 4,* and truncated protein (denoted *2DL4*t* genotype containing *Mamu-KIR2DL4 allele-5* through *allele-7* and *predicted allele-5*); Mamu-KIR3DH including HVL-alleles or *3DH*h* genotype (*allele-2, 3, 6, 10, 11, 13,* and *14*), LVL-alleles or *3DH*l* genotype (*allele-4, 5,* and *12*), and others (*allele-1, 7, 8,* and *9*); and finally, *Mamu-KIR3DL alleles* which were regarded as the SNP at position H159Q containing *allele-13* and *14*, denoted *3DL*q* genotype, while at the same position H159H containing *allele-1* through *allele-12* and *variant A,* denoted *3DL*wt* genotype (Table 5.11). Five animals in our cohort were undetectable for their allelic expression of KIRs as measured with these primer sets.Additionally, these five animals obtained from 3 samples in RM-HVL cohort (sample ID mm 5, 6, and 17) and 2 samples in RM-LVL cohort (sample ID mm 13 and 31).

The odds ratio (OR) analysis were aimed to identify any statistical significance ($p < 0.05$) of the association between *Mamu-KIR* genotypes with high as compared with low VLs (Table 5.12). The homozygous *Mamu-KIR3DH*h/*h* genotype showed high expression in SIV-infected RMs with high levels of plasma VLs when compared to infectious macaques with low VLs (OR = 21.67, p = 0.047). Meanwhile macaques in LVL cohort had high expression of *Mamu-KIR3DH*l/*l* genotype. Interestingly, Mamu-KIR alleles showing statistical significance with influencial by VLs were the animals that expressed the *Mamu-KIR3DH*h/*h* or **h/*allele-9* genotype as compared with animals that expressed the *Mamu-KIR3DH*l/*l* or **l/*allele-8* genotype giving OR equal 35.00 (p = 0.015) (Table 5.12). When association between multiple Mamu-KIR loci and VLs were analyzed, animals expressing *Mamu-KIR3DH*h/*h* or **h/*allele-9* combined with *Mamu-KIR3DL*q/*wt* were associated with high VLs as compared with animals that expressed *Mamu-KIR3DH*l/*l* or **l/*allele-8* combined with *Mamu-KIR3DL*q/*wt* in low VLs (OR = 25.67, p = 0.034). These data provide support to the view that select Mamu-KIR loci appear to be associated with influencing plasma VLs in SIV-

infected RMs. A trend forward showed the animals with high VLs had pattern of Mamu-KIR expression in *1D*i/*i-2DL4*1/*1-3DH*h/*h-3DL*q/*q* genotypes whereas the animals with low VLs had *1D*n/*n-2DL4*2/*2-3DH*l/*l-3DL*wt/*wt* genotypes. Interestingly, *Mamu-KIR1D* genotypes associated with plasma VLs related to the regulation of signal transduction in the inhibitory NK cell activity. Because animals who had *Mamu-KIR1D*i/*i* genotype could show high expression of KIR1D molecues containing ITIMs in their cytoplasmic tail and plays an important role in the inhibition of the infected cell killing by NK cells. By contrast, the SIV-infected RMs who had chronic infectious disease associated with *Mamu-KIR1D*n/*n* genotype that was a null phenotype. Genotypic variations of other KIRs in this study were associated with diversity of KIR polymorphisms that plays roles in the diagnosis for separation of acute and chronic infection. Although the relationship between *Mamu-KIR3DH* and *Mamu-KIR3DL* genes had a statistically significant difference giving a p-value for 0.034, unfortunately, our observation was not found the genetic linkage of all five KIR loci in the family. Despite that there were two animals in RM-HVL cohort had *Mamu-KIR1D*i/2DL4*1/3DL*q* genotypes and 3 animals in the same cohort had *Mamu-KIR2DL4*1/3DH*h/3DL*q* genotype, while these two genotyoes were no found in RM-LVL cohort. The data showed low level of animals had the *Mamu-KIR1D* either **i,*n* or both alleles combined with *Mamu-KIR3DH*h* and **o* alleles, but the combinated expression of *KIR1D* with *KIR3DH*l* allele was not found (Table 5.13).

5.4.2. Forming new *KIRs* in the lineages of Old World monkeys and Hominoids

Gibbs *et al* who analyzed to understand the evolution of gemomic DNA in the human-chimpanzee-RM (HCR) trio that described in the RM genome sequencing and analysis consortium in 2007 (44). They proposed that RM is closely related to human and shares a last common ancestor from about 25 Mya (44). The genomic sequences were also identified into the lineage-specific expansions and contraction of gene families. For KIR loci, Rajalinggam R and colleges proposed in 2004 (42), the genomic DNA of individual KIR domains and their full-length from favored animal models such as gorilla (*Gorilla gorilla*, Gg), common chimpanzee

(*Pan troglodytes*, Pt), Bonobo or Pygmy chimpanzee (*Pan paniscus*, Pp), orangutan (*Pongo pygmaeus*, Popy), rhesus macaque (*Macaca mulatta*, Mm), and human (*Homo sapien*s, Hu) showed five major lineages (42). In recent study, Bimber *et al* determined the KIR loci of Mauritian cynomolgus macaque (*Macaca fascicularis*, Mf) and designed the microsatellite model to compare these KIR loci with Mamu-KIR loci. Therefore, we attempted to challenge the new Mamu-KIR sequences in our study with previous KIRs with those of other Old World monkeys and hominoids and to provide an excellent system for identification of closely related species. On the basic of overall sequence similarity and phylogenetic analysis of the complete cDNA sequences, *Mamu-KIR1D* and *Mamu-KIR2DL4* genes appear closely related to *Mf-KIR1D* and *Mf-KIR2DL4* genes, respectively. Phylogenetic analysis of *KIR1D* genes from RM, Mauritian cynomolgus macaque, and human (no publishing from other species) were performed by using BioEdit software version 7.0.9 (Figure 5.22). A phylogram showing the distances between individual sequences containing *Mamu (Mm)-KIR1D allele-1* to *allele-11* include their variants, *sv-3, sv-5, sv-7,* and *sv-8*; three sequences of *Mf-KIR1D* in the GenBank ac. no. EU419110, EU419120, and EU419124; *Hu-KIR1D* alleles/variants refer to the GenBank in the numbering of AY102623 and AY102624. Subsequently, seven groups were created according to a shared ancestor (internal node) as shown in Figure 5.22; lineage I (*Hu-KIR1D* alleles) and II (*Mamu-KIR1D allele-1, 2,* and *10*) had long distance for 0.72667 in length. Additionally, a pairwise alignment analysis showed a new *Mamu-KIR1D allele-10* and their variants were close to *Hu-KIR1D* at ~43% aa homology. While the distance between Mamu-KIR1D (lineage V) and Mf-KIR1D (lineage VI) had 0.06316 in length that related to the pairwise alignment analysis which showed that a new *Mamu-KIR1D allele-11* and previous *Mamu-KIR1D allele-7* were close to *Mf-KIR1D alleles* (ac. no. EU419110 and EU419124) at ~88% aa homology. Generation of a rectangular cladogram for KIR2DL analysis according to the NCBI and EBI databases includes 8 alleles/vairants from RMs (allele-1-6, 7A and 7B), 3 alleles from Mauritian cynomolgus macaques (ac. no. EU419108, EU419110, and EU419114), 7 alleles from gorillas (ac. no. AY122865, AY122866, AY122870-AY122874), 4 alleles from common chimpanzees (ac. no. AF258804-AF258806, and AF274005), an allele from orangutans (ac. no. AF470389), and 24 alleles from humans (Table 5.14).

Table 5.11. Genetic variations of *Mamu-KIR* genes according to allelic grouping.

Genes	*Mamu-KIR1D gene*		*Mamu-KIR2DL4 gene*					*Mamu-KIR3DH gene*			*Mamu-KIR3DL gene*	
Alleles/Clusters	Cluster I	Cluster II	1	2	3	4	truncated proteins	HVL alleles	LVL alleles	Others	H159Q	H159H
RM-HVL cohort												
mm01		■	■					■				■
mm03			■		■			■		■	■	■
mm05												
mm06												
mm07		■	■				■			■		
mm08				■			■	■			■	■
mm09										■		■
mm10	■	■	■					■				■
mm16											■	
mm17												
mm18	■		■				■	■			■	
mm19	■		■	■						■	■	
mm22	■	■					■					
mm23		■					■				■	■
mm24				■				■			■	■
mm25			■	■			■					
mm26	■		■				■					■
mm27			■			■		■			■	
mm29	■		■					■				■
mm33				■			■			■		■
RM-LVL cohort												
mm02				■						■		■
mm04				■			■					■
mm11												■
mm12									■			■
mm13												
mm14			■				■					■
mm15	■	■	■									
mm20	■	■	■	■			■					■
mm21		■	■									
mm28	■	■		■						■		
mm30												■
mm31												
mm32				■					■		■	■
mm34				■				■			■	■
mm35				■						■		■
mm36									■	■		■
mm37	■	■		■						■	■	
mm38	■		■						■			■

Mamu-KIR1D-Cluster I containing *allele-3, 4, 5, 7, 8, 9,* and *11*; Mamu-KIR1D-Cluster II containing *allele-1, 2, 6,* and *10*; *Mamu-KIR2DL4 allele-1, 2, 3, 4,* and truncated protein containing *Mamu-KIR2DL4 allele-5* through *allele-7*; Mamu-KIR3DH HVL-alleles containing *allele-2, 3, 6, 10, 11, 13,* and *14*, LVL-alleles containing *allele-4, 5,* and *12,* and others containing *allele-1, 7, 8,* and *9*; and *Mamu-KIR3DL alleles* H159Q containing *allele-13* and *14*, H159H containing *allele-1* through *allele-12* and *variant A.*

Table 5.12. Univariate analysis of the association between *Mamu-KIR1D*, Mamu-KIR2DL4, Mamu-KIR3DH, and Mamu-KIR3DL genes with plasma VLs in SIV-infected RMs.

Genotypes	HVL (n)	LVL (n)	OR	95%CI		*p*-value
				lower	upper	
*1D*i/*i*	4	1	1.33	0.06	31.12	0.858
*1D*n/*n*	3	1				
*2DL4*1/*1*	3	3	6.00	0.42	85.25	0.164
*2DL4*2/*2*	1	6				
*3DH*h/*h*	7	1	21.67	0.64	730.08	0.047
*3DH*l/*l*	0	3				
*3DH*h/*h or *al9*	8	1	35.00	1.12	1094.79	0.015
*3DH*l/*l or *al8*	0	4				
*3DL*q/*q*	4	1	7.33	0.66	81.37	0.078
*3DL*wt/*wt*	6	11				
*1D*i/*i+2DL4*1/*1*	1	1	1.00	0.01	92.43	1.000
*1D*n/*n+2DL4*2/*2*	0	2				
*1D*i/*i+3DL*q/*q*	2	0	1.00	0.01	92.43	1.000
*1D*n/*n+3DL*wt/*wt*	1	1				
*2DL4*1/*1+3DH*h/*h*	3	0	5.00	0.04	711.87	0.505
*2DL4*2/*2+3DH*l/*l*	0	1				
*2DL4*1/*1+3DL*wt/*wt*	3	1	5.00	0.11	220.64	0.386
*2DL4*2/*2+3DL*wt/*wt*	0	2				
*2DL4*f/*f+3DL*q/*q*	2	1	2.00	0.11	35.81	0.635
*2DL4*f/*t+3DL*wt/*wt*	3	3				
*2DL4*f/*t+3DL*q/*q or *wt*	3	0	5.00	0.15	166.60	0.346
*2DL4*f/*t+3DL*wt/*wt*	2	3				
*3DH*h/*h+3DL*q/*q*	2	0	9.00	0.10	831.85	0.317
*3DH*l/*l+3DL*wt/*wt*	0	2				
*3DH*h/*h+3DL*wt/*wt*	3	0	15.00	0.18	1236.28	0.192
*3DH*l/*l +3DL*wt/*wt*	0	2				
*3DH*h/*h or *al9+3DL*q/*wt*	6	1	25.67	0.80	824.78	0.034
*3DH*l/*l or *al8+3DL*q/*wt*	0	4				
*1D*i/*i+2DL4*1/*2,*6,*7+3DL*q/*q*	2	0	3.00	0.02	473.1	0.665
*1D*n/*al5+2DL4*2/*1,p5+3DL*wt/*wt*	0	1				
*2DL4*1/*x+3DH*h/*h or *al9 +3DL*q/*q or *al2*	3	0	5.00	0.04	711.87	0.505
*2DL4*2/*2+3DH*l/*l+3DL*wt/*q*	0	1				

Abbreviation: *1D*i, Mamu-KIR1D allele-3, 4, 5, 7, 8, 9,* and *11; 1D*n, Mamu-KIR1D allele-1, 2, 6,* and *10*; *1D*al5, Mamu-KIR1D allele-5*; *2DL4*1, Mamu-KIR2DL4 allele-1*; *2DL4*2, Mamu-KIR2DL4 allele-2*; *2DL4*f, Mamu-KIR2DL4 allele-1-4; 2DL4*t, Mamu-KIR2DL4 allele-5-7* including predicted allele-5 (p5*); 2DL4*x, Mamu-KIR2DL4 allele-1, 3, 4, 6,* and *7*; *3DH*h, Mamu-KIR3DH allele-2, 3, 6, 10, 11, 13,* and *14*; *3DH*l, Mamu-KIR3DH allele-4, 5,* and *12*; *3DH*al8* and **al9, Mamu-KIR3DH allele-8* and *allele-9,* respectively*; 3DL*q, Mamu-KIR3DL allele-13* and *14*; *3DL*wt, Mamu-KIR3DL allele-1-12* and *variant A*; *3DL*al2, Mamu-KIR3DL allele-2*; OR is the odds ratio; and CI is confidence interval.

Table 5.13. The genotypic combination between *Mamu-KIR1D* and *Mamu-KIR3DH* genes in SIV-infected RMs.

Genotypic combination		HVL	LVL
Mamu-KIR1D	*Mamu-KIR3DH*	(n)	(n)
*1D*i/*i*	*3DH*h/*h*	2	0
*1D*i/*i*	*3DH*o/*o*	1	0
*1D*i/*n*	*3DH*h/*h*	1	0
*1D*i/*n*	*3DH*o/*o*	0	2
*1D*n/*n*	*3DH*h/*h*	1	0
*1D*n/*n*	*3DH*o/*o*	1	0

Abbreviations: *1D*i/*i* and *1D*n/*n* genotypes are a homozygous for allelic expression of *Mamu-KIR1D* gene in Cluster I (*allele-3, 4, 5, 7, 8, 9,* and *11*) and in Cluster II (*allele-1, 2, 6,* and *10*), respectively; *1D*i/*n* genotype is a heterozygous for *Mamu-KIR1D* gene in both two clusters; *3DH*h/*h* and *3DH*o/*o* genotypes are *Mamu-KIR3DH-HVL alleles* (*allele-2, 3, 6, 10, 11, 13,* and *14*) and *Mamu-KIR3DH-other alleles* containing *allele-1, 7, 8,* and *9*, respectively.

Table 5.14. Lists of *Hu-KIR2DL4* alleles from European Bioinformatics Institute 2010.

Allele Name	Local Names	Cells Sequenced	Accession No.	Description	Protein ID
2DL4*00101	NK3.3#27	NK3.3,	X99480,	mRNA	CAA67843
2DL4*00102	2DL4v1	AA1,	AF034771,	mRNA	AAB95164
2DL4*0010301	2DL4*00102v1-g	JBUSH,	AY789058,	mRNA	AAX23103
2DL4*0010302	2DL4*00102v2-g	GU1183,	AY727762,	Genomic DNA*	AAW32093
2DL4*00104	2DL4*00101v-g	GU324,	AY727760,	Genomic DNA*	AAW32091
2DL4*00105	2DL4-00102JB	J101,	AY789059,	mRNA	AAX23104
2DL4*00201	pcl.15.212	NKDonor#1,	X97229,	mRNA	CAA65868
2DL4*00202	2DL4v2	PP,	AF034772,	mRNA	AF034772
2DL4*003	KIR103AS	NK-92, YT(NK)	U71199,	mRNA	AAB49756
2DL4*004	KIR-103LP	Lopez,	AF002979,	mRNA	AAB71387
2DL4*00501	2DL4v3,	COX,	AF034773,	mRNA	AAB95166
2DL4*00502	9082959	RDP30,	DQ979374,	Genomic DNA	ABL09830
2DL4*00601	2DL4v4	RR,	AF285436,	mRNA	AAG34927
2DL4*00602	2DL4-006J	J42,	AY789062,	mRNA	AAX23107
2DL4*007	-	LP,	AF276292,	mRNA	AAG44820
2DL4*0080101	2DL4*00202v1	UV5HL9-5B,	AY789060,	mRNA	AAX23105
2DL4*0080103	2DL4*00202v1-g	GU321,	AY727758,	Genomic DNA*	AAW32089
2DL4*0080104	RDP56	RDP56,	EF095157,	Genomic DNA, partial	ABN13877
2DL4*0080201	2DL4*00201v2-g	HOM-2,	AY727763,	Genomic DNA*	AAW32094
2DL4*0080202	2DL4*00201v1-g	GU321,	AY727757,	Genomic DNA*	AAW32088
2DL4*009	2DL4*00202v2-g	GU324,	AY727759,	Genomic DNA*	AAW32090
2DL4*010	2DL4*006v	GU2015,	AY727764,	Genomic DNA*	AAW32095
2DL4*011	2DL4*005v	VAVY,	AY789061,	mRNA	AAX23106
2DL4*012	AA1	AA1,	EF091490,	Genomic DNA, partial	ABO14699

*Genomic DNA, exons 1 through 3, 5 through 9 and partial cds

Reference: http://www.ebi.ac.uk/

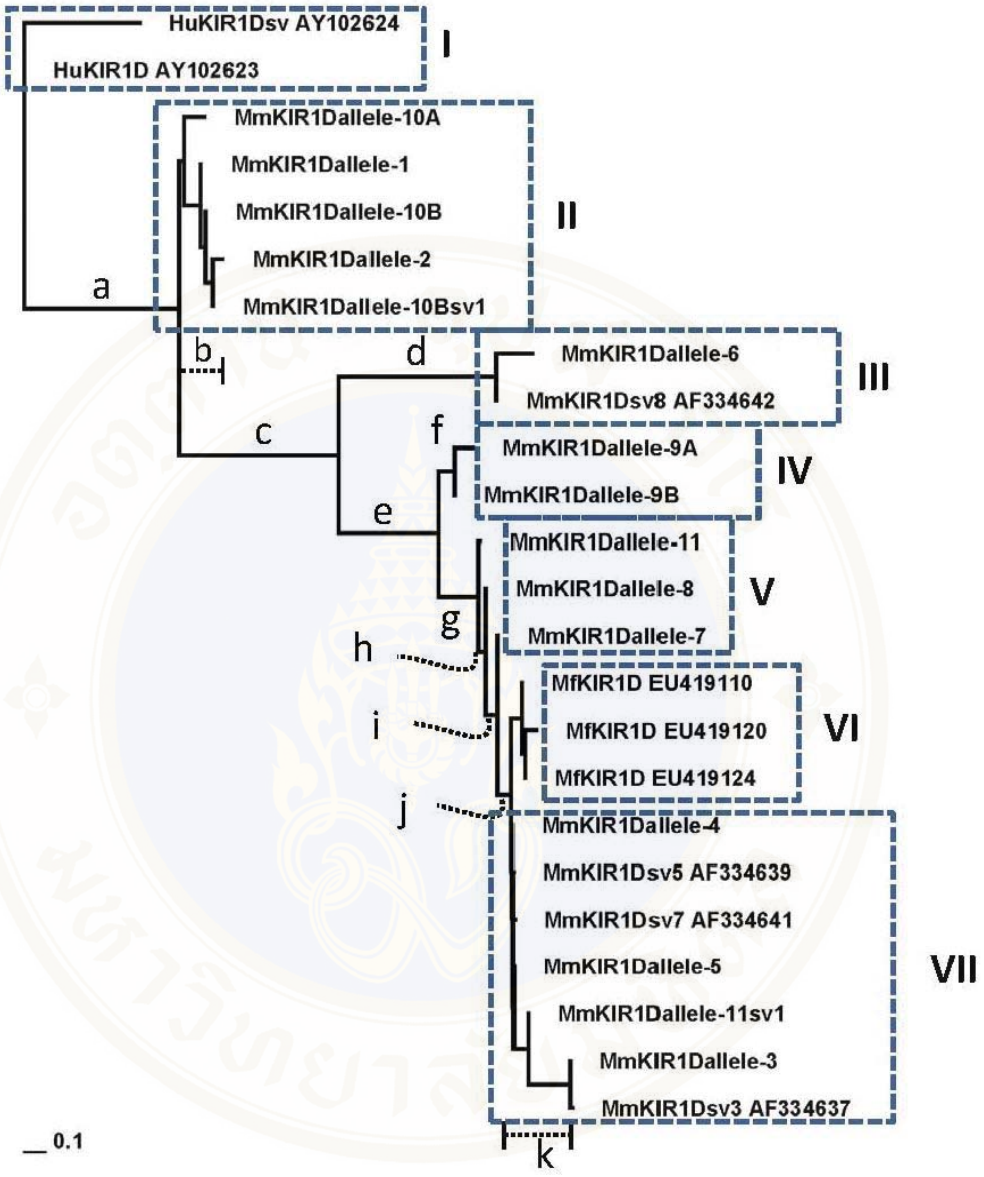

Figure 5.22. Phylogenetic tree of *KIR1D* loci at protein level. KIR1D cDNA sequences obtained from rhesus macaque (*Macaca mulatta*, Mm), Mauritian cynomolgus macaque (*Macaca fascicularis*, Mf), and human (*Homo sapien*s, Hu) were encoded into protein sequences. Subsequently, protein sequences were aligned and analyzed by using BioEdit software version 7.0.9. The phylogram of KIR1D alleles were characterized into seven major lineages of these analysis (lineages I – VII). The branch lengths were following; a = 0.72667, b = 0.15834, c = 0.74842, d = 0.73817, e = 0.46703, f = 0.07623, g = 0.18711, h = 0.03469, i = 0.05650, j = 0.06316, and k = 0.27529.

The distance in length of each allele was performed and illustrated in Figure 5.23. We created four groups of KIR2DL-related species according to a phylogenetic tree analysis at protein level. The first group (lineage I) was divided into 2 subgroups (lineages I.1 and I.2) due to sharing sequences of the same root. All *Mamu-KIR2DL4* sequencs were grouped into lineage I.2 that include *Mf-KIR2DL4* (refer to GenBank ac. no. EU419111 and EU419114) and *Gg-KIR2DL4* (ac. no. AY122865). This lineage was spliced into two branches; the individual *Gg-KIR2DL4* and all sequences from *Mamu-* and *Mf-KIR2DL4*. *Mamu-KIR2DL4 allele-1* through *allele-5* including the same ancestor with *Mf-KIR2DL4* sequences. Meanwhile *Mamu-KIR2DL4 allele-6* and *7*, including their variants, were separated into another branch. These results related to the pairwise alignment analysis (Needle-Wunch algorithm, BioEdit software version 7.0.9) that showed *Gg-KIR2DL4* had ~53-61% aa homology to *Mamu-KIR2DL4* alleles and ~68-69% aa homology to *Mf-KIR2DL4* alleles. While *Mamu-KIR2DL4 allele-5* had ~70% aa homology to *Mf-KIR2DL4* alleles.

Without additional information, Hu-KIR2DL4 had highly genetic variation as shown in Table 5.14, Mamu-KIR2DL4 alleles shared a root with Hu-KIR2DL4 allele-7, 8, 9, and 11. However, Mamu-KIRs also appeared to be the only KIR common to hominoids as described in previous study (42).

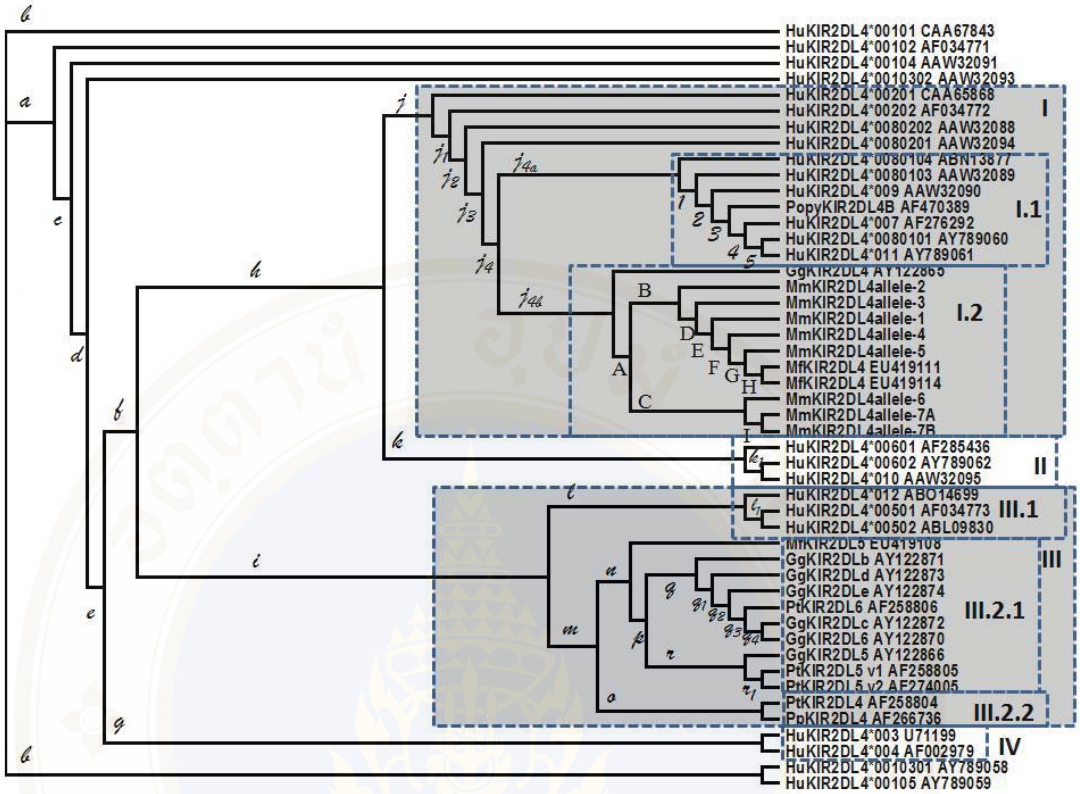

Figure 5.23. Phylogenetic tree of *KIR2DL* loci at protein level. KIR2DL cDNA sequences obtained from rhesus macaque (*Macaca mulatta*, Mm), Mauritian cynomolgus macaque (*Macaca fascicularis*, Mf), gorilla (*Gorilla gorilla*, Gg), common chimpanzee (*Pan troglodytes*, Pt), orangutan (*Pongo pygmaeus*, Popy), and human (*Homo sapien*s, Hu) were encoded into protein sequences. Subsequently, protein sequences were aligned and analyzed by using BioEdit software version 7.0.9. The rectangular cladogram of KIR2DL alleles showed four major lineages of these analysis (lineages I – IV). The branch lengths were following; a = 0.00001, b = 0, c and d = 0.00006, e = 0.00518, f = 0.00378, g = 0.00468, h = 0.00090, i = 0.00115, j = 0.00075, j_1 = 0.00076, j_2 = 0.04121, j_3 = 0.01609, j_4 = 0.01602, j_{4a} = 0.01676, j_{4a}-1 = 0.05716, j_{4a}-2 = 0.10697, j_{4a}-3 = 0.14391, j_{4a}-4 = 0.05955, j_{4a}-5 = 0.01365, j_{4b} = 0.06316, j_{4b}-A = 0.09060, j_{4b}-B =0.01103, j_{4b}-C = 0.15693, j_{4b}-D = 0.01582, j_{4b}-E = 0.00413, j_{4b}-F = 0.00342, j_{4b}-G = 0.02152, j_{4b}-H = 0.04452, j_{4b}-I = 0.29650, k = 0.00479, k_1 = 0.00006, l = 0.00435, l_1 = 0.00019, m = 0.03373, n = 0.18954, o = 0.02508, p = 0.03154, q = 0.29265, q_1 = 0.21208, q_2 = 0.01804, q_3 = 0.03585, q_4 = 0.03707, r = 0.09350, and r_1 = 0.02040.

CHAPTER VI
DISCUSSION

The fact that the kinetics of viral replication in both HIV-1-infected humans and SIV-infected RMs show a marked and rapid decline following the peak levels within a 2-3 week period when adaptive immune responses have not fully matured, strongly indicates that cell lineages of the innate immune system most likely play a major role in this decline of viremia (56). The degree of this initial decline in viremia during the acute infection sets a footprint for the pace at which disease progression ensues, suggests that the detailed mechanisms by which such differences in decline of viremia occurs should be one of the top research priorities. Recognizing this issue has prompted our laboratory to focus on the potential role of NK cells as perhaps one of the major effector mechanisms that potentially mediate such an effect. As Pereira *et al* demonstrated that the depletion of $CD16^{+}CD56^{-}$ NK cells in chronically SIV-infected RMs correlates with disease progressive, a role for such NK cells because evident. The fact that both the frequency and the function of NK cells increase in SIV disease resistant SMs as compared with a decrease in frequency and function in disease subceptible RM suggests that NK cells most play a role in SIV pathogenesis. As stated above, NK cells are in fact phenotypically and functionally heterogenous (2) and mediate their effector function by the net interactions of a large number of activating and inhibitory receptors decorating their cell surface. Among these receptors are the KIR molecules. There have been several reports proposed that the inherent genetic variability between human MHC class I and KIR genes showed an association with delay to AIDS progression via HIV-1-infected individuals (2). These foundings prompted us to can your studies to determine whether such as association is also present in the SIV-infected RM.

We therefore performed Mamu typing for *A.01, B.01, B.08,* and *B.17* in our cohort animals, and that these alleles were associated with slow disease progression (Table A.1 in Appendix section) (57, 58). Subsequently, a cohort of

animals with post-infection had a statistically significant difference of plasma VLs, $CD4^+$T cell count, and NK cell activity when compared to animals with LVLs at *p*-value < 0.001 (Table A.2). The changes in the data differented post-SIV infection vs the pre-SIV infection (baseline) of animals in HVL cohort were low level of NK function and $CD4^+$T cell count ($p < 0.001$). We utilized these baseline data to causing only shares on differencing the potential role of KIR polymorphisms on influence viral load. Our studies this focused on identifying the genotypic variations of KIR family expressed by purified $NKG2A^+$ NK cells obtained from SIV-infected RMs with the goal of identifying those KIR loci and alleles that are associated with the initial decline of viremia described above.

The WHO Nomenclature Committee for Factors of the HLA System that are responsible for naming KIR genes approached by the HGNC (http://www.ebi.ac.uk/). This committee assigned the name of KIR genes based on the structures of the molecules they encode. Briefly, the first digit following the KIR acronym corresponds to the number of Ig-like domains in the molecule, and the 'D' denotes 'domain'. The 'D' is followed by either an 'L' indicating a 'Long' cytoplasmic tail, an 'S' indicating a 'Short' cytoplasmic tail, or a 'P' for pseudogenes. The final digit indicates the number of the gene encoding a protein with this structure. After the gene name, an asterisk is used as a separator before a numerical allele designation. It is important to note that we chose to assign alleles/variants which is distinct from that HGNC assigns.The naming of *Mamu-KIR alleles/variants* in our study was based on sequences of a single locus that shared > 98% homology at the nucleotide and protein levels as belonging to a single allele (2). By contrast, the assignment of KIR alleles naming based on the classical definition of HGNC suggested that the alleles with three digits after an asterisk in addition to the first three digits of the numerical designation are used to indicate alleles that differ in the sequences of their encoded proteins. The next two digits are used to distinguish alleles that only differ by synonymous (non-coding) differences within the coding sequence. The final two digits are used to distinguish alleles that only differ by substitutions in an intron, promoter, or other non-coding region of the sequence. The rationale for using our strategy is that if we were to use the classical definition of an allele as being sequences that would differ by a single amino acid, it would lead to the assignments

of hundreds of alleles which would make it difficult to examine the association between KIR alleles and plasma VLs. In addition, our focus was to identify differences in the sequences of the KIR genes and its alleles that had functional subficience. Thus, on interests were to identify differences in the sequences that are involved in binding to MHC molecules and there that are involved in intracellular signaling.

Our laboratory has focused on KIR sequences that are associated with function such as those that are primarily localized to extracellular domains that have been previously shown to participate in binding to MHC molecules and/or are involved in select cases in coding for intracellular sequences involved in signaling such as ITIMs and positive charged arginine mediated ITAM activation. Such a strategy clearly has led to some interesting data as described herein. In general, the encoding KIR1D, KIR2DL4, and KIR3DL molecules what are responded to serve as the inhibitory NK cell receptors via the signal transduction of ITIMs were identified as playing a major role. While KIR2DL4 and KIR3DH contain an AGG sequence in their TM which codes for a positively charged arginine residue to facilitate binding to the corresponding negatively charged TM residues of the ITAM-encoding adaptor proteins. Results from previous studies have found that the KIR2DL4 could gene as both activating and inhibitory receptors (10). It is possible that the function of the KIR2DL4 molecules may differ in species because of the ITIM expression in their cytoplasmic tails. Both human and chimpanzee KIR2DL4 molecules have only one ITIM while in the macaque molecules contain two ITIMs in their cytoplasmic domains (10). Total mRNA isolated from NKG2A cells from animals in our cohort were also amplified and cloned for *Mamu-KIR2DL4* genes by using primer sets as shown in Table 4.3. Although the full-length protein could not be amplified, overlapping sections of the extracellular and intracellular domains were aligned to ensure complete coverage of the cDNA sequences. The intracellular sequences including the ITIMs were found to share >98% aa homology to allele-2. The allelic expression of this KIR2DL4 gene was identified into seven alleles, interestingly; allele-1 and 2 were expressed at a highly frequency in our cohort. While allele-5 through allele-7 had rare expression and encoded for truncated proteins. If these proteins were expressed on the cell surface, they could still bind their ligands resulting

in an inhibitory signal to the NK cells. There have been several reports that have identified HLA-G molecule as the ligand for Hu-KIR2DL4 molecule (20). However, the precise sequence that is involved in recognition of the HLA-G molecule by KIR2DL4 remains unknown at present. It is possible that the Ig-like domains of KIR2DL4 might function in ligand-receptor interaction similar to the interaction noted for the HLA Bw4-KIR3DL binding (9).

As *Mamu-KIR2DL4* alleles which are encoded for truncated proteins, we found two different KIR1D phenotypes which play an important role in the regulation of NK cell function. The fact that our laboratory identified 11 *Mamu-KIR1D* alleles that appeared to two different phenotypes based on the presence or absence of an ITIM(s). These 11 alleles were grouped into two clusters; Cluster I and Cluster II. As denoted; *Mamu-KIR1D*i* genotype contains *Mamu-KIR1D allele-3, 4, 5, 7, 8, 9,* and *11*. It is interesting to note that these sets of KIR alleles formed a Cluster I was distinct from the other alleles encoded by this locus and also displays the ITIMs in their cytoplasmic tail. We believe that KIR1D molecules encoding from a Cluster I could regulate the inhibitory function in NK cells. In contrast, *Mamu-KIR1D*n* genotype (allele-1, 2, 6, and 10) was thus characterized into a Cluster II and we believe that these alleles were encoded into a null phenotype. Studies reported by Pando *et al* proposed the founding that Hu-KIR3DL1*004 molecule fails to lead to protein folding and is retained in the endoplasmic reticulum with little or no expression at the cell surface (59). The *Hu-KIR3DL1*004* allele is unique since the Hu-KIR3DL1 allotype characteristic has led to its functionality being called into question. Martin *et al* investigated HIV-1 infected patients who had combined *Hu-KIR3DL1*004* with *HLA-B Bw4* and showed the possibility that the KIR3DL1*004 molecule may actually bind HLA-B Bw4 molecules intracellularly with functionally relevant consequences to slow progression to AIDS (9). Whether Mamu-KIR1D*n molecule is responsible for this requires further investigation in protein folding, expression, and also in the function in the KIR cDNA sequences. Moreover, we also found that *Mamu-KIR1D allele-1, 2, 3, 6,* and *10* had no TM domain. It remains unclear whether the proteins encoding from these alleles are still functional (Figure 5.4).

For successful characterization of allele/genomic polymorphisms of Mamu-KIR family in our cohort, we included the identification of the *Mamu-KIR3DH* (unpublished) and *Mamu-KIR3DL* (2) allelic expression obtained from our previous observation in this thesis. Previously, Bostik *et al* characterized 14 new Mamu-KIR3DL alleles and a variant from cDNA sequences obtained from purified NKG2A^{+}NK cells isolated from animals with high and low plasma VLs (2). Importantly, the higher frequency of inheritance of *Mamu-KIR3DL allele-13* and *14* characterized by a SNP H159Q was associated with SIV-infected RMs that exhibited RM-HVL cohort. These two alleles were classified into *Mamu-KIR3DL*q* genotype. The other 12 Mamu-KIR3DL alleles and a variant which had generally histidine expression at position 159 were classified into *Mamu-KIR3DL*wt* genotype.

In addition, cDNA isolated from NKG2A^{+} cell from animals in our cohort were amplified and cloned for *Mamu-KIR3DH* alleles by using two forward primers; 5'-TGTGTTGGGTTCTTCTTGGTCCAG-3' and 5'-CACACGGGTGGTCAGGACA AGAC-3' with reverse primer 5'-TCTGAGAAGGGCGAGTGATTTTTC-3'. Mamu-KIR3DH as noted by its name is a hybrid KIR molecule between Mamu-KIR3DL and Mamu-KIR2DL4 allele-2 molecules. Mamu-KIR3DH molecule is composed of 370 aa in length with three Ig-like domains and a stem sequence which is similar to Mamu-KIR3DL molecule while the TM is identical to Mamu-KIR2DL4 allele-2 which contains an arginine residue. The nucleotide sequence of exon 8 expected to be part of the Mamu-KIR3DH molecule has been found so far. The deletion of 53 bases leads to a frame shift translation and the novel molecules terminate after encoding only 10 aa in length. This early termination occurs before the ITIMs seen in the Mm-KIR3DL and Mm-KIR2DL4 molecules (Figure 6.1) (10). From our analyses, Mamu-KIR3DH alleles are expressed predominantly by animals of that one can define as those expressing "HVL alleles" (expressed only in RM-HVL animals, *Mamu-KIR3DH*h* genotype), "LVL alleles" (expressed only in RM-LVL animals, *Mamu-KIR3DH*l* genotype), or "Other alleles" (expressed in both cohorts, *Mamu-KIR3DH*o* genotype).

Finally, we also attempted to amplify, clone and sequence alleles encoded by the *Mamu-KIR2DL5* locus using the primer pairs listed in Table 4.3 and Table 5.8. Unfortunately, samples from only 3 of the 10 animals in cohort gave results with data

Figure 6.1. A hybrid Mamu-KIR3DH molecule. Asterisk is the arginine residue which regulates the signal transduction in NK cell activity. The GenBank numbering of Mamu-KIR3DL7, Mamu-KIR2DL4 allele-2, and Mamu-KIR3DH1 are AF334622, AY728182, and AY728190, respectively.

on most of the sequences that have already been published for *Mamu-KIR2DL5 allele-1* and *2* (the GenBank ac. no. AF334646 and AF334647) or were identified as *Mamu-KIR3DL20* (the GenBank ac. no. NM_001104552). Mamu-KIR2DL5 molecule has two Ig-like domains and ITIMs in their cytoplasmic tail such as to Mamu-KIR2DL4 molecule but it lacks the arginine in their TM. Similar findings have been reported in Mamu-KIR2DL5/Mamu-KIR3DL20. It is likely that these are alternatively spliced transcripts from the same locus. The KIR2DL5/KIR3DL20 locus has been speculated to represent an evolutionary intermediate between KIR2DL and KIR3DL genes because the KIR3DL version of this transcript lacks a stop codon with the region sequenced (Figure 5.20) (38).

Statistical analysis of the data presented herein show a high degree of significance between plasma VLs and the association with *KIR3DH*h* genotype and *KIR3DH*h* genotype combined with *KIR3DL*q* genotype as determined by calculating the OR (Table 5.12). Clearly, the number of animals studied herein is a relatively small number to derive any major conclusions and larger groups of animals need to be studied. However, we submit that these findings are interesting and encourage the need for additional study. Data from the studies reported herein appear to show some interesting trends in terms of KIR polymorphisms and the initial attempt to study the genetic expression of Mamu-KIR genes in animals with fast and slow AIDS progressive showed that macaques that expressed *Mamu-KIR1D*i, Mamu-KIR2DL4*1, Mamu-KIR3DH*h,* and *Mamu-KIR3DL*q* appeared to belong to the HVL category while animals that expressed *Mamu-KIR1D*n, Mamu-KIR2DL4*2, Mamu-KIR3DH*l,* and *Mamu-KIR3DL*wt* appeared to belong to the LVL category (Table 5.12). Although statistical analysis showed a significant difference of KIR3DH loci and VLs, the frequency of each individual KIR3DH allelic expression diverge with respect to the use for primer/probe design in KIR typing. Other important associations between KIR loci and VLs were a strongly genomic expression of KIR2DL4 and KIR3DL. The RMs that expressed *Mamu-KIR2DL4* either expressed *allele-1* or *2* supports a need for Mamu-KIR typing in the prediction of the relatively viremia as done in the TaqMan probe designed to analysis of the expression of *Mamu-KIR3DL* alleles in genomic DNA samples from the animals belong to the two cohorts. In the future, we will design the probes to determine *Mamu-KIR2DL4 allele-1* and *2*

by the specific motifs that the *allele-1* shows a 'VT-X_3-A-X_{18}-H-X_5-D' motif meanwhile the *allele-2* shows either a 'TR-X_3-I-X_{18}-L-X_5-D/N' or 'VR-X_3-A-X_{18}-L-X_5-D' motifs at the same position.

It is also important to note that these findings will add significance in terms of the mechanisms when the MHC ligands for such Mamu-KIR loci are identified. In addition, when a more complete set of data on the other Mamu-KIR loci becomes available, it would be important to determine if the loci segregate into haplotypes much like in humans. Thus, human KIR haplotypes have been shown to form 2 major groups. Haplotype A which is the most common haplotype contains two activating KIR genes (KIR2DL4 and KIR2DS4) and five inhibitory KIR genes (KIR2DL1, KIR2DL3, KIR3DL1, KIR3DL2, and KIR3DL3). On the other hand haplotype B includes 6 activating KIR genes (KIR2DS1, S2, S3, S5.A, S5.B, and KIR3DS1), two inhibitory KIR genes (KIR2DL2 and KIR2DL5) and two KIR pseudogenes (KIR2DP1 and KIR3DP1) (31).

It should also be noted that there are 2 other groups of molecules expressed by NK cells that could also potentially be involved in regulating their functional activity. These include the killer cell lectin-like receptor's (KLR) and the non-immunoglobulin like NK cell receptors (60). Among the KLR's, both an activating (NKG2A) and an inhibitory form (NKG2C) have been identified in the RM which interestingly have been shown to share 85% homology at the protein level with the human homologues (61). The non-classical human MHC class I HLA-E molecule has been shown to be the ligand for these receptors and a rhesus homologue for HLA-E has been identified (62). In this regard, it is important to note that human HLA-E tetramer reagent binds to RM NKG2A expressing NK and CD3 expressing cells which is not surprising because HLA-E homologues have limited polymorphisms and are the among the most phylogenetically conserved MHC class I genes in primates (63). Relevant to the present study, a role for NKG2C/C2 has been implicated in SIV-infected RMs (64), and a role for NKG2A in human HIV-1 infection (65, 66). It thus appears that the interaction between NK cells and its subsets with target cells following infection involve the interactions between multiple receptors and ligands and the nature of the net signals generating from such interaction result in either killing of the target cells or the generation of multiple cytokines and chemokines that

influence the quantity and quality of the immune response. These issues have to be taken into consideration in the interpretation of data such as those presented in the present communication.

There are, in addition, a compile of important issues that need to be taken into consideration in the interpretation of data that are presented as a part of this study. First of all, the expression pattern of the KIR genes and its loci do not appear to be influenced by SIV infection. Thus, the pattern of KIR gene/allele expression profile appears as the same pre- and to post-SIV infection. Secondly, the levels of viral load were only shown to influence the related levels of mRNA loading for the KIR gene and its alleles but not the nature of the KIR gene. Thus, differences induced by SIV infection appear to influence in quantization but not qualization of difference in the expression of the KIR genes/alleles. This is an important issue such the $NKG2A^{+}$ cells used for the exhibited of mRNA included cells for the animals exhibited chronic SIV infection. Nonetheless, one needs to keep these issues in mind in the analyzing data presented in the present communication.

In summary, it should be noted that which clearly a large number of animals need to be typed for MHC and then corresponding KIR genes/alleles, studies performed herein are the foundation upon that further studies used to be caused and on effects to objectively analyze the potential role of KIR genes/alleles and SIV pathogenesis.

CHAPTER VII
CONCLUSION

It is important to note that results of these studies were combined with previous studies (2) were initially aimed to characterize genomic polymorphisms of Mamu-KIR family in SIV-infected RMs and to delineate potential correlation between these loci and viral control. Animals in our cohort were housed at the Yerkes National Primate Research Center, Emory University. Animals were infected with SIV_{mac251} or SIV_{mac239} and were separated into two cohorts based on the levels of plasma VL at the chronic stage of infection or disease progression. Animals in RM-HVL cohort had progressed toward AIDS-like disease within 8 months. Results of our studies using multiple sequence expression analysis demonstrated that these animals expressed different alleles of five Mamu-KIR loci and showed their unequal distribution between animals which exhibit good vs poor control of SIV replication.

KIR cDNA sequences were amplified and analyzed by using bioinformatic tools. A total of KIR loci that expressed in our cohort were herein identified 11 alleles from *Mamu-KIR1D* gene and 7 alleles from *Mamu-KIR2DL4* gene combined with previous study as reported by Bostik *et al*. They found 14 alleles from *Mamu-KIR3DH* gene and 14 from *Mamu-KIR3DL* gene (2). We also amplified *Mamu-KIR2DL5* gene by using primer sets as described in the section of Materials and Methods, the sequence results have already been previously published or crossover to *Mamu-KIR3DL20* amplification. Although mostly KIR alleles that expressed in the cohort have already been published, new KIR alleles/variants were also found in addition 3 new *Mamu-KIR1D* alleles contain *allele-9* and *10* had lack the ITIMs in their cytoplasmic tail and *allele-11* that had different encoding protein and this a variant of this allele-11 had deleted nucleotide at TM. Five new *Mamu-KIR2DL4* alleles were identified. These included allele-3 and 4 with a full-length in the extracellular domain through a part of cytoplasmic tail meanwhile allele-5 through allele-7 including their variants were encoded into the truncated proteins that have led

to their functionality being called into question. Data showed high diversity of allelic KIR expression in each individual animal, clearly, we found the association between KIR loci and VLs that showed some interesting trends in animals with high VLs that expressed *Mamu-KIR1D*i, Mamu-KIR2DL4*1, Mamu-KIR3DH*h,* and *Mamu-KIR3DL*q* genotypes while animals with low VLs that expressed *Mamu-KIR1D*n, Mamu-KIR2DL4*2, Mamu-KIR3DH*l,* and *Mamu-KIR3DL*wt* genotypes. Statistical analysis showed that *Mamu-KIR3DH* and *Mamu-KIR3DL* alleles appeared to be a strongly associated with influencing plasma VLs in SIV-infected RMs. The segregation of the RM-HVL and RM-LVL categories in *Mamu-KIR2DL4* gene is great and definitely a good candidate to try for the TaqMan probe detection including the motifs that the *allele-1* showed a 'VT-X_3-A-X_{18}-H-X_5-D' motif meanwhile the *allele-2* showed either a 'TR-X_3-I-X_{18}-L-X_5-D/N' or 'VR-X_3-A-X_{18}-L-X_5-D' motifs at the same position. It is important in tandem this finding *with Mamu-KIR3DL* at SNP H159Q as described previously (2).

In summary, results of these studies combined with previous studies suggest that selected *Mamu-KIR2DL4* and *Mamu-KIR3DL* alleles appear to be associated with influencing high VLs in SIV-infected RMs in our colony at the Yerkes National Primate Research Center. It would be important to determine if a similar association is also seen in macaques of Indian origin at other Primate Centers.

REFERENCES

1. Fauci AS, Mavilio D, Kottilil S. NK cells in HIV infection: paradigm for protection or targets for ambush. Nat Rev Immunol. 2005 Nov;5(11):835-43.
2. Bostik P, Kobkitjaroen J, Tang W, Villinger F, Pereira LE, Little DM, et al. Decreased NK cell frequency and function is associated with increased risk of KIR3DL allele polymorphism in simian immunodeficiency virus-infected rhesus macaques with high viral loads. J Immunol. 2009 Mar 15;182(6):3638-49.
3. Lanier LL. Up on the tightrope: natural killer cell activation and inhibition. Nat Immunol. 2008 May;9(5):495-502.
4. Barrow AD, Trowsdale J. You say ITAM and I say ITIM, let's call the whole thing off: the ambiguity of immunoreceptor signalling. Eur J Immunol. 2006 Jul;36(7):1646-53.
5. Miah SM, Hughes TL, Campbell KS. KIR2DL4 differentially signals downstream functions in human NK cells through distinct structural modules. J Immunol. 2008 Mar 1;180(5):2922-32.
6. Iannello A, Debbeche O, Samarani S, Ahmad A. Antiviral NK cell responses in HIV infection: I. NK cell receptor genes as determinants of HIV resistance and progression to AIDS. J Leukoc Biol. 2008 Jul;84(1):1-26.
7. Martin MP, Gao X, Lee JH, Nelson GW, Detels R, Goedert JJ, et al. Epistatic interaction between KIR3DS1 and HLA-B delays the progression to AIDS. Nat Genet. 2002 Aug;31(4):429-34.
8. Alter G, Rihn S, Walter K, Nolting A, Martin M, Rosenberg ES, et al. HLA class I subtype-dependent expansion of KIR3DS1+ and KIR3DL1+ NK cells during acute human immunodeficiency virus type 1 infection. J Virol. 2009 Jul;83(13):6798-805.

9. Martin MP, Qi Y, Gao X, Yamada E, Martin JN, Pereyra F, et al. Innate partnership of HLA-B and KIR3DL1 subtypes against HIV-1. Nat Genet. 2007 Jun;39(6):733-40.
10. Hershberger KL, Shyam R, Miura A, Letvin NL. Diversity of the killer cell Ig-like receptors of rhesus monkeys. J Immunol. 2001 Apr 1;166(7):4380-90.
11. van Rompay KK, Dailey PJ, Tarara RP, Canfield DR, Aguirre NL, Cherrington JM, et al. Early short-term 9-[2-(R)-(phosphonomethoxy)propyl]adenine treatment favorably alters the subsequent disease course in simian immunodeficiency virus-infected newborn Rhesus macaques. J Virol. 1999 Apr;73(4):2947-55.
12. Taber R, Rajakumar PA, Fuller DH, Trichel AM, Dowling P, Meleason D, et al. Effects of monotherapy with (R)-9-(2-phosphonylmethoxypropyl)adenine (PMPA) on the evolution of a primary Simian immunodeficiency virus (SIV) isolate. Virology. 2006 Oct 10;354(1):116-31.
13. Boyton RJ, Altmann DM. Natural killer cells, killer immunoglobulin-like receptors and human leucocyte antigen class I in disease. Clin Exp Immunol. 2007 Jul;149(1):1-8.
14. Wold AS, Arici A. Natural killer cells and reproductive failure. Curr Opin Obstet Gynecol. 2005 Jun;17(3):237-41.
15. Cooper MA, Fehniger TA, Caligiuri MA. The biology of human natural killer-cell subsets. Trends Immunol. 2001 Nov;22(11):633-40.
16. Iannello A, Debbeche O, Samarani S, Ahmad A. Antiviral NK cell responses in HIV infection: I. NK cell receptor genes as determinants of HIV resistance and progression to AIDS. J Leukoc Biol. 2008 Apr 3.
17. Andersen H, Rossio JL, Coalter V, Poore B, Martin MP, Carrington M, et al. Characterization of rhesus macaque natural killer activity against a rhesus-derived target cell line at the single-cell level. Cell Immunol. 2004 Sep-Oct;231(1-2):85-95.
18. Moretta A, Biassoni R, Bottino C, Mingari MC, Moretta L. Natural cytotoxicity receptors that trigger human NK-cell-mediated cytolysis. Immunol Today. 2000 May;21(5):228-34.

19. Newman KC, Riley EM. Whatever turns you on: accessory-cell-dependent activation of NK cells by pathogens. Nat Rev Immunol. 2007 Apr;7(4):279-91.
20. Biassoni R. Human natural killer receptors, co-receptors, and their ligands. Curr Protoc Immunol. 2009 Feb;Chapter 14:Unit 14 0.
21. Altfeld M, Goulder P. 'Unleashed' natural killers hinder HIV. Nat Genet. 2007 Jun;39(6):708-10.
22. Kumar V, McNerney ME. A new self: MHC-class-I-independent natural-killer-cell self-tolerance. Nat Rev Immunol. 2005 May;5(5):363-74.
23. Chiesa S, Tomasello E, Vivier E, Vely F. Coordination of activating and inhibitory signals in natural killer cells. Mol Immunol. 2005 Feb;42(4):477-84.
24. Vilches C, Pando MJ, Parham P. Genes encoding human killer-cell Ig-like receptors with D1 and D2 extracellular domains all contain untranslated pseudoexons encoding a third Ig-like domain. Immunogenetics. 2000 Jul;51(8-9):639-46.
25. Velickovic M, Velickovic Z, Panigoro R, Dunckley H. Diversity of killer cell immunoglobulin-like receptor genes in Indonesian populations of Java, Kalimantan, Timor and Irian Jaya. Tissue Antigens. 2009 Jan;73(1):9-16.
26. Trowsdale J, Barten R, Haude A, Stewart CA, Beck S, Wilson MJ. The genomic context of natural killer receptor extended gene families. Immunol Rev. 2001 Jun;181:20-38.
27. Parham P. MHC class I molecules and KIRs in human history, health and survival. Nat Rev Immunol. 2005 Mar;5(3):201-14.
28. Borrego F, Kabat J, Kim DK, Lieto L, Maasho K, Pena J, et al. Structure and function of major histocompatibility complex (MHC) class I specific receptors expressed on human natural killer (NK) cells. Mol Immunol. 2002 Feb;38(9):637-60.
29. Zheng D, Frankish A, Baertsch R, Kapranov P, Reymond A, Choo SW, et al. Pseudogenes in the ENCODE regions: consensus annotation, analysis of transcription, and evolution. Genome Res. 2007 Jun;17(6):839-51.

30. Marsh SG, Parham P, Dupont B, Geraghty DE, Trowsdale J, Middleton D, et al. Killer-cell immunoglobulin-like receptor (KIR) nomenclature report, 2002. Immunogenetics. 2003 Jul;55(4):220-6.
31. Khakoo SI, Carrington M. KIR and disease: a model system or system of models? Immunol Rev. 2006 Dec;214:186-201.
32. Gumperz JE, Valiante NM, Parham P, Lanier LL, Tyan D. Heterogeneous phenotypes of expression of the NKB1 natural killer cell class I receptor among individuals of different human histocompatibility leukocyte antigens types appear genetically regulated, but not linked to major histocompatibililty complex haplotype. J Exp Med. 1996 Apr 1;183(4):1817-27.
33. Gardiner CM, Guethlein LA, Shilling HG, Pando M, Carr WH, Rajalingam R, et al. Different NK cell surface phenotypes defined by the DX9 antibody are due to KIR3DL1 gene polymorphism. J Immunol. 2001 Mar 1;166(5):2992-3001.
34. O'Connor GM, Guinan KJ, Cunningham RT, Middleton D, Parham P, Gardiner CM. Functional polymorphism of the KIR3DL1/S1 receptor on human NK cells. J Immunol. 2007 Jan 1;178(1):235-41.
35. Shilling HG, Guethlein LA, Cheng NW, Gardiner CM, Rodriguez R, Tyan D, et al. Allelic polymorphism synergizes with variable gene content to individualize human KIR genotype. J Immunol. 2002 Mar 1;168(5):2307-15.
36. Gardiner CM. Killer cell immunoglobulin-like receptors on NK cells: the how, where and why. Int J Immunogenet. 2008 Feb;35(1):1-8.
37. Zahn RC, Hermann FG, Kim EY, Rett MD, Wolinsky SM, Johnson RP, et al. Efficient entry inhibition of human and nonhuman primate immunodeficiency virus by cell surface-expressed gp41-derived peptides. Gene Ther. 2008 May 1.
38. Bimber BN, Moreland AJ, Wiseman RW, Hughes AL, O'Connor DH. Complete Characterization of Killer Ig-Like Receptor (KIR) Haplotypes in Mauritian Cynomolgus Macaques: Novel Insights into Nonhuman Primate KIR Gene Content and Organization. J Immunol. 2008 Nov 1;181(9):6301-8.

39. Parham P. Killer cell immunoglobulin-like receptor diversity: balancing signals in the natural killer cell response. Immunol Lett. 2004 Mar 29;92(1-2):11-3.
40. Khakoo SI, Rajalingam R, Shum BP, Weidenbach K, Flodin L, Muir DG, et al. Rapid evolution of NK cell receptor systems demonstrated by comparison of chimpanzees and humans. Immunity. 2000 Jun;12(6):687-98.
41. Rajalingam R, Hong M, Adams EJ, Shum BP, Guethlein LA, Parham P. Short KIR haplotypes in pygmy chimpanzee (Bonobo) resemble the conserved framework of diverse human KIR haplotypes. J Exp Med. 2001 Jan 1;193(1):135-46.
42. Rajalingam R, Parham P, Abi-Rached L. Domain shuffling has been the main mechanism forming new hominoid killer cell Ig-like receptors. J Immunol. 2004 Jan 1;172(1):356-69.
43. Guethlein LA, Flodin LR, Adams EJ, Parham P. NK cell receptors of the orangutan (Pongo pygmaeus): a pivotal species for tracking the coevolution of killer cell Ig-like receptors with MHC-C. J Immunol. 2002 Jul 1;169(1):220-9.
44. Gibbs RA, Rogers J, Katze MG, Bumgarner R, Weinstock GM, Mardis ER, et al. Evolutionary and biomedical insights from the rhesus macaque genome. Science. 2007 Apr 13;316(5822):222-34.
45. Glazko GV, Nei M. Estimation of divergence times for major lineages of primate species. Mol Biol Evol. 2003 Mar;20(3):424-34.
46. Sambrook JG, Sehra H, Coggill P, Humphray S, Palmer S, Sims S, et al. Identification of a single killer immunoglobulin-like receptor (KIR) gene in the porcine leukocyte receptor complex on chromosome 6q. Immunogenetics. 2006 Jun;58(5-6):481-6.
47. Williams KC, Burdo TH. HIV and SIV infection: the role of cellular restriction and immune responses in viral replication and pathogenesis. Apmis. 2009 May;117(5-6):400-12.
48. Silvestri G. AIDS pathogenesis: a tale of two monkeys. J Med Primatol. 2008 Dec;37Suppl2:6-12.

49. Dunham R, Pagliardini P, Gordon S, Sumpter B, Engram J, Moanna A, et al. The AIDS resistance of naturally SIV-infected sooty mangabeys is independent of cellular immunity to the virus. Blood. 2006 Jul 1;108(1):209-17.
50. Betts MR, Ambrozak DR, Douek DC, Bonhoeffer S, Brenchley JM, Casazza JP, et al. Analysis of total human immunodeficiency virus (HIV)-specific CD4(+) and CD8(+) T-cell responses: relationship to viral load in untreated HIV infection. J Virol. 2001 Dec;75(24):11983-91.
51. Bontrop RE, Watkins DI. MHC polymorphism: AIDS susceptibility in non-human primates. Trends Immunol. 2005 Apr;26(4):227-33.
52. Bland JM, Altman DG. Statistics notes. The odds ratio. Bmj. 2000 May 27;320(7247):1468.
53. Blokhuis JH, van der Wiel MK, Doxiadis GG, Bontrop RE. Evidence for balancing selection acting on KIR2DL4 genotypes in rhesus macaques of Indian origin. Immunogenetics. 2009 Jul;61(7):503-12.
54. Rajagopalan S, Long EO. A human histocompatibility leukocyte antigen (HLA)-G-specific receptor expressed on all natural killer cells. J Exp Med. 1999 Apr 5;189(7):1093-100.
55. Yu YR, Tian XH, Wang Y, Feng MF. Rapid production of human KIR2DL4 extracellular domain and verification of its interaction with HLA-G. Biochemistry (Mosc). 2006;71 Suppl 1:S60-4, 4-5.
56. Pereira LE, Ansari AA. A case for innate immune effector mechanisms as contributors to disease resistance in SIV-infected sooty mangabeys. Curr HIV Res. 2009 Jan;7(1):12-22.
57. Kaizu M, Borchardt GJ, Glidden CE, Fisk DL, Loffredo JT, Watkins DI, et al. Molecular typing of major histocompatibility complex class I alleles in the Indian rhesus macaque which restrict SIV CD8+ T cell epitopes. Immunogenetics. 2007 Sep;59(9):693-703.
58. Wojcechowskyj JA, Yant LJ, Wiseman RW, O'Connor SL, O'Connor DH. Control of simian immunodeficiency virus SIVmac239 is not predicted by inheritance of Mamu-B*17-containing haplotypes. J Virol. 2007 Jan;81(1):406-10.

59. Pando MJ, Gardiner CM, Gleimer M, McQueen KL, Parham P. The protein made from a common allele of KIR3DL1 (3DL1*004) is poorly expressed at cell surfaces due to substitution at positions 86 in Ig domain 0 and 182 in Ig domain 1. J Immunol. 2003 Dec 15;171(12):6640-9.
60. Averdam A, Petersen B, Rosner C, Neff J, Roos C, Eberle M, et al. A novel system of polymorphic and diverse NK cell receptors in primates. PLoS Genet. 2009 Oct;5(10):e1000688.
61. LaBonte ML, Levy DB, Letvin NL. Characterization of rhesus monkey CD94/NKG2 family members and identification of novel transmembrane-deleted forms of NKG2-A, B, C, and D. Immunogenetics. 2000 May;51(6):496-9.
62. Boyson JE, McAdam SN, Gallimore A, Golos TG, Liu X, Gotch FM, et al. The MHC E locus in macaques is polymorphic and is conserved between macaques and humans. Immunogenetics. 1995;41(2-3):59-68.
63. Evans DT, Knapp LA, Jing P, Mitchen JL, Dykhuizen M, Montefiori DC, et al. Rapid and slow progressors differ by a single MHC class I haplotype in a family of MHC-defined rhesus macaques infected with SIV. Immunol Lett. 1999 Mar;66(1-3):53-9.
64. LaBonte ML, McKay PF, Letvin NL. Evidence of NK cell dysfunction in SIV-infected rhesus monkeys: impairment of cytokine secretion and NKG2C/C2 expression. Eur J Immunol. 2006 Sep;36(9):2424-33.
65. Zeddou M, Rahmouni S, Vandamme A, Jacobs N, Frippiat F, Leonard P, et al. Downregulation of CD94/NKG2A inhibitory receptors on CD8+ T cells in HIV infection is more pronounced in subjects with detected viral load than in their aviraemic counterparts. Retrovirology. 2007;4:72.
66. Yunis EJ, Romero V, Diaz-Giffero F, Zuniga J, Koka P. Natural Killer Cell Receptor NKG2A/HLA-E Interaction Dependent Differential Thymopoiesis of Hematopoietic Progenitor Cells Influences the Outcome of HIV Infection. Journal of stem cells. 2007;2(4):237-48.

APPENDIX

Table A.1. Clinical history of SIV-infected RMs in the cohort.

Sample ID	MHC Class I typing (Mamu)*	SIV strains	PMPA treatment	viral loads (copies/ml)	NK cell activity (lytic units)		% CD4+T cell count	
					Pre-infection	Post-infection	Pre-infection	Post-infection
RM-HVL cohort								
mm 1		SIVmac239	Yes	6,000,000	776	101	33.4	15.5
mm 3		SIVmac239	No	28,841,600	673	824	30.6	25.3
mm 5		SIVmac239	Yes	8,763,600	926	148	28.9	27.1
mm 6		SIVmac239	Yes	6,912,600	887	88	32.1	15.4
mm 7	B.01	SIVmac239	Yes	1,200,000	776	172	24.4	9.5
mm 8	B.01	SIVmac239	No	31,426,100	721	122	35.1	34.4
mm 9	B.01	SIVmac239	No	27,000,000	709	154	25.1	30.5
mm 10		SIVmac239	Yes	6,200,000	921	210	35.9	10.5
mm 16		SIVmac239	Yes	18,000,000	578	122	26.4	21.6
mm 17		SIVmac239	No	36,831,700	822	321	23.3	8.9
mm 18		SIVmac239	Yes	3,434,500	876	212	27.6	15.7
mm 19	A.01	SIVmac251	Yes	2,950,000	984	98	29.1	11.8
mm 22		SIVmac239	No	2,000,000	498	98	32.2	3.2
mm 23	A.01	SIVmac251	Yes	6,000,000	574	108	31.9	22.9
mm 24	A.01,B.01	SIVmac239	No	3,300,000	582	232	21.1	10.8
mm 25		SIVmac251	No	4,000,000	621	164	31.4	5.2
mm 26		SIVmac239	Yes	5,041,100	602	173	30.8	13.9
mm 27		SIVmac251	No	2,000,000	548	182	41.1	11.8
mm 29		SIVmac239	No	1,500,000	733	167	22.2	12.6
mm 33		SIVmac239	Yes	3,000,000	678	186	31.8	10.7
RM-LVL cohort								
mm 2		SIVmac239	Yes	11,000	645	764	34.5	35.8
mm 4		SIVmac239	Yes	70,184	833	722	31.1	37.2
mm 11	A.01	SIVmac239	No	800	887	776	19.3	15.7
mm 12		SIVmac239	No	2,000	567	698	23.2	18.1
mm 13	A.01,B.01,B.17	SIVmac239	Yes	1,000	587	859	28.8	17.2
mm 14	A.01	SIVmac239	Yes	10,000	902	770	31.2	29.6
mm 15	A.01	SIVmac239	Yes	20,000	768	623	33.8	25.9
mm 20	A.01	SIVmac239	Yes	15,000	772	632	32.7	31.4
mm 21		SIVmac239	Yes	4,000	664	662	25.8	20.7
mm 28		SIVmac239	No	2,770	776	589	31.1	27.2
mm 30		SIVmac239	No	1,100	784	634	28.3	38.1
mm 31		SIVmac239	No	300	698	702	38.2	33.5
mm 32		SIVmac239	Yes	700	802	874	25.5	15.4
mm 34	A.01	SIVmac251	Yes	4,000	712	668	32.6	14.8
mm 35		SIVmac239	No	300	823	668	41.9	34.1
mm 36	B.08	SIVmac239	No	9,100	776	721	35.9	26.8
mm 37	B.17	SIVmac239	Yes	20,000	715	693	29.1	16.3
mm 38	A.01	SIVmac251	Yes	1,500	756	922	36.7	18.1

*Animals typed for *Mamu A.01, B.01, B.08, and B.17*; only positive results are in lists.

Table A.2. Statistical analysis of the pre- and the post-infection of SIV-infected RMs.

Cohort	plasma viral loads* (copies/ml)		CD4+T cell count (%)				NK cell activity (lytic units)			
			pre-infection		post-infection*		pre-infection		post-infection*	
	mean	SD	mean	SD	mean	SD	mean	SD	mean	SD
HVL	1.00E+07	1.10E+07	29.72	5.00	15.87**	8.42	724.25	142.99	194.10**	158.55
LVL	9653	16497	31.09	5.55	25.33	26.35	748.17	92.02	720.94	91.85

*$p < 0.001$, compared to animals with low VLs.

**$p<0.001$, compared to the pre-infection.

BIOGRAPHY

NAME Miss Porntip Chaichompoo
DATE OF BIRTH 16 September 1982
PLACE OF BIRTH Chon buri, Thailand
INSTITUTIONS ATTENDED Chiang Mai University, 2000-2003:
Bachelor of Science (Medical Technology)
Mahidol University, 2004-2006:
Master of Science (Immunology)
Mahidol University, 2007-2009:
Doctor of Philosophy (Immunology)
HOME ADDRESS 161/16 Sukumvit Rd., Saen suk,
Chon buri 20130 Thailand
E-mail: panion15@hotmail.com
SCHOLARSHIP Siriraj Graduate Scholarship,
Faculty of Medicine Siriraj hospital,
Mahidol University, 2004-2005
Royal Golden Jubilee (RGJ)-Ph.D. program,
Thailand Research Fund (TRF), 2006-2009

PUBLICATIONS

1. Pattanapanyasat K, Gonwong S, Chaichompoo P, Noulsri E, Lerdwana S, Sukapirom K, Siritanaratkul N, Fucharoen S. Activated platelet-derived microparticles in thalassaemia. Br J Haematol. 2007 Feb;136(3):462-71.
2. Chaichompoo P, Bostik P, Kobkitjaroen J, Stephenson S, Udompunturuk S, Pattanapanyasat K, Ansari AA. Multiple KIR gene polymorphisms are associated with plasma viral loads in SIV infected rhesus macaques. Cellular Immunol. Submitted, Copyright©2010 Published by Elsevier Inc. (doi:10.1016/j.cellimm.2010.03.014)